Water Research

Streambed microbial communities in the transition zone between groundwater and a first-order stream as impacted by bidirectional water exchange

--Manuscript Draft--

Manuscript Number:	WR67033
Article Type:	Research Paper
Keywords:	headwater stream; streambed microbiomes; nitrate reduction; losing and gaining stream; groundwater-surface water exchange
Corresponding Author:	Tillmann Lueders University of Bayreuth Bayreuth, GERMANY
First Author:	Tillmann Lueders
Order of Authors:	Tillmann Lueders
	Zhe Wang
	Oscar Jimenez-Fernandez
	Karsten Osenbrück
	Marc Schwientek
	Michael Schloter
	Jan H. Fleckenstein
Abstract:	The input of nitrate and other agricultural pollutants in higher order streams largely derives from first-order streams. The streambed as the transition zone between groundwater and stream water has a decisive impact on the attenuation of such pollutants. This reactivity is not yet well-understood for lower-order agricultural streams, which are often anthropogenically altered and lack streambed complexity allowing for extensive hyporheic exchange. Reactive hot-spots in the streambed have been hypothesized as a function of hydrology, controlling either the local gaining or losing of water by the stream. However, streambed microbial communities and activities associated with such reactive zones remain mostly uncharted. In this study, sediments of a first-order, agriculturally impacted stream in southern Germany were investigated. Along with a hydraulic dissection of distinct gaining and losing reaches along the stream, community composition and the abundance of bacterial communities in the streambed were investigated using PacBio long-read sequencing of bacterial 16S rRNA amplicons and qPCR of bacterial 16S rRNA and denitrification genes. We show that bidirectional water exchange between groundwater and the stream represents an important control for sediment microbiota, especially for nitrate-reducing populations. Typical heterotrophic denitrifiers were most abundant in a midstream losing section, while up- and downstream gaining sections were associated with an enrichment of sulfur-oxidizing potential nitrate reducers affiliated with *Sulfuricurvum* and *Thiobacillus* spp. Dispersal-based community assembly was found to dominate such spots of groundwater exfiltration. Our results indicate a coupling of N- and S-cycling processes in headwater streambeds, and a prominent control of microbiology by hydrology and hydrochemistry *in situ*. Such detailed local heterogeneities in exchange fluxes and microbial community structure in streambed sediments have not been reported to date, but may clearly be relevant to understand streambed reactivity *in situ*.
Suggested Reviewers:	Virginia I Rich rich.270@osu.edu
	Alyson Santoro asantoro@ucsb.edu
	Feng Ju jufeng@westlake.edu.cn
	Philips Akinwole

Powered by Editorial Manager® and ProduXion Manager® from Aries Systems Corporation

	philipsakinwole@depauw.edu

Powered by Editorial Manager® and ProduXion Manager® from Aries Systems Corporation

Streambed microbial communities in the transition zone between groundwater and a first-order stream as impacted by bidirectional water exchange

Highlights

- Bidirectional water fluxes affect streambed microbial community assembly.
- Interactions between N- and S-cycles stimulated by bidirectional water exchange.
- Full-length amplicon sequencing of headwater streambed microbiomes.
- *Sulfuricurvum* spp. and *Thiobacillus* spp. are prominent taxa.
- Agricultural headwaters are not only drainage channels, but reactors.

Graphical Abstract

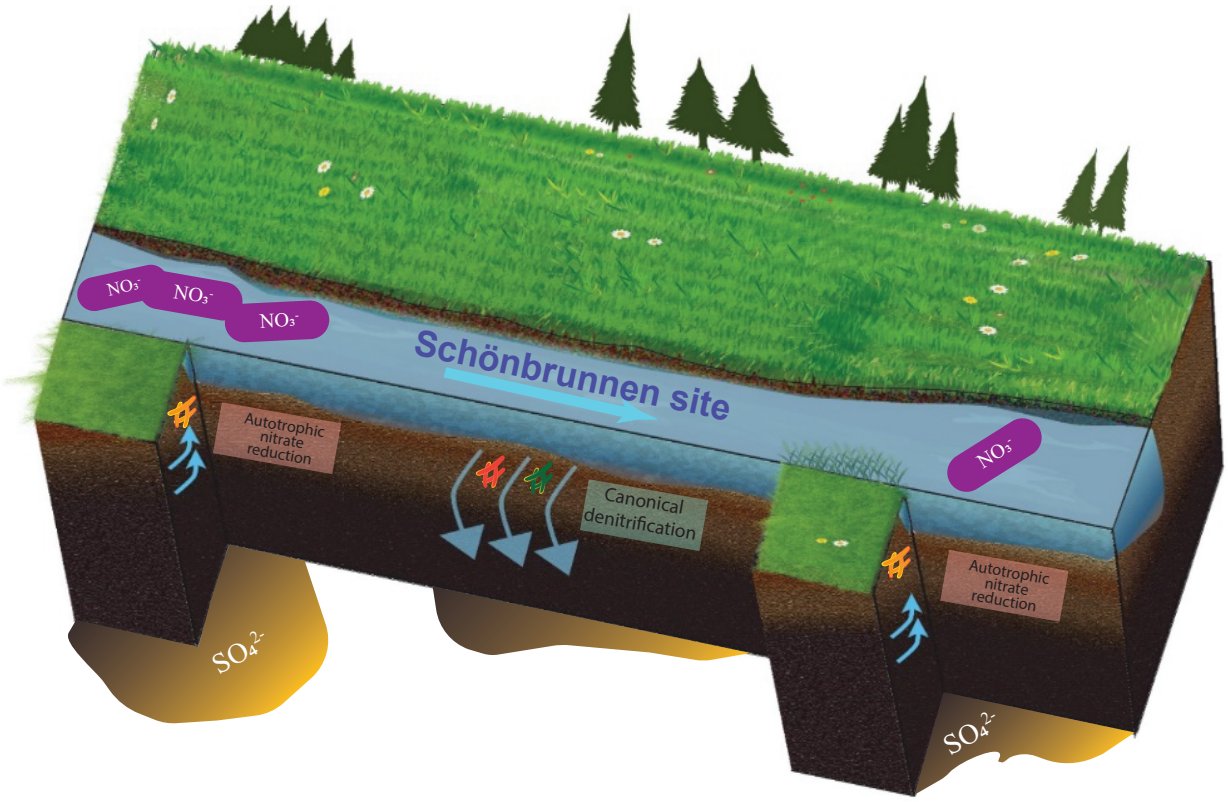

Declaration of interests

☒The authors declare that they have no known competing financial interests or personal relationships that could have appeared to influence the work reported in this paper.

☐The authors declare the following financial interests/personal relationships which may be considered as potential competing interests:

Manuscript Click here to view linked References

Streambed microbial communities in the transition zone between groundwater and a first-order stream as impacted by bidirectional water exchange

Zhe Wang[1,2,8], Oscar Jimenez-Fernandez[3,4], Karsten Osenbrück[3,9], Marc Schwientek[3], Michael Schloter[5,7], Jan H. Fleckenstein[4,6], Tillmann Lueders[1,*]

[1] Chair of Ecological Microbiology, Bayreuth Center of Ecology and Environmental Research (BayCEER), University of Bayreuth, Bayreuth, Germany

[2] Institute of Groundwater Ecology, Helmholtz Zentrum München - German Research Centre for Environmental Health, Neuherberg, Germany

[3] Center for Applied Geoscience, University of Tübingen, Tübingen, Germany

[4] Department of Hydrogeology, Helmholtz-Zentrum für Umweltforschung GmbH - UFZ, Leipzig, Germany

[5] Chair of Soil Science, Technical University of Munich, Freising, Germany

[6] Hydrologic Modelling Unit, Bayreuth Center of Ecology and Environmental Research (BayCEER), University of Bayreuth, Bayreuth, Germany

[7] Research Unit for Comparative Microbiome Analyses, Helmholtz Zentrum München - German Research Centre for Environmental Health, Neuherberg, Germany

[8] School of Life Sciences, Technical University of Munich, Freising, Germany

[9] Federal Institute for Geosciences and Natural Resources (BGR), Hannover, Germany

[*]Corresponding author. E-mail address: tillmann.lueders@uni-bayreuth.de

Keywords: headwater stream, streambed microbiomes, nitrate reduction, losing and gaining stream, groundwater-surface water exchange

Abstract

The input of nitrate and other agricultural pollutants in higher order streams largely derives from first-order streams. The streambed as the transition zone between groundwater and stream water has a decisive impact on the attenuation of such pollutants. This reactivity is not yet well-understood for lower-order agricultural streams, which are often anthropogenically altered and lack streambed complexity allowing for extensive hyporheic exchange. Reactive hot-spots in the streambed have been hypothesized as a function of hydrology, controlling either the local gaining or losing of water by the stream. However, streambed microbial communities and activities associated with such reactive zones remain mostly uncharted. In this study, sediments of a first-order, agriculturally impacted stream in southern Germany were investigated. Along with a hydraulic dissection of distinct gaining and losing reaches along the stream, community composition and the abundance of bacterial communities in the streambed were investigated using PacBio long-read sequencing of bacterial 16S rRNA amplicons and qPCR of bacterial 16S rRNA and denitrification genes. We show that bidirectional water exchange between groundwater and the stream represents an important control for sediment microbiota, especially for nitrate-reducing populations. Typical heterotrophic denitrifiers were most abundant in a midstream losing section, while up- and downstream gaining sections were associated with an enrichment of sulfur-oxidizing potential nitrate reducers affiliated with *Sulfuricurvum* and *Thiobacillus* spp. Dispersal-based community assembly was found to dominate such spots of groundwater exfiltration. Our results indicate a coupling of N- and S-cycling processes in headwater streambeds, and a prominent control of microbiology by hydrology and hydrochemistry *in situ*. Such detailed local heterogeneities in exchange fluxes and microbial community structure in streambed sediments have not been reported to date, but may clearly be relevant to understand streambed reactivity *in situ*.

Introduction

Up to 85 % of the total stream length in a river system consist of headwater streams, typically classified as first- and second- order streams (Horton, 1945; Peterson et al., 2001; Scheidegger, 1965). Lower-order streams act as the fountainhead of fluvial networks and have a substantial imprint on streamwater chemisty (Peterson et al., 2001). However, their reactivity and elimination potential towards incoming pollutants, in particular from diffuse agricultural sources, are not well understood. Especially, the partitioning of this reactivity between instream processing and the streambed remain sparsely addressed. Higher order streams are typically connected to extensive hyporheic and parafluvial flow paths, which move stream water through streambed and riparian sediments to subsequently return to the stream (Boano et al., 2014; Gomez-Velez et al., 2015; Krause et al., 2011; McClain et al., 2003). Water passage through hyporheic zones can significantly stimulate biogeochemical turnover of pollutants and nutrient elimination because of elongated transit times (compared to instream transit times) and increased biogeochemical and physical heterogeneity. In contrast, lower-order agricultural streams have often been strongly modified, straightened and typically are of low streambed morphological complexity, thus minimizing the potential for hyporheic exchange. Therefore, such streams have often been considered to act predominantly as drainage systems, largely receiving water from the surrounding landscape (Kaandorp et al., 2018; Needelman et al., 2007; Yu et al., 2018). This currently limits the perspective of how hydrology and biogeochemistry can interact to control oxidative and reductive pollutant transformation in lower-order agricultural streams.

Nitrate loading, mainly stemming from agricultural fertilizer inputs and also nitrification of ammonia arising from livestock manure, is of a particular concern for stream and groundwater quality (Peterson et al., 2001; Starry et al., 2005). Capacities for the assimilative removal of nitrate in the stream itself mostly involve algal or macrophyte growth

(Gooseff et al., 2004; Smith et al., 2006). More importantly, nitrate can also be removed by stream sediment microbial communities through heterotrophic denitrification and/or dissimilatory nitrate reduction to ammonium (DNRA) (Kuypers et al., 2018; Mulholland et al., 2008; Storey et al., 2004; Tiedje, 1988). Nitrate reduction can also occur autotrophically, coupled to the oxidation of iron and sulfur species, hydrogen, or methane (Kuypers et al., 2018). However, as all of these processes require microoxic or anoxic conditions, the local hydraulic patterns becomes a decisive parameter of control (Seitzinger et al., 2002; Zarnetske et al., 2011). It is now recognized that lower-order streams not only receive water, but steadily interact with the surrounding groundwater along successive and seasonally variable gaining (groundwater exfiltration) or losing (stream water infiltration) reaches (Covino and McGlynn, 2007; Mallard et al., 2014; Zhang et al., 2021). This sequential exchange and replacement of water along the flow of a lower-order stream has been termed as hydrologic turnover, which can substantially influence the biogeochemistry of the stream (Mallard et al., 2014). Depending on the local availability of electron donors such as organic carbon, reduced iron and/or sulfur species in the sediment, reactive hot-spots for denitrification may thus be generated in the streambed especially in losing reaches (Trauth et al., 2018). In an agriculturally impacted first-order stream in southern Germany, we have recently identified substantial and seasonally variable bidirectional exchange fluxes between the stream and surrounding groundwater, contributing significantly to nitrate reduction in water entering the near-stream anoxic aquifer (Jimenez-Fernandez et al., 2022). However, the interplay of hydrological and biogeochemical processes in shaping sedimentary bacterial communities and their activities in nitrogen cycling has not been addressed.

Previous studies addressing the microbiology of rivers and streams report that sediment microbial communities are typically distinct to those found in surface water and the surrounding groundwater, and suggest a depth-dependent stratification (Danczak et al., 2016;

Graham et al., 2017; Lin et al., 2012; Saup et al., 2019). Longitudinally, successions in microbial community structure have been investigated from headwaters to large rivers and even estuaries, and are taken to be controlled by local stream characteristics, landscape type, and anthropogenic impact (Battin et al., 2008; Crump et al., 2004; Hullar et al., 2006; Liao et al., 2019; Winter et al., 2007). It is also assumed that local sediment community assembly is dominated by deterministic selection (Danczak et al., 2016; Graham et al., 2017). In contrast, mechanisms of dispersal based stochastic assembly were observed for zones impacted by direct hydrologic transport, such as hyporheic mixing (Danczak et al., 2016; Graham et al., 2017; Stegen et al., 2016).

To date, studies on structural patterns of microbial communities in sediment of agricultural impacted lower-order streams remain scarce, especially in a dedicated hydrologic perspective. Here, we address this research gap by dissecting sedimentary bacterial communities in the same agricultural first-order stream mentioned above via qPCR and PacBio full-length 16S rRNA gene amplicon sequencing. Long-read amplicon sequencing was chosen to provide more reliable phylogenetic resolution on possible taxon distribution patterns associated with local hydrology characteristics. We posit that typical hydrological and geochemical parameters alone are not sufficient to understand nitrate reduction mechanisms in such systems, and explicitly address the interplay of hydrologic and microbial process controls (Harvey et al., 2013; Mulholland et al., 2008). We hypothesize that (1) sediment microbial communities along successive gaining and losing sections of the first-order stream are distinct and impacted by local hydrology, (2) the impact of hydrology on sediment microbial communities should be apparent in distinct assembly patterns between communities over longitudinal sections and over depth, and (3) local hydrologic turnover caused by simultaneous bidirectional water exchange impacts the distribution and abundance of nitrate reducing populations.

Materials and methods

Site description.

The Schönbrunnen stream (48.32°N latitude and 8.57°E longitude) is a first-order stream located in a predominantly agricultural area. It is a tributary of the second-order Käsbach stream, within the Ammer catchment in the west of the city of Tübingen, Germany (Fig. 1). Both hydrology and hydrochemistry of the site (Table 1) are comprehensively described in a parallel manuscript (Jimenez-Fernandez et al., 2022). The studied section of the stream has a length of approximately 550 m, a mean discharge of approximately 1 L s^{-1}, and drains an area of approximately 1 km^2. The mean stream water depth varies between 5 and 13 cm. The stream section runs in the Käsbach valley, mainly filled with fine alluvial quaternary sediments overlying the geological unit of the Lower Keuper (Erfurt-Formation), dolomites, sand- and claystones, which act as the primary bedrock. Along the eastern hillslopes, the Lower Keuper is overlain by the Grabfeld-Formation of the Middle Keuper. This formation contains thick gypsum units interspersed with dolomite and limestone banks and forms a local aquifer draining hillslope groundwater towards the alluvial groundwater system (D'Affonseca et al., 2020). The eastern hillslope groundwater exhibits higher sulfate concentrations than the alluvial groundwater. During this study, the majority of the surrounding area of the studied Schönbrunnen section was covered by meadows due to crop and fallow rotation, with the exception of the northwestern area, which was utilized as farming- and pasture-land.

The streambed sediment is comprised of silty, clayey, and loamy materials. Hydraulic parameters of groundwater were calculated by performing a series two slug tests per groundwater monitoring well. The hydraulic conductivity (k_f) of the streambed sediments was calculated by tracing a perpendicular line to groundwater flow direction on the head contours maps. By assessing the influence of the stream on the mean groundwater levels, we defined the hydraulic head differences (Δh) at a given distance (Δl). Groundwater discharge (Q) was

taken from the results of a series of tracer tests (Jimenez-Fernandez et al., 2022). Defining a fixed sediment area within each of the tracer test reaches, we could determine the hydraulic conductivity for each reach. This parameter was assumed to be constant alongside the studied stream section. The permeability value (K) of the streambed was between 10^{-7} to 10^{-9} $cm^2 \cdot s^{-1}$ according to hydraulic conductivity (k_f) (Table 1) calculated using the equation below:

$$K = k_f \cdot \frac{\eta}{\rho \cdot g} \quad (1)$$

where η = dynamic viscosity = 10^{-3} Ps at 10 °C, ρ = mass density of water, g = gravitational acceleration.

Sediment sampling

Stream sediments were collected in August 2017 at selected locations along the Schönbrunnen stream (Fig. 1 & Table S1) by taking sediment push-cores using a stainless steel piston corer (Eijkelkamp, Giesbeek, Netherlands). There had not been any major precipitation events (< 5 mm) one week preceding the sampling campaign (Agrometeorology of Baden-Württemberg, 2017). After coring, sediments were dispensed onto clean plastic furrows, and sediment subsamples were collected using sterile spatula at two distinct sediment depths (5 cm and 15 cm below streambed surface). Replicate cores were taken within ~30 cm distances from the first core to minimize lateral disturbances. Subsamples were stored in sterile 50 mL PE tubes (Fisher Scientific GmbH, Schwerte, Germany) and cooled during immediate transport back to the lab, then stored at -80 °C until further processing. Some fresh sediment cores (~25 cm in length) were also stored in sterilized glass cylinders in duplicates, covered with 5 cm of stream water, before transport to the 15 °C sample storage room in the lab, which was similar to the average stream water temperature 13.2 °C during the sampling month.

Hydrological description and water chemistry.

The interaction between the stream and adjacent groundwater, and the hydrologic turnover were quantified by repeated field measurements and tracer tests done between summer 2017 and summer 2018 (Jimenez-Fernandez et al., 2022). Thus, the Schönbrunnen stream was divided into six reaches (R1 – R6) characterized by distinct and seasonally variable net water gains or losses to or from the stream, respectively (Fig. 1). Water exchange fluxes in the summer season were characterized by net gaining conditions in the further upstream of the reach R1 (major water source of the Schönbrunnen owing to the spring), generally net losing but locally variable conditions in midstream R2 to R4, and again mostly gaining but locally variable conditions in downstream R5 and R6 (Fig. 2A). However, gross water fluxes in both directions (infiltration and exfiltration) occured in all reaches. These reach-scale exchange fluxes had been further investigated with salt tracer tests. Gaining conditions were relatively more important in downstream R5 and R6, whereas locally variable but generally net losing conditions were observed in midstream reaches (R2 and R4). For R3, salt tracers indicated a similar magnitude of stream water gaining and losing fluxes (Fig. 2A).

Water samples for major ions and DOC (dissolved organic carbon) analyses were obtained from the stream and the surrounding network of groundwater monitoring wells in August 2018. For both stream and groundwater samples, 100 mL and 25 mL samples were taken in glass bottles and filtered through 0.45 µm filters (MillexHA, Darmstadt, Germany) within 48 hours for the analysis of major ions and DOC, respectively. The samples were kept at 4°C in the dark upon analysis. Major ions were determined by ion chromatography (Dionex DX 500, Thermo Fisher Scientific, Waltham, MA, USA; LOQ = 0.1 mg/L for chloride and nitrate, and 0.3 mg/L for sulfate). The DOC sample's pH was adjusted to 2 and measured on a TOC analyzer (elementar HighTOC, Langenselbold, Germany).

At selected locations, sediment porewater was sampled using mini piezometers (≤ 2.5 mL min^{-1}) with depth differentiation (0-30 cm below streambed) (Fig. S1) (Duff et al., 1998).

All samples were filtered and kept at 4 °C in the dark until further analysis as mentioned above. Stream water electrical conductivity (EC) was monitored using vented pressure transducers integrated in CTD probes with data loggers (UIT GmbH, Dresden, Germany) which were installed *in situ*. Groundwater EC (± 0.5% of value; temperature compensation to 25°C) was measured in the field by hand-held probes (WTW GmbH, Weilheim in Oberbayern, Germany). The assessment of other parameters, including discharge Q, water mixing ratios, and groundwater heads, are described elsewhere (Jimenez-Fernandez et al., 2022).

Nucleic Acid Extraction and 16S rRNA gene sequencing.

Samples from replicate sediment cores of each location and depth were homogenized before further processing. Genomic DNA of sediment samples was extracted as described (Pilloni et al., 2012) with minor modifications (all was done at 4 °C). About 0.6 g wet sediment was used for each DNA extraction, and DNA was extracted in triplicates from each sample. DNA quality and quantity in extracts was determined with agarose gel electrophoresis and by using the Quant-iT PicoGreen dsDNA Assay Kit (Thermo Fisher, Waltham, USA) on an MX3000p cycler (Agilent, Santa Clara, USA).

For full-length 16S rRNA gene sequencing, a two-step PCR was performed. The first amplification was done with the KAPA HiFi HotStart PCR Kit (Kapa Biosystems, Boston, MA, USA) and universal primers for the bacterial 16S rRNA gene (forward and reverse) tailed with PacBio universal sequence adapters (Table S2). The detailed information on PCR reactions is described in Supplementary Appendix. Sequencing library construction was performed utilizing the SMRTbell® Template Prep Kit 1.0, following the PacBio online documentation “Procedure & Checklist – Amplification of Full-Length 16S Gene with Barcoded Primers for Multiplexed SMRTbell Library Preparation and Sequencing” (version June, 2018). The libraries were sequenced on a PacBio Sequel platform.

Sequencing data analysis.

Raw sequencing data was processed using the SMRTLink implemented secondary analysis platform provided by PacBio (version 6.0) to generate demultiplexed sequences and Circular Consensus Sequence (CCS) reads, which were converted to .fastq files (Table S4). Primers were trimmed using CUTADAPT v1.14 (Martin, 2011). Reads lengths were filtered and retained by Geneious R10 (Biomatters, New Zealand) to an average range of 1400-1600 bp. Samples with a total read number <1500 were excluded (n=3) from downstream analysis. Sequence data were deposited in the European Nucleotide Archive (ENA) with the study accession number: PRJEB49634.

Sequence data were further processed in R (version 3.5.0) (R Core Team, 2019) using the DADA2 (version 1.10.1) algorithms for quality filtering, generating high accuracy exact amplicon sequence variants (ASVs) with single-nucleotide resolution, and chimera removal, according to the "DADA2 + PacBio" workflow (Callahan et al., 2019). However, we did not manually discard ASVs low in abundance across all samples prior to taxonomic classification. IDTAXA Classifier (Wright, 2016) was used with a confidence level of 50% (high) to map ASV sequences against the SILVA SSU database (release 132) for taxonomic classification (Quast et al., 2013). ASVs classified as "mitochondria", "chloroplasts", or "unclassified root" were removed. The FastTree (Price et al., 2009) algorithm was applied for generating a midpoint-rooted phylogenetic tree after ASVs sequence alignment by the DECIPHER package (version 2.12.0) (Wright, 2015). Maximum likelihood phylogenetic trees were constructed for specific taxa (i.e. *Sulfuricurvum* spp. and *Thiobacillus* spp.) with MEGA-X (Kumar et al., 2018), aligned with selected reference 16S rRNA gene sequences from NCBI and IMG/M databases (Agarwala et al., 2018; Chen et al., 2019), using the ClustralW algorithm with default settings (1,000 bootstrap replications). Phylogenetic trees for *Sulfuricurvum* spp. and *Thiobacillus* spp. were then visualized and analyzed with iTol v6 (Letunic and Bork, 2019).

We utilized raw read counts and proportions for alpha diversity and beta diversity analysis, respectively (Cameron et al., 2020; McMurdie and Holmes, 2014). Alpha diversity indices, including the Shannon Index and Shannon diversity based evenness index were calculated using the phyloseq package (version 1.28.0) (McMurdie and Holmes, 2013). Differences in alpha diversity were assessed by non-parametric Kruskal-Wallis analysis in combination with Dunn's tests for multiple comparisons, and Benjamini-Hochberg correction for multiple comparisons using DescTools package (version 0.99.41) (Signorelli, 2020). Bray-Curtis dissimilarities calculated to demonstrate differences in microbial community composition among samples at the family level using hierarchical clustering method (average-linkage) and non-metric multi-dimensional scaling (NMDS) using the vegan package (version 2.5-5) (Oksanen et al., 2019). Similarity percentage (SIMPER) analysis was applied to evaluate which taxa contributed to the structural differences of two communities using the vegan package (permutations = 1000) (version 2.5-5) (Oksanen et al., 2019).

Bacterial community structure was investigated in order to evaluate the assembly mechanisms under the impact of bidirectional water exchange in the streambed. Therefore, a two-step null model approach, taking both phylogenetic distance and abundance into consideration, was applied as first-step. This is based on the assumption that phylogenetically close taxa are more likely to have similar ecological niches (Stegen et al., 2013). We first calculated β-mean nearest taxa distance (β-MNTD) in order to quantify the phylogenetic distance of a species in one community to its closest relatives in another. β -MNTD was calculated with 999 randomizations. Then β-nearest taxon index (β-NTI), which represents the number of standard deviations between the observed β-MNTD and the mean of the null distribution, was calculated to indicate whether species in two compared communities are phylogenetically significantly more close or different than expected by chance. If $|\beta\text{-NTI}| > 2$, a significant deviation from the null distribution is assumed; indicating that species in two compared communities are phylogenetically significantly more close or distinct. Likely, this

is because of deterministic environmental selection processes, such as homogeneous and variable selection. If $|\beta\text{-NTI}| < 2$, dispersal-based and other stochastic processes should be further examined. We applied the Bray-Curtis distance based Raup-Crick index (RC_{bray}) (Chase and Myers, 2011) to evaluate stochastic assembly mechanisms. RC_{bray} only requires species occurrence and abundance in one community. $|RC_{bray}| > 0.95$ suggests that two communities have significantly more or less common species than expected by chance; indicating homogenizing dispersal or dispersal limitation and drift processes. $|RC_{bray}| < 0.95$ indicates drift or undominated processes. RC_{bray} was also calculated with 999 randomizations. In assembly analysis, all samples were rarefied to the 1800 reads (seed = 123), the minimum number of reads among all samples. Reads from duplicate samples were merged using the Picante package (version 1.7) (Kembel et al., 2010). Moreover, in this analysis, we omitted samples from the confluence as we only applied this approach to samples with comprehensive hydrological metadata.

Correlations between gene abundances and geodesic distance were calculated using Spearman correlation and least square linear models in the R package stats (version 4.0.3), respectively (R Core Team, 2019). Other major packages used for data visualization include phyloseq (version 1.34.0), ggplot2 (version 3.3.2), tidyverse (version 1.3.0), ComplexHeatmap (version 2.7.6.1002), ggpubr (version 0.4.0), ComplexUpset (version 1.1.0) (Ginestet, 2011; Gu et al., 2016; Kassambara, 2020; Li, 2020; M Krassowski, 2020; McMurdie and Holmes, 2013; Wickham et al., 2019).

Quantitative PCR (qPCR) of bacterial 16S rRNA and nitrite reduction genes.

Abundances of bacterial 16S rRNA, *nirK*, and *nirS* genes were determined via qPCR on an MX3000p qPCR System (Agilent, Santa Clara, USA). The primers used are listed in Table S3. Triplicate DNA extracts per sample were quantified in technical duplicates. For bacterial 16S rRNA genes, 40 µL reactions consisting of 1 x Takyon SYBR MasterMix (Eurogentec, Cologne, Germany) with 0.6 µL 50 x ROX reference dye (Thermo Fisher

Scientific, Waltham, MA, USA), 0.2 µM bovine serum albumin (BSA) (Roche Diagnostics GmbH, Basel, Switzerland), 0.3 µM of each of the forward and reverse primer and 2 µL of adequately diluted DNA template were used. For amplification of the nitrite reductase genes, all components were identical except that 1 x Brilliant III Ultra-Fast qPCR Master Mix (Agilent, Santa Clara, CA, USA) was used in 40 µL qPCR reactions.

The temperature and cycling profile for each assay were as follows: initial denaturation at 95 °C (3 min), 35 – 40 cycles of denaturation at 95 °C (30 s) , annealing at a given temperature (30 s), elongation at 72 °C (30 s), followed by a final a melting at 95 °C (30 s) and a melting curve recorded between 60 and 95 °C. Primer annealing temperature was set to 54 °C for bacterial 16S genes, and to 58 °C for *nirK* and *nirS* genes, respectively. Standardization was done via ten-fold dilution series of synthetic gene fragments (gBlocks, Integrated DNA Technologies, Leuven, Belgium) of known concentration covering all respective primer sites. For 16S rRNA genes, a 980 bp-fragment of the *E. coli* 16S rRNA gene was used. For *nirK*, a 450 bp-fragment of the respective gene of *Sinorhizobium meliloti* 1021 and for *nirS*, a 660 bp-fragment of the respective gene of *Pseudomonas stutzeri* DSM 4166 was employed. Each standard curve reached R-square value greater than 0.99 and amplification efficiency of all genes was at 100 ± 15 %. Absolute abundances of target genes were reported as copies g^{-1} of fresh sediment (g_{ww}^{-1} of sediment). Relative abundances of nitrite reductases are shown as the $\log_{10}$ ratio of each gene to the bacterial 16S rRNA gene copies g_{ww}^{-1} of sediment.

Results

Hydrology and hydrochemistry of the Schönbrunnen

Nitrate concentrations in Schönbrunnen stream water and the alluvial aquifer were repeatedly measured over several years, and a representative set of water chemistry data

corresponding to our sampling season is shown in Fig. 2B. Nitrate was generally highest in the northwestern, most upstream section of the Schönbrunnen, with concentrations > 50 mg·L^{-1}, consistent with the intensive agricultural activities in this area. This was also reflected in highest nitrate concentrations (> 60 mg·L^{-1}) found in the surrounding groundwater monitoring wells of the northwestern hillslope. Interestingly, the high nitrate concentrations clearly decreased along the course of the Schönbrunnen, and were lowest (< 30 mg·L^{-1}) before the confluence with the Käsbach. At selected streambed locations, fine-scale depth-resolved pore water analyses of nitrate, nitrite and DOC were also conducted (Fig. S1). These data showed a strong decline of nitrate concentrations between 0 and 20 cm below the streambed, which was also the depth (~10-20 cm below streambed) where pore water DOC concentrations were highest (Fig. S1).

In contrast to nitrate concentrations, sulfate concentrations in the stream increased over the Schönbrunnen reaches, with concentrations > 200 mg L^{-1} at the confluence (Fig. 2C). Sulfate concentrations were generally lower in groundwater from the northwestern hillslope, but higher in eastern groundwater (> 1200 mg·L^{-1}) in between Käsbach and Schönbrunnen, an indicative of groundwater influenced by gypsum dissolution flowing from the east. The ditch upstream of R1 was also characterized by elevated sulfate concentrations (> 170 mg L^{-1}, Fig. 2C), indicative of sulfate-rich groundwater entering the stream in this upstream gaining section.

Bacterial communities in streambed sediments

Triplicate sampling of sediment microbial communities was done in three major sections of the Schönbrunnen, two upstream locations (*Up-A* and *Up-B*; further upstream of R1), two in the midstream losing sections (*Mid-A*; R3. *Mid-B*; Boundary of R3-R4), as well as one location each in the downstream gaining section (*Down*; Boundary of R6) and directly after the confluence with the Käsbach (*Conf*). For all sampling locations, full-length 16S

rRNA gene amplicon sequencing was done at 5 and 15 cm depths corresponding to the nitrate reduction zone (Fig. S1). Alpha diversity indices were similar ($H' = 5.27 \pm 0.88$) across all sediment samples taken along the Schönbrunnen (Fig. 3), whereas confluence samples displayed a significantly lower diversity both at 5 and at 15 cm depth (Dunn's Kruskal-Wallis, $p < 0.01$). Samples from *Up-A* and the two midstream locations showed greater Evenness (J') (Dunn's Kruskal-Wallis, $p < 0.05$) than the confluence samples. Depth had no consistent effect on diversity indices, although some significant differences were observed for specific locations. E.g., *Up-A* 5 cm samples showed a higher Shannon diversity (Dunn's Kruskal-Wallis, $p < 0.01$) than corresponding 15 cm samples.

Hierarchical clustering of Bray-Curtis dissimilarities between samples revealed three major clusters (Fig. 4). Samples from the confluence formed a disparate cluster, connoting that taxonomic composition was distinct here from all other samples. A second, major cluster mainly comprised samples from 5 cm depth, as well as one set of 15 cm samples (*Mid-B*). The majority of the third cluster were samples from 15 cm depth, plus one set of shallow depth samples from *Mid-A*. Generally, triplicate (or duplicate) libraries always grouped closely, except for one replicate of the *Down* 5 cm site, which was more similar to the *Mid-B* 15 cm samples, possibly reflecting small-scale local heterogeneities of the sampled streambed.

The 9024 unique ASVs identified could be assigned to 55 phyla (Table S5). All samples were dominated by three phyla, *Proteobacteria* (2173 ASVs), *Bacteroidota* (1125 ASVs), and *Acidobacteriota* (1160 ASVs), which all together accounted for up to ~50% of each library. In total, 429 families were assigned. *Nitrosomonadaceae* (216 ASVs), *Chitinophagaceae* (187 ASVs), and *Vicinamibacteraceae* (391 ASVs) appeared as the most abundant families within those three dominant phyla, respectively, accounting for ~10% relative abundance of the respective phylum on average. *Chitinophagaceae* were generally more abundant in 5 cm samples, while *Nitrosomonadaceae* were mostly more abundant in 15

cm samples, especially mid- and down- stream. Additional to these phyla, the *Sulfurimonadaceae* (phylum *Campilobacterota*) were the most abundant family (mean relative abundance 3.5%), especially in 5 cm samples taken midstream and at the confluence. From up- to down- stream and the confluence, 12% (1083 ASVs) of all ASVs belonging to 167 families were shared between at least five out of the six sampling locations (Fig. S2A). As for the five locations within the Schönbrunnen, 793 ASVs were presented from up- to downstream. The samples from 5 cm generally shared a greater number of common ASVs than samples from 15 cm depth (Figs. S2B & S2C).

Differences in bacterial community structure along the Schönbrunnen were further investigated via non-metric multidimensional scaling (NMDS) and similarity percentage (SIMPER) analyses (Fig. 5). The 5 cm samples generally featured a higher abundance of typical heterotrophic, aerobic or facultative anaerobic microbial lineages. These included *Rhodanobacteraceae* (dominated by *Ahniella* spp.), *Rhodobacteraceae* (dominated by *Rhodobacter* and *Tabrizicola* spp.), *Microscillaceae* (dominated by *Chryseolinea* spp.), *Xanthomonadaceae* (dominated by *Arenimonas* spp.), *Chitinophagaceae* (dominated by *Dinghuibacter* and *Terrimonas* spp.) and the *Saprospiraceae*. Members of the *Rhodocyclaceae* were also particularly abundant in 5 cm samples taken from *Up-B* and *Mid-B* (~2-3 %), mainly including reads associated with *Denitratisoma*, *Dechloromonas*, and *Rhodocyclus* spp. (Fig. 6). However, samples from 5 cm depth of *Up-A*, *Mid-A* and *Down* also featured taxa similarly abundant at 15 cm depth of *Mid-B*. These included the *Nitrosomonadaceae* (~3%) and *Nitrospiraceae* (~1%). In contrast, the dissimilarity of bacterial communities observed in other samples from 15 cm depth was mainly driven by typical anaerobic or microaerophilic lineages. This included typical fermenters (*Anaerolineaceae*, *Anaerovoracaceae*, *Clostridiaceae*, and *Prevotellaceae*), potential sulfate reducers (*Desulfobaccaceae*, *Thermodesulfovibrionia*), but also potential iron-oxidizing

bacteria within the *Gallionellaceae* (*Sideroxydans* spp.). The confluence samples were clearly distinguished from the other Schönbrunnen samples. Taxa typical for inorganic sulfide- and sulfur-oxidation (*Sulfuricellaceae, Sulfurimonadaceae,* and *Thiobacillus* spp. within the *Hydrogenophilaceae*) were among the major drivers of dissimilarity between those samples. Moreover, *Flavobacteriaceae* (*Flavobacterium* spp.) and *Comamonadaceae* (*Rhizobacter* spp.) were also relevant for the separation of confluence samples and others.

Typical sulfur-oxidizing bacteria (SOB) were rather abundant throughout the Schönbrunnen sediments, not only at the confluence (Fig. 4). Consider their potential role in linking sulfur and nitrogen cycling in the streambed, the distribution at ASV-level was further investigated, facilitated by the high resolution of full-length 16S amplicon reads. We specifically focused on ASVs within two dominating genera, *Sulfuricurvum* spp. (relative abundance up to 14.79%) and *Thiobacillus* spp. (relative abundance up to ~5.6%). *Sulfuricurvum* spp. was the only taxon within the *Sulfurimonadaceae* detected in this study. *Thiobacillus* spp. (73 ASVs; took up 99.88% of the family *Hydrogenophilaceae*) and unclassified *Hydrogenophilaceae* (2 ASVs; took up 0.12% of the family *Hydrogenophilaceae*) were genera detected within *Hydrogenophilaceae*. In total, 65 ASVs were identified within the genus *Sulfuricurvum*, including 34 of them were only detected within Schönbrunnen samples, such as the most dominant ASV9 (relative abundance up to ~1.99%) (Fig. 7A). However, also ASVs exclusive to the confluence samples, especially ASV2 and ASV8 (relative abundance up to 3.71% and 3.23%, respectively), were found.

Another typical sulfur-oxidizing lineage detected was *Thiobacillus*. Here, out of 73 ASVs detected in total (Fig. 7B), only two ASVs appeared specifically enriched at the confluence, ASV19 (relative abundance up to ~1.26%) and ASV127 (relative abundance up to ~0.61%). In the Schönbrunnen streambed, ASV3 (relative abundance up to ~1.12%) and ASV291 (relative abundance up to ~0.33%) were relatively more abundant. For further

context on the detected ASVs, ASVs within both *Sulfuricurvum* spp. and *Thiobacillus* spp. were embedded in phylogenetic dendrograms (Figs. 8A & 8B). The phylogenetic tree of *Sulfuricurvum* spp. revealed, that Schönbrunnen and confluence ASVs were separated into two distinct clusters (nominal Schönbrunnen cluster and Käsbach cluster) (Fig. 8A). The phylogenetic tree of *Thiobacillus* spp. suggested, that Schönbrunnen and confluence ASVs of *Thiobacillus* spp. were closely related to *Thiobacillus thioparus*, whereas ASV19 and ASV291 were more related to *Thiobacillus thiophilus* and *Thiobacillus denitrificans*, respectively (Fig. 8B).

Streambed community assembly

To investigate the potential impact of hydrologic turnover on bacterial communities in the streambed, the β-nearest taxon (β-NTI) and RC_{bray} indices were inferred. The importance of deterministic versus stochastic microbial community assembly can thus be estimated (Stegen et al., 2013, 2012). For our samples, over half of pairwise comparisons resulted in β-NTI values > 2, significantly different from the expectation of the null model (Fig. 9). This indicated that community assembly of Schönbrunnen sediments was largely triggered by deterministic variable selection. A $|\beta\text{-NTI}|$ index < 2 generally suggests that a pair of samples is likely to be selected by stochastic processes. The RC_{bray} index was calculated to further delineate these patterns. An RC_{bray} index < -0.95 or > 0.95 indicates that two samples are sharing more ASVs or less ASVs than expected, respectively. We assume that homogenizing dispersal could be relevant between samples from 5 cm and 15 cm of the same sampling location, depending on the local hydraulic conditions. Indeed, a homogenizing dispersal was suggested at *Up-A* and *Mid-A* sampling spots. Moreover, a longitudinal homogenizing dispersal was observed between 5 cm samples of *Up-A* and *Mid-A*, and between 15 cm samples of *Mid-A* and *Down*.

Quantification of denitrifying communities

In addition to 16S rRNA gene amplicon sequencing, we also quantified absolute abundances of bacterial 16S rRNA and nitrite reduction genes, indicative of denitrifying communities, along the Schönbrunnen. Bacterial 16S rRNA genes ranged from $9.1 \pm 2.5 \times 10^6$ to $9 \pm 0.8 \times 10^7$ copies g_{ww}^{-1} of sediment (Fig. 10A). *nirK* genes were more abundant than *nirS* across all samples, ranging from $2.2 \pm 1.2 \times 10^5$ to $5.3 \pm 2.5 \times 10^6$ copies g_{ww}^{-1} of sediment. The abundance of bacterial 16S rRNA genes was positively correlated with the abundance of *nirK* ($r = 0.791$, $p < 0.001$; Pearson's) and *nirS* ($r = 0.909$, $p < 0.001$; Pearson's) genes. A notable increase in relative abundance of *nirK* genes to up to ~10% of total bacterial 16S rRNA gene counts was observed from upstream to downstream samples, especially at 15 cm depth (Fig. 10B). A similar but less pronounced positive linear relationship ($p < 0.05$, Adjusted $R^2 = 0.235$) was noted between relative abundance of *nirK* and geodesic distance of the sampling locations from upstream to confluence.

Discussion

In this study, we comprehensively interrogate sediment microbial community structure of the Schönbrunnen, an agriculturally impacted first-order stream. We differentiate microbes in sections of the streambed where seasonal bidirectional gaining and losing fluxes are occurring. We propose that the demonstrated longitudinal and vertical heterogeneity of streambed microbial communities and the distribution of distinct functional capacities were impacted by this specific hydrologic setting. Here, we discuss the evidence supporting these conclusions, as well as the implications for our understanding of the reactivity of lower-order streams.

Bidirectional water exchange as a control of water chemistry and streambed bacterial communities

The influence of bidirectional water exchange on the biogeochemistry of lower-order streams may represent an under-regarded mechanism for the control of solute fluxes in headwater catchments (Trauth et al., 2018; Zarnetske et al., 2011). Our hydrological analyses mainly delineate six successive reaches, of which especially the midstream R3 was identified as net losing reach. It has been proposed that such losing reaches could represent reactive hot-spots for denitrification along infiltrating flow paths (Trauth et al., 2018). Under losing conditions, microbial denitrification will largely depend on sediment-borne electron donors or on DOC that is still available after oxygen depletion from the infiltrating stream water. Water leaving the Schönbrunnen through midstream losing sections may not directly return to the stream, or only after a long travel distance and mixing with the surrounding groundwater. Therefore, stream and groundwater mixing is not likely to happen in the first few decimeters of the flowpath. This differentiates the hydrologic setting from typical hyporheic flow, defined as flowpaths that originate and end in the stream over short distances, mainly induced by complex streambed morphology (Hester et al., 2013).

However, if nitrate reduction is largely associated with infiltrating water fluxes, nitrate concentrations in the losing section (e.g. midstream) should remain relatively constant. This was observed in our study (Fig. 2B), and instream nitrate concentrations only gradually decreased in downstream gaining reaches (R5 and R6), where adjacent groundwater depleted in nitrate (Fig. S1) and enriched in sulfate (and likely also sulfide or other reduced sulfur species) entered the Schönbrunnen. Under gaining scenarios, mixing of groundwater and reduced solutes with the stream water in the upper streambed should thus result in a distinct reactivity compared to spots of stream water infiltration. Over the Schönbrunnen longitudinal profile, nitrate concentrations appeared negatively correlated with that of sulfate, indicating that sulfur and nitrogen cycling in downstream gaining reaches were possibly linked.

We propose that bidirectional water exchange fluxes not only affected water chemistry, but also shaped streambed bacterial communities. The high spatial variability of abiotic factors that determined the local presence and relative abundance of microbial taxa should be apparent in strong deterministic variable selection patterns (Dini-Andreote et al., 2015) along the Schönbrunnen stream. In accordance, microbial communities in top sediments of the Schönbrunnen mostly showed high ßNTI values (> 2), suggesting strong variable selection (Stegen et al., 2013). This was consistent with previous studies on river sediment bacterial community assembly processes (Danczak et al., 2016; Graham et al., 2017). However, dispersal-based stochastic processes, especially homogenizing dispersal processes ($RC_{Bray} < -0.95$), were found in samples from typical gaining reaches (e.g. *up-A*, and *down*). Homogenizing dispersal patterns can be an indicator of actual physical transport of organisms (Stegen et al., 2016) and thus could indicate the impact of groundwater exfiltration under the specific hydrologic setting of Schönbrunnen. Homogenizing dispersal patterns were also observed at *Mid-A*, which was located in reach R3 predominated by net losing condition according to the groundwater heads (Figs. 2A & 9). However, several lines of circumstantial evidence indicate that *Mid-A* was impacted by local exfiltration fluxes of groundwater, similar to upstream and downstream samples. On the one hand, bidirectional gross fluxes are likely in all reaches. Tracer tests showed that the gaining and losing water fluxes in R3 could be very similar (Figure 2A). On the other hand, the *Mid-A* 5 cm samples showed similar bacterial community composition as other 15 cm samples, whereas *Mid-B* appeared more representative of the generally losing conditions in this reach (Fig. 4). Moreover, the presence of a greater abundance of ASVs affiliated with *Sulfuricurvum* spp. was also observed at *up-A*, and *down*, two obvious groundwater exfiltration spots.

Dispersal-based assembly processes can lead to rather maladapted local communities and can therefore restrict the biogeochemical potentials and functional stability of specific

communities (Graham and Stegen, 2017). However, in our study, dispersal-based assembly processes were found at locations dominated by exfiltration, in concert with a high abundance of sulfur-oxidizing and autotrophic nitrate reduction bacteria. Thus, chemolithoautotrophic nitrate reduction communities (i.e. sulfur-oxidizing bacteria) and autotrophic nitrate reduction mechanisms rather than canonical denitrification processes might actually be prioritized at groundwater exfiltration sections. Such fine-scale heterogeneities in exchange fluxes and microbial community structure in streambed sediments have not been reported to date, but may become relevant indicators of streambed reactivity *in situ*.

Microbial communities potentially involved in nitrate reduction

Our data suggest that distinct mechanisms could be driving microbial nitrate reduction in different sections of the Schönbrunnen. Firstly, the losing section appeared to be associated with heterotrophic denitrification in the streambed. Although absolute or relative abundances of denitrification genes were not highest in this section (Fig. 10), respective sediment communities (especially in *Mid-B*) were clearly enriched in typical canonical heterotrophic denitrifier lineages. These included members of the *Rhodobacteraceae* (Tarhriz et al., 2013; Tosques et al., 1997), *Flavobacteriaceae* (Tekedar et al., 2017), *Comamonadaceae* (Khan et al., 2002; Wang and Chu, 2016), *Rhodocyclaceae* (Fahrbach et al., 2006), all known to host typical *nirK*- or *nirS*-carrying denitrifiers. The abundance of these potential denitrifiers, especially the *Rhodocyclaceae*, was increased in 5 cm depths of *Up-B* and *Mid-B*, whereas the relative abundance of potential sulfur associated autotrophic nitrate reducers, including *Sulfuricurvum* and *Thiobacillus* (Beller et al., 2006; Kodama and Watanabe, 2004), was relatively low here (Figs. 6 & 7). Dominant genera within the *Rhodocyclaceae* were well-known denitrifiers such as *Denitratisoma, Dechloromonas* (Fahrbach et al., 2006; Horn et al., 2005), as well as *Rhodocyclus* spp. (Tang et al., 2020). In turn, potential sulfur-driven nitrate reducing populations were more abundant in groundwater exfiltration locations, such as *Up-A*,

Mid-A, and *Down*. The phylogenetic tree for *Sulfuricurvum* spp. revealed two major clusters of ASVs distributed between Schönbrunnen and Käsbach (Fig. 8A). Species-level taxonomy of *Sulfuricurvum* spp. reads was not fully resolved, due to the existence of only few pure culture isolates (Fida et al., 2021; Han et al., 2012; Kodama and Watanabe, 2004; Li et al., 2019). Even though the Schönbrunnen cluster was mostly related to *Sulfuricurvum kujiense* (Kodama and Watanabe, 2004), the Käsbach cluster did not include any previously reported *Sulfuricurvum* isolates. The currently known *Sulfuricurvum* strains are known for respiratory reduction of nitrate, but not of nitrite (Fida et al., 2021).

In addition, the ASVs of another typical sulfide- and sulfur-oxidizer, *Thiobacillus* spp. (*Hydrogenophilaceae*), were widespread in both Schönbrunnen and confluence sediments. Currently, three species have been described within the genus, *T. thioparus, T. thiophilus*, and *T. denitrificans* (Boden et al., 2017). *T. denitrificans* is a well-defined denitrifier and carrying *nirS* genes (Beller et al., 2006). *T. thioparus* and *T. thiophilus* may perform only partial denitrification, reducing nitrate to nitrite (Hutt et al., 2017; Kellerman and Griebler, 2009). Thus, both, the detected *Sulfuricurvum* and *Thiobacillus* spp. could have contributed to a sulfide- and/or other sulfur species driven nitrate reduction, especially in gaining conditions impacted streambed.

It has been previously proposed that the infiltration of stream water rich in nitrate and organic carbon may trigger heterotrophic denitrification in streambeds, whereas the exfiltration of reduced groundwater could prioritize autotrophic denitrifiers and DNRA (Graham et al., 2017; Storey et al., 2004). While high ratios between organic carbon and nitrate are known to generally trigger DNRA (Wang et al., 2020), also high sulfides levels in aquatic environments may favor this process (Delgado Vela et al., 2020). DNRA was reported to dominate over denitrification in salt marsh sediments amended with 100 µM sulfide (Murphy et al., 2020). Although sulfide was not routinely measured in our regular field

sampling across the Schönbrunnen catchment during our study, total sulfide concentrations measured in sediments in a following year reached values of ~50 µM at a depth of 2 cm (data not shown). Apart from such exemplary porewater measurements, groundwater from the southeastern monitoring wells (e.g. GWS 25) clearly smelled sulfidic upon sampling.

Apart from *Sulfuricurvum* spp., several other lineages detected in our libraries are also known for DNRA, such as *Geobacter* spp. (van den Berg et al., 2017), members of the *Desulfocapsaceae* (Arshad et al., 2017; Bell et al., 2020), or *Sulfurimonas* spp. (Bell et al., 2020). Generally, *nirK*-carrying denitrifiers have a greater probability of harboring a respiratory DNRA pathway (*Nrf*A) as well, while *nirS*-carrying nitrate reducers are more likely to perform complete denitrification (Helen et al., 2016). Despite some bacteria can carry both *nirK* or *nirS* genes, most known nitrate reducers only have one copy of either of the two genes (Etchebehere and Tiedje, 2005; Graf et al., 2014).

PacBio long-read sequencing to dissect sediment microbial communities at high resolution

PacBio long-read sequencing of full-length 16S rRNA gene amplicons provided us with a valuable opportunity in this study to dissect sediment bacterial communities at a robust and taxonomically informative ASV-level (Lam et al., 2020). In contrast to the more widely used short Illumina reads, long-read ASVs can likely be resolved beyond the genus level (Callahan et al., 2017). As exemplified for the species-level resolution for ASVs of sulfur-oxidizing populations here, this may well be relevant to assess spatial patterns in investigated populations and to infer their potential impact on streambed biogeochemistry. Although 16S rRNA genes affiliation can clearly only be an indicator, not a diagnostic for actual process relevance within environmental microbiomes, functionally relevant context like a reliable differentiation between *T. denitrificans* and other *Thiobacillus*–related ASVs would not have been possible using shorter reads. Though PacBio long-read sequencing does not produce

comparable amounts of total sequencing output as other platforms, it can offer comparable biodiversity coverage for more frequent taxa (Lam et al., 2020). As shown here, this may be relevant for the functional interpretation of environmental amplicon datasets.

Conclusion

In this study, we show that bidirectional water exchange between an agricultural first-order stream and the surrounding alluvial aquifer is important not only for stream water chemistry, but also for sediment microbial populations and their presumed activities in attenuating agricultural solute inputs. By disentangling the stream into gaining and losing sections, we show that sediment microbial community assembly was mostly dominated by deterministic heterogeneous processes, except for zones of the streambed strongly influenced by groundwater exfiltration. Such gaining spots were associated with an enrichment of typical sulfur-oxidizing lineages, indicative of possibly ongoing sulfur-driven autotrophic nitrate attenuation processes. In contrast, canonical heterotrophic denitrifying populations were more abundant in midstream losing reaches of the Schönbrunnen. Our study thus advances the current understanding of the reactivity of lower-order streams towards incoming agricultural pollutants, which is important for stream management and restoration, as well as for the prediction of watershed-level pollutant attenuation and water quality in river networks.

Acknowledgements

This study was supported by collaborative research project 1253 CAMPOS (Project 2: Sub-Catchemnts), funded by the German Research Foundation (DFG, Grant agreement SFB 1253/1). We thank Research Unit for Comparative Microbiome Analyses at the Helmholtz Zentrum München for providing laboratory and computing resources, especially Susanne Kublik and Dr. Silvia Gschwendtner for technical support on PacBio Sequel sequencing. We

additionally thank Gabriele Barthel for assistance during field sampling, and Dr. Lucas Fillinger (Univ. Vienna) for constructive feedback on the manuscript.

References

Agarwala, R., Barrett, T., Beck, J., Benson, D.A., Bollin, C., Bolton, E., Bourexis, D., Brister, J.R., Bryant, S.H., Canese, K., Cavanaugh, M., Charowhas, C., Clark, K., Dondoshansky, I., Feolo, M., Fitzpatrick, L., Funk, K., Geer, L.Y., Gorelenkov, V., Graeff, A., Hlavina, W., Holmes, B., Johnson, M., Kattman, B., Khotomlianski, V., Kimchi, A., Kimelman, M., Kimura, M., Kitts, P., Klimke, W., Kotliarov, A., Krasnov, S., Kuznetsov, A., Landrum, M.J., Landsman, D., Lathrop, S., Lee, J.M., Leubsdorf, C., Lu, Z., Madden, T.L., Marchler-Bauer, A., Malheiro, A., Meric, P., Karsch-Mizrachi, I., Mnev, A., Murphy, T., Orris, R., Ostell, J., O'Sullivan, C., Palanigobu, V., Panchenko, A.R., Phan, L., Pierov, B., Pruitt, K.D., Rodarmer, K., Sayers, E.W., Schneider, V., Schoch, C.L., Schuler, G.D., Sherry, S.T., Siyan, K., Soboleva, A., Soussov, V., Starchenko, G., Tatusova, T.A., Thibaud-Nissen, F., Todorov, K., Trawick, B.W., Vakatov, D., Ward, M., Yaschenko, E., Zasypkin, A., Zbicz, K., 2018. Database resources of the National Center for Biotechnology Information. Nucleic Acids Res. 46. https://doi.org/10.1093/nar/gkx1095

Agrometeorology of Baden-Württemberg, 2017. Agrarmeteorologie Baden-Württemberg [WWW Document]. URL https://www.wetter-bw.de/Agrarmeteorologie-BW/Wetterdaten/Stationskarte

Arshad, A., Dalcin Martins, P., Frank, J., Jetten, M.S.M., Op den Camp, H.J.M., Welte, C.U., 2017. Mimicking microbial interactions under nitrate-reducing conditions in an anoxic bioreactor: enrichment of novel Nitrospirae bacteria distantly related to Thermodesulfovibrio. Environ. Microbiol. 19, 4965–4977. https://doi.org/10.1111/1462-2920.13977

Battin, T.J., Kaplan, L.A., Findlay, S., Hopkinson, C.S., Marti, E., Packman, A.I., Newbold, J.D., Sabater, F., 2008. Biophysical controls on organic carbon fluxes in fluvial networks. Nat. Geosci. 1, 95–100.

Bell, E., Lamminmäki, T., Alneberg, J., Andersson, A.F., Qian, C., Xiong, W., Hettich, R.L., Frutschi, M., Bernier-Latmani, R., 2020. Active sulfur cycling in the terrestrial deep subsurface. ISME J. 14, 1260–1272. https://doi.org/10.1038/s41396-020-0602-x

Beller, H.R., Chain, P.S.G., Letain, T.E., Chakicherla, A., Larimer, F.W., Richardson, P.M., Coleman, M.A., Wood, A.P., Kelly, D.P., 2006. The genome sequence of the obligately chemolithoautotrophic, facultatively anaerobic bacterium Thiobacillus denitrificans. J. Bacteriol. 188. https://doi.org/10.1128/JB.188.4.1473-1488.2006

Boano, F., Harvey, J.W., Marion, A., Packman, A.I., Revelli, R., Ridolfi, L., Wörman, A., 2014. Hyporheic flow and transport processes: Mechanisms, models, and biogeochemical implications. Rev. Geophys. https://doi.org/10.1002/2012RG000417

Boden, R., Hutt, L.P., Rae, A.W., 2017. Reclassification of Thiobacillus aquaesulis (Wood & Kelly, 1995) as Annwoodia aquaesulis gen. nov., comb. nov., transfer of Thiobacillus

(Beijerinck, 1904) from the Hydrogenophilales to the Nitrosomonadales, proposal of Hydrogenophilalia class. nov. withi. Int. J. Syst. Evol. Microbiol. 67, 1191–1205. https://doi.org/10.1099/ijsem.0.001927

Callahan, B.J., McMurdie, P.J., Holmes, S.P., 2017. Exact sequence variants should replace operational taxonomic units in marker-gene data analysis. ISME J. 11. https://doi.org/10.1038/ismej.2017.119

Callahan, B.J., Wong, J., Heiner, C., Oh, S., Theriot, C.M., Gulati, A.S., McGill, S.K., Dougherty, M.K., 2019. High-throughput amplicon sequencing of the full-length 16S rRNA gene with single-nucleotide resolution. Nucleic Acids Res. 47. https://doi.org/10.1093/nar/gkz569

Cameron, E.S., Schmidt, P.J., Tremblay, B.J.M., Emelko, M.B., Müller, K.M., 2020. To rarefy or not to rarefy: Enhancing microbial community analysis through next-generation sequencing. bioRxiv. https://doi.org/10.1101/2020.09.09.290049

Chase, J.M., Myers, J.A., 2011. Disentangling the importance of ecological niches from stochastic processes across scales. Philos. Trans. R. Soc. B Biol. Sci. 366. https://doi.org/10.1098/rstb.2011.0063

Chen, I.M.A., Chu, K., Palaniappan, K., Pillay, M., Ratner, A., Huang, J., Huntemann, M., Varghese, N., White, J.R., Seshadri, R., Smirnova, T., Kirton, E., Jungbluth, S.P., Woyke, T., Eloe-Fadrosh, E.A., Ivanova, N.N., Kyrpides, N.C., 2019. IMG/M v.5.0: An integrated data management and comparative analysis system for microbial genomes and microbiomes. Nucleic Acids Res. 47. https://doi.org/10.1093/nar/gky901

Covino, T.P., McGlynn, B.L., 2007. Stream gains and losses across a mountain-to-valley transition: Impacts on watershed hydrology and stream water chemistry. Water Resour. Res. 43. https://doi.org/10.1029/2006WR005544

Crump, B.C., Hopkinson, C.S., Sogin, M.L., Hobbie, J.E., 2004. Microbial Biogeography along an Estuarine Salinity Gradient: Combined Influences of Bacterial Growth and Residence Time. Appl. Environ. Microbiol. 70. https://doi.org/10.1128/AEM.70.3.1494-1505.2004

D'Affonseca, F.M., Finkel, M., Cirpka, O.A., 2020. Combining implicit geological modeling, field surveys, and hydrogeological modeling to describe groundwater flow in a karst aquifer. Hydrogeol. J. 28. https://doi.org/10.1007/s10040-020-02220-z

Danczak, R.E., Sawyer, A.H., Williams, K.H., Stegen, J.C., Hobson, C., Wilkins, M.J., 2016. Seasonal hyporheic dynamics control coupled microbiology and geochemistry in Colorado River sediments. J. Geophys. Res. Biogeosciences 121, 2976–2987. https://doi.org/10.1002/2016JG003527

Delgado Vela, J., Bristow, L.A., Marchant, H.K., Love, N.G., Dick, G.J., 2020. Sulfide alters microbial functional potential in a methane and nitrogen cycling biofilm reactor. Environ. Microbiol. 0–2. https://doi.org/10.1111/1462-2920.15352

Dini-Andreote, F., Stegen, J.C., Van Elsas, J.D., Salles, J.F., 2015. Disentangling mechanisms that mediate the balance between stochastic and deterministic processes in microbial succession. Proc. Natl. Acad. Sci. U. S. A. 112, E1326–E1332. https://doi.org/10.1073/pnas.1414261112

Duff, J.H., Murphy, F., Fuller, C.C., Triska, F.J., 1998. A mini drivepoint sampler for measuring pore water solute concentrations in the hyporheic zone of sand-bottom

streams. Limnol. Oceanogr. 43. https://doi.org/10.4319/lo.1998.43.6.1378

Etchebehere, C., Tiedje, J., 2005. Presence of two different active nirS nitrite reductase genes in a denitrifying Thauera sp. from a high-nitrate-removal-rate reactor. Appl. Environ. Microbiol. 71. https://doi.org/10.1128/AEM.71.9.5642-5645.2005

Fahrbach, M., Kuever, J., Meinke, R., Kämpfer, P., Hollender, J., 2006. Denitratisoma oestradiolicum gen. nov., sp. nov., a 17 β-oestradiol-degrading, denitrifying betaproteobacterium. Int. J. Syst. Evol. Microbiol. 56, 1547–1552. https://doi.org/10.1099/ijs.0.63672-0

Fida, T.T., Sharma, M., Shen, Y., Voordouw, G., 2021. Microbial sulfite oxidation coupled to nitrate reduction in makeup water for oil production. Chemosphere 284. https://doi.org/10.1016/j.chemosphere.2021.131298

Ginestet, C., 2011. ggplot2: Elegant Graphics for Data Analysis. J. R. Stat. Soc. Ser. A (Statistics Soc. 174. https://doi.org/10.1111/j.1467-985x.2010.00676_9.x

Gomez-Velez, J.D., Harvey, J.W., Cardenas, M.B., Kiel, B., 2015. Denitrification in the Mississippi River network controlled by flow through river bedforms. Nat. Geosci. 8. https://doi.org/10.1038/ngeo2567

Gooseff, M.N., McKnight, D.M., Runkel, R.L., Duff, J.H., 2004. Denitrification and hydrologic transient storage in a glacial meltwater stream, McMurdo Dry Valleys, Antarctica. Limnol. Oceanogr. 49. https://doi.org/10.4319/lo.2004.49.5.1884

Graf, D.R.H., Jones, C.M., Hallin, S., 2014. Intergenomic comparisons highlight modularity of the denitrification pathway and underpin the importance of community structure for N2O emissions. PLoS One 9. https://doi.org/10.1371/journal.pone.0114118

Graham, E.B., Crump, A.R., Resch, C.T., Fansler, S., Arntzen, E., Kennedy, D.W., Fredrickson, J.K., Stegen, J.C., 2017. Deterministic influences exceed dispersal effects on hydrologically-connected microbiomes. Environ. Microbiol. 19. https://doi.org/10.1111/1462-2920.13720

Graham, E.B., Stegen, J.C., 2017. Dispersal-based microbial community assembly decreases biogeochemical function. Processes 5. https://doi.org/10.3390/pr5040065

Gu, Z., Eils, R., Schlesner, M., 2016. Complex heatmaps reveal patterns and correlations in multidimensional genomic data. Bioinformatics 32. https://doi.org/10.1093/bioinformatics/btw313

Han, C., Kotsyurbenko, O., Chertkov, O., Held, B., Lapidus, A., Nolan, M., Lucas, S., Hammon, N., Deshpande, S., Cheng, J.F., Tapia, R., Goodwin, L., Pitluck, S., Liolios, K., Pagani, I., Ivanova, N., Mavromatis, K., Mikhailova, N., Pati, A., Chen, A., Palaniappan, K., Land, M., Hauser, L., Chang, Y. juan, Jeffries, C.D., Brambilla, E.M., Rohde, M., Spring, S., Sikorski, J., Göker, M., Woyke, T., Bristow, J., Eisen, J.A., Markowitz, V., Hugenholtz, P., Kyrpides, N.C., Klenk, H.P., Detter, J.C., 2012. Complete genome sequence of the sulfur compounds oxidizing chemolithoautotroph Sulfuricurvum kujiense type strain (YK-1 T). Stand. Genomic Sci. 6. https://doi.org/10.4056/sigs.2456004

Harvey, J.W., Böhlke, J.K., Voytek, M.A., Scott, D., Tobias, C.R., 2013. Hyporheic zone denitrification: Controls on effective reaction depth and contribution to whole-stream mass balance. Water Resour. Res. 49. https://doi.org/10.1002/wrcr.20492

Helen, D., Kim, H., Tytgat, B., Anne, W., 2016. Highly diverse nirK genes comprise two major clades that harbour ammonium-producing denitrifiers. BMC Genomics 17. https://doi.org/10.1186/s12864-016-2465-0

Hester, E.T., Young, K.I., Widdowson, M.A., 2013. Mixing of surface and groundwater induced by riverbed dunes: Implications for hyporheic zone definitions and pollutant reactions. Water Resour. Res. 49. https://doi.org/10.1002/wrcr.20399

Horn, M.A., Ihssen, J., Matthies, C., Schramm, A., Acker, G., Drake, H.L., 2005. Dechloromonas denitrificans sp. nov., Flavobacterium denitrificans sp. nov., Paenibacillus anaericanus sp. nov. and Paenibacillus terrae strain MH72, N2O-producing bacteria isolated from the gut of the earthworm Aporrectodea caliginosa. Int. J. Syst. Evol. Microbiol. 55, 1255–1265. https://doi.org/10.1099/ijs.0.63484-0

Horton, R.E., 1945. Erosional development of streams and their drainage basins; hydrophysical approach to quantitative morphology. Geol. Soc. Am. Bull. 56, 275–370.

Hullar, M.A.J., Kaplan, L.A., Stahl, D.A., 2006. Recurring seasonal dynamics of microbial communities in stream habitats. Appl. Environ. Microbiol. 72. https://doi.org/10.1128/AEM.72.1.713-722.2006

Hutt, L.P., Huntemann, M., Clum, A., Pillay, M., Palaniappan, K., Varghese, N., Mikhailova, N., Stamatis, D., Reddy, T., Daum, C., Shapiro, N., Ivanova, N., Kyrpides, N., Woyke, T., Boden, R., 2017. Permanent draft genome of Thiobacillus thioparus DSM 505T, an obligately chemolithoautotrophic member of the Betaproteobacteria. Stand. Genomic Sci. 12. https://doi.org/10.1186/s40793-017-0229-3

Jimenez-Fernandez, O., Schwientek, M., Osenbrück, K., Glaser, C., Schmidt, C., Fleckenstein, J.H., 2022. Groundwater-surface water exchange and hydrologic turnover as key controls for instream and groundwater nitrate concentrations in first-order agricultural stream catchments. Hydrol. Process. (resubmitted after revisions)

Kaandorp, V.P., de Louw, P.G.B., van der Velde, Y., Broers, H.P., 2018. Transient Groundwater Travel Time Distributions and Age-Ranked Storage-Discharge Relationships of Three Lowland Catchments. Water Resour. Res. 54. https://doi.org/10.1029/2017WR022461

Kassambara, A., 2020. ggpubr: “ggplot2” Based Publication Ready Plots. R Packag. version 0.4.0.

Kellerman, C., Griebler, C., 2009. Thiobacillus thiophilus sp. nov., a chemolithoautotrophic, thiosulfate-oxidizing bacterium isolated from contaminated aquifer sediments. Int. J. Syst. Evol. Microbiol. 59. https://doi.org/10.1099/ijs.0.002808-0

Kembel, S.W., Cowan, P.D., Helmus, M.R., Cornwell, W.K., Morlon, H., Ackerly, D.D., Blomberg, S.P., Webb, C.O., 2010. Picante: R tools for integrating phylogenies and ecology. Bioinformatics 26. https://doi.org/10.1093/bioinformatics/btq166

Khan, S.T., Horiba, Y., Yamamoto, M., Hiraishi, A., 2002. Members of the family Comamonadaceae as primary poly(3-hydroxybutyrate-co-3-hydroxyvalerate)-degrading denitrifiers in activated sludge as revealed by a polyphasic approach. Appl. Environ. Microbiol. 68, 3206–3214. https://doi.org/10.1128/AEM.68.7.3206-3214.2002

Kodama, Y., Watanabe, K., 2004. Sulfuricurvum kujiense gen. nov., sp. nov., a facultatively anaerobic, chemolithoautotrophic, sulfur-oxidizing bacterium isolated from an underground crude-oil storage cavity. Int. J. Syst. Evol. Microbiol. 54, 2297–2300.

https://doi.org/10.1099/ijs.0.63243-0

Krause, S., Hannah, D.M., Fleckenstein, J.H., Heppell, C.M., Kaeser, D., Pickup, R., Pinay, G., Robertson, A.L., Wood, P.J., 2011. Inter-disciplinary perspectives on processes in the hyporheic zone. Ecohydrology. https://doi.org/10.1002/eco.176

Kumar, S., Stecher, G., Li, M., Knyaz, C., Tamura, K., 2018. MEGA X: Molecular evolutionary genetics analysis across computing platforms. Mol. Biol. Evol. 35. https://doi.org/10.1093/molbev/msy096

Kuypers, M.M.M., Marchant, H.K., Kartal, B., 2018. The microbial nitrogen-cycling network. Nat. Rev. Microbiol. 16, 263–276. https://doi.org/10.1038/nrmicro.2018.9

Lam, T.Y.C., Mei, R., Wu, Z., Lee, P.K.H., Liu, W.T., Lee, P.H., 2020. Superior resolution characterisation of microbial diversity in anaerobic digesters using full-length 16S rRNA gene amplicon sequencing. Water Res. 178, 115815. https://doi.org/10.1016/j.watres.2020.115815

Letunic, I., Bork, P., 2019. Interactive Tree of Life (iTOL) v4: Recent updates and new developments. Nucleic Acids Res. 47. https://doi.org/10.1093/nar/gkz239

Li, C., 2020. GitHub - cxli233/customized_upset_plots [WWW Document]. https://doi.org/https://github.com/cxli233/customized_upset_plots

Li, X., Yang, Y., Zeng, X., Wang, J., Jin, H., Sheng, Z., Yan, J., 2019. Metagenome-Assembled Genome Sequence of Sulfuricurvum sp. Strain IAE1, Isolated from a 4-Chlorophenol-Degrading Consortium . Microbiol. Resour. Announc. 8. https://doi.org/10.1128/mra.00296-19

Liao, H., Yu, K., Duan, Y., Ning, Z., Li, B., He, L., Liu, C., 2019. Profiling microbial communities in a watershed undergoing intensive anthropogenic activities. Sci. Total Environ. 647, 1137–1147. https://doi.org/10.1016/j.scitotenv.2018.08.103

Lin, X., Kennedy, D., Fredrickson, J., Bjornstad, B., Konopka, A., 2012. Vertical stratification of subsurface microbial community composition across geological formations at the Hanford Site. Environ. Microbiol. 14. https://doi.org/10.1111/j.1462-2920.2011.02659.x

M Krassowski, 2020. ComplexUpset. [WWW Document]. https://doi.org/10.5281/zenodo.3700590

Mallard, J., McGlynn, B., Covino, T., 2014. Lateral inflows, stream-groundwater exchange, and network geometry influence stream water composition. Water Resour. Res. 50. https://doi.org/10.1002/2013WR014944

Martin, M., 2011. Cutadapt removes adapter sequences from high-throughput sequencing reads. EMBnet.journal 17. https://doi.org/10.14806/ej.17.1.200

McClain, M.E., Boyer, E.W., Dent, C.L., Gergel, S.E., Grimm, N.B., Groffman, P.M., Hart, S.C., Harvey, J.W., Johnston, C.A., Mayorga, E., 2003. Biogeochemical hot spots and hot moments at the interface of terrestrial and aquatic ecosystems. Ecosystems 301–312.

McMurdie, P.J., Holmes, S., 2014. Waste Not, Want Not: Why Rarefying Microbiome Data Is Inadmissible. PLoS Comput. Biol. 10. https://doi.org/10.1371/journal.pcbi.1003531

McMurdie, P.J., Holmes, S., 2013. Phyloseq: An R Package for Reproducible Interactive Analysis and Graphics of Microbiome Census Data. PLoS One 8.

https://doi.org/10.1371/journal.pone.0061217

Mulholland, P.J., Helton, A.M., Poole, G.C., Hall, R.O., Hamilton, S.K., Peterson, B.J., Tank, J.L., Ashkenas, L.R., Cooper, L.W., Dahm, C.N., Dodds, W.K., Findlay, S.E.G., Gregory, S. V., Grimm, N.B., Johnson, S.L., McDowell, W.H., Meyer, J.L., Valett, H.M., Webster, J.R., Arango, C.P., Beaulieu, J.J., Bernot, M.J., Burgin, A.J., Crenshaw, C.L., Johnson, L.T., Niederlehner, B.R., O'Brien, J.M., Potter, J.D., Sheibley, R.W., Sobota, D.J., Thomas, S.M., 2008. Stream denitrification across biomes and its response to anthropogenic nitrate loading. Nature 452. https://doi.org/10.1038/nature06686

Murphy, A.E., Bulseco, A.N., Ackerman, R., Vineis, J.H., Bowen, J.L., 2020. Sulphide addition favours respiratory ammonification (DNRA) over complete denitrification and alters the active microbial community in salt marsh sediments. Environ. Microbiol. 22, 2124–2139. https://doi.org/10.1111/1462-2920.14969

Needelman, B.A., Kleinman, P.J.A., Strock, J.S., Allen, A.L., 2007. Improved management of agricultural drainage ditches for water quality protection: An overview. J. Soil Water Conserv.

Oksanen, J., Blanchet, F.G., Friendly, M., Kindt, R., Legendre, P., Mcglinn, D., Minchin, P.R., O'hara, R.B., Simpson, G.L., Solymos, P., Henry, M., Stevens, H., Szoecs, E., Maintainer, H.W., 2019. vegan: Community Ecology Package. R package version 2.5-5. https://CRAN.R-project.org/package=vegan. Community Ecol. Packag. 2.

Peterson, B.J., Wollheim, W.M., Mulholland, P.J., Webster, J.R., Meyer, J.L., Tank, J.L., Marti, E., Bowden, W.B., Valett, H.M., Hershey, A.E., McDowell, W.H., Dodds, W.K., Hamilton, S.K., Gregory, S., Morrall, D.D., 2001. Control of nitrogen export from watersheds by headwater streams. Science (80-.). 292. https://doi.org/10.1126/science.1056874

Pilloni, G., Granitsiotis, M.S., Engel, M., Lueders, T., 2012. Testing the limits of 454 pyrotag sequencing: Reproducibility, quantitative assessment and comparison to T-RFLP fingerprinting of aquifer microbes. PLoS One 7. https://doi.org/10.1371/journal.pone.0040467

Price, M.N., Dehal, P.S., Arkin, A.P., 2009. Fasttree: Computing large minimum evolution trees with profiles instead of a distance matrix. Mol. Biol. Evol. 26. https://doi.org/10.1093/molbev/msp077

Quast, C., Pruesse, E., Yilmaz, P., Gerken, J., Schweer, T., Yarza, P., Peplies, J., Glöckner, F.O., 2013. The SILVA ribosomal RNA gene database project: Improved data processing and web-based tools. Nucleic Acids Res. 41. https://doi.org/10.1093/nar/gks1219

R Core Team, 2019. R: A language and environment for statistical computing. R Found. Stat. Comput.

Saup, C.M., Bryant, S.R., Nelson, A.R., Harris, K.D., Sawyer, A.H., Christensen, J.N., Tfaily, M.M., Williams, K.H., Wilkins, M.J., 2019. Hyporheic Zone Microbiome Assembly Is Linked to Dynamic Water Mixing Patterns in Snowmelt-Dominated Headwater Catchments. J. Geophys. Res. Biogeosciences 124, 3269–3280. https://doi.org/10.1029/2019JG005189

Scheidegger, A.E., 1965. The algebra of stream-order numbers. United States Geol. Surv. Prof. Pap. 525, 187–189.

Seitzinger, S.P., Styles, R. V., Boyer, E.W., Alexander, R.B., Billen, G., Howarth, R.W., Mayer, B., Van Breemen, N., 2002. Nitrogen retention in rivers: Model development and application to watersheds in the northeastern U.S.A., in: Biogeochemistry. https://doi.org/10.1023/A:1015745629794

Signorelli, A., 2020. DescTools: Tools for Descriptive Statistics. R package version 0.99.37. Cran.

Smith, L.K., Voytek, M.A., Böhlke, J.K., Harvey, J.W., 2006. Denitrification in nitrate-rich streams: Application of N2:Ar and 15N-tracer methods in intact cores. Ecol. Appl. 16. https://doi.org/10.1890/1051-0761(2006)016[2191:DINSAO]2.0.CO;2

Starry, O.S., Valett, H.M., Schreiber, M.E., 2005. Nitrification rates in a headwater stream: Influences of seasonal variation in C and N supply. J. North Am. Benthol. Soc. 24, 753–768. https://doi.org/10.1899/05-015.1

Stegen, J.C., Fredrickson, J.K., Wilkins, M.J., Konopka, A.E., Nelson, W.C., Arntzen, E. V., Chrisler, W.B., Chu, R.K., Danczak, R.E., Fansler, S.J., Kennedy, D.W., Resch, C.T., Tfaily, M., 2016. Groundwater-surface water mixing shifts ecological assembly processes and stimulates organic carbon turnover. Nat. Commun. 7. https://doi.org/10.1038/ncomms11237

Stegen, J.C., Lin, X., Fredrickson, J.K., Chen, X., Kennedy, D.W., Murray, C.J., Rockhold, M.L., Konopka, A., 2013. Quantifying community assembly processes and identifying features that impose them. ISME J. 7, 2069–2079. https://doi.org/10.1038/ismej.2013.93

Stegen, J.C., Lin, X., Konopka, A.E., Fredrickson, J.K., 2012. Stochastic and deterministic assembly processes in subsurface microbial communities. ISME J. 6, 1653–1664. https://doi.org/10.1038/ismej.2012.22

Storey, R.G., Williams, D.D., Fulthorpe, R.R., 2004. Nitrogen processing in the hyporheic zone of a pastoral stream. Biogeochemistry 69. https://doi.org/10.1023/B:BIOG.0000031049.95805.ec

Tang, S., Liao, Y., Xu, Y., Dang, Z., Zhu, X., Ji, G., 2020. Microbial coupling mechanisms of nitrogen removal in constructed wetlands: A review. Bioresour. Technol. https://doi.org/10.1016/j.biortech.2020.123759

Tarhriz, V., Thiel, V., Nematzadeh, G., Hejazi, M.A., Imhoff, J.F., Hejazi, M.S., 2013. Tabrizicola aquatica gen. nov. sp. nov., a novel alphaproteobacterium isolated from Qurugöl Lake nearby Tabriz city, Iran. Antonie van Leeuwenhoek, Int. J. Gen. Mol. Microbiol. 104, 1205–1215. https://doi.org/10.1007/s10482-013-0042-y

Tekedar, H.C., Karsi, A., Reddy, J.S., Nho, S.W., Kalindamar, S., Lawrence, M.L., 2017. Comparative genomics and transcriptional analysis of Flavobacterium columnare strain ATCC 49512. Front. Microbiol. 8. https://doi.org/10.3389/fmicb.2017.00588

Tiedje, J.M., 1988. Ecology of denitrification and dissimilatory nitrate reduction to ammonium. Environ. Microbiol. Anaerobes.

Tosques, I.E., Kwiatkowski, A. V., Shi, J., Shapleigh, J.P., 1997. Characterization and regulation of the gene encoding nitrite reductase in Rhodobacter sphaeroides 2.4.3. J. Bacteriol. 179. https://doi.org/10.1128/jb.179.4.1090-1095.1997

Trauth, N., Musolff, A., Knöller, K., Kaden, U.S., Keller, T., Werban, U., Fleckenstein, J.H., 2018. River water infiltration enhances denitrification efficiency in riparian groundwater.

Water Res. 130, 185–199. https://doi.org/10.1016/j.watres.2017.11.058

van den Berg, E.M., Elisário, M.P., Kuenen, J.G., Kleerebezem, R., van Loosdrecht, M.C.M., 2017. Fermentative bacteria influence the competition between denitrifiers and DNRA bacteria. Front. Microbiol. 8, 1–13. https://doi.org/10.3389/fmicb.2017.01684

Wang, J., Chu, L., 2016. Biological nitrate removal from water and wastewater by solid-phase denitrification process. Biotechnol. Adv. https://doi.org/10.1016/j.biotechadv.2016.07.001

Wang, S., Pi, Y., Song, Y., Jiang, Y., Zhou, L., Liu, W., Zhu, G., 2020. Hotspot of dissimilatory nitrate reduction to ammonium (DNRA) process in freshwater sediments of riparian zones. Water Res. 173. https://doi.org/10.1016/j.watres.2020.115539

Wickham, H., Averick, M., Bryan, J., Chang, W., McGowan, L., François, R., Grolemund, G., Hayes, A., Henry, L., Hester, J., Kuhn, M., Pedersen, T., Miller, E., Bache, S., Müller, K., Ooms, J., Robinson, D., Seidel, D., Spinu, V., Takahashi, K., Vaughan, D., Wilke, C., Woo, K., Yutani, H., 2019. Welcome to the Tidyverse. J. Open Source Softw. 4. https://doi.org/10.21105/joss.01686

Winter, C., Hein, T., Kavka, G., Mach, R.L., Farnleitner, A.H., 2007. Longitudinal changes in the bacterial community composition of the Danube River: A whole-river approach. Appl. Environ. Microbiol. 73. https://doi.org/10.1128/AEM.01849-06

Wright, E.S., 2016. Using DECIPHER v2.0 to analyze big biological sequence data in R. R J. 8. https://doi.org/10.32614/rj-2016-025

Wright, E.S., 2015. DECIPHER: Harnessing local sequence context to improve protein multiple sequence alignment. BMC Bioinformatics 16. https://doi.org/10.1186/s12859-015-0749-z

Yu, L., Rozemeijer, J., Van Breukelen, B.M., Ouboter, M., Van Der Vlugt, C., Broers, H.P., 2018. Groundwater impacts on surface water quality and nutrient loads in lowland polder catchments: Monitoring the greater Amsterdam area. Hydrol. Earth Syst. Sci. 22. https://doi.org/10.5194/hess-22-487-2018

Zarnetske, J.P., Haggerty, R., Wondzell, S.M., Baker, M.A., 2011. Dynamics of nitrate production and removal as a function of residence time in the hyporheic zone. J. Geophys. Res. Biogeosciences 116. https://doi.org/10.1029/2010JG001356

Zhang, Z.-Y., Schmidt, C., Nixdorf, E., Kuang, X., Fleckenstein, J.H., 2021. Effects of Heterogeneous Stream-Groundwater Exchange on the Source Composition of Stream Discharge and Solute Load. Water Resour. Res. 57, e2020WR029079. https://doi.org/https://doi.org/10.1029/2020WR029079

Table 1: Water chemistry and hydrology of Schöbrunnen stream water and adjacent groundwater.

Sampling locations	Hydraulic conductivity K_f [m/s]	Q [L/s]	Water mixing		EC [µS/cm]	DOC [mg/L]	Na^+ [mg/L]	K^+ [mg/L]	Ca^{2+} [mg/L]	Mg^{2+} [mg/L]	NH_4^+ [mg/L]	NO_3^- [mg/L]	Cl^- [mg/L]	SO_4^{2-} [mg/L]
			% Stream	% GW										
Schönbrunnen stream														
Up-A	-	0.11	0	100	1032	1.2	4.6	1.4	168	45.3	0	59.0	18.8	191
Up-B	-	0.57	-	-	1015	1.4	5.0	1.6	162	46.0	0	60.5	18.2	179
Mid-A	-	-	-	-	-	-	-	-	-	-	-	-	-	-
Mid-B	-	0.31	88.1	11.9	930	1.7	4.8	1.6	143	46.7	0	58.9	17.9	179
Down	-	-	-	-	1099	1.0	7.8	2.5	179	45.0	0	42.0	27.3	237
Conf	-	-	-	-	2280	1.6	18.7	6.9	512	78.8	0	31.0	38.2	1123
Groundwater (GW)														
GWS 2	2.9E-04	-	-	-	1035	1.4	4.6	1.3	168	45.1	0	64.4	19.8	201
GWS 7	5.9E-06	-	-	-	983	2.5	5.4	0.3	157	47.3	0	6.4	16.8	195
GWS 12	5.7E-04	-	-	-	956	1.3	4.8	1.5	153	47.0	0	16.6	16.5	183
GWS 15	8.0E-06	-	-	-	970	3.1	4.8	0.8	167	39.9	0.6	3.3	17.5	209
GWS 16	8.6E-04	-	-	-	780	1.9	4.9	0.8	120	35.2	0	3.1	21.7	65
GWS 23	7.1E-04	-	-	-	1004	2.8	5.0	0.7	160	47.5	0	2.8	15.6	122
GWS 25	1.8E-04	-	-	-	1950	7.1	10.3	7.0	383	63.9	3.7	4.9	33.8	409

* DOC and major ions are given as mean values of samples collected on several dates in summer.

Fig 1

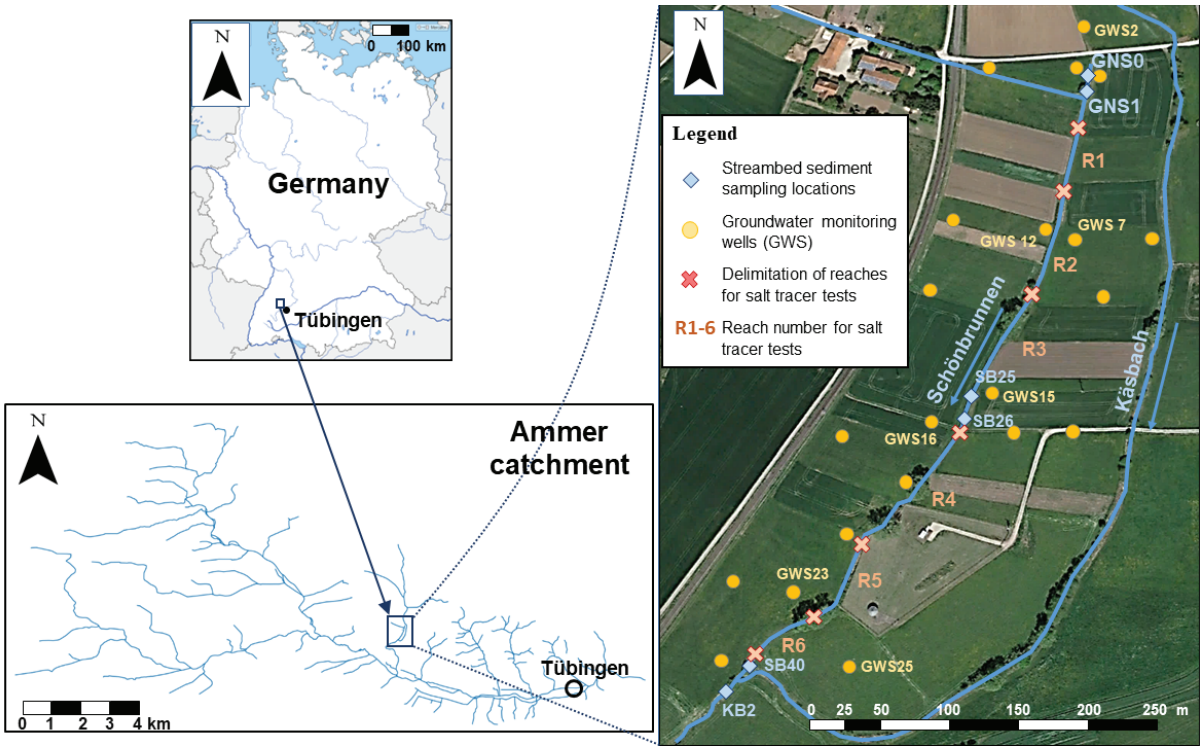

Fig. 1: Location of the first-order stream Schönbrunnen in the Ammer catchment near Tübingen, Germany. Sediment sampling locations and groundwater monitoring wells are indicated with respective symbols. These are: *Up-A* - GNS0, *Up-B* - GNS1, *Mid-A* - SB25, *Mid-B* - SB26, *Down* - SB40, *Conf* - KB2. Successive hydraulic reaches of the stream as delineated by tracer test are indicated as R1 – R6 (Jimenez-Fernandez et al., 2022).

Fig 2

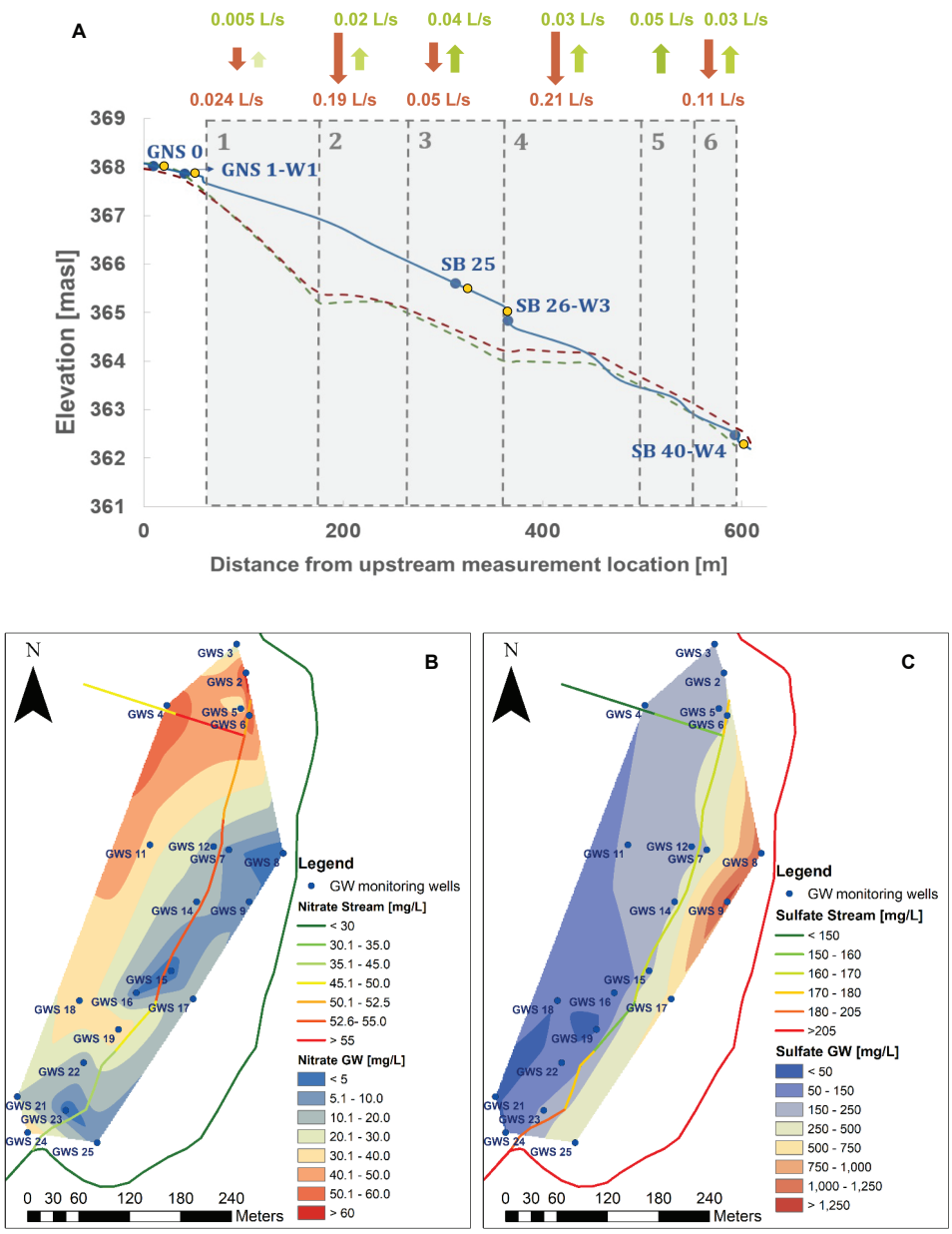

Fig. 2: (A) Stream-groundwater exchange fluxes, stream water elevation, and groundwater heads in the Schönbrunnen. Numbers give gross bidirectional stream-groundwater exchange fluxes determined by tracer tests (Jimenez-Fernandez et al., 2022). The length of the arrows indicates the magnitude of stream water gain (green color) and loss (red color). The plot shows stream water elevation and groundwater heads. Blue color line represents the stream water stage. The two dashed lines represent groundwater head elevations 10 meters away from the Schönbrunnen, from either western side (blue color) or eastern side (green color). The head elevations were extracted from the interpolated groundwater contour map (Jimenez-Fernandez et al., 2022). The location of weirs installed in the field are shown as blue dots. Locations for sediment sampling are shown as yellow dots, corresponding to sample name code in Table1. (B) Contour maps of concentrations of nitrate and (C) sulfate mapped for both stream and groundwater of the Schönbrunnen and Käsbach catchment in summer 2018.

Fig 3

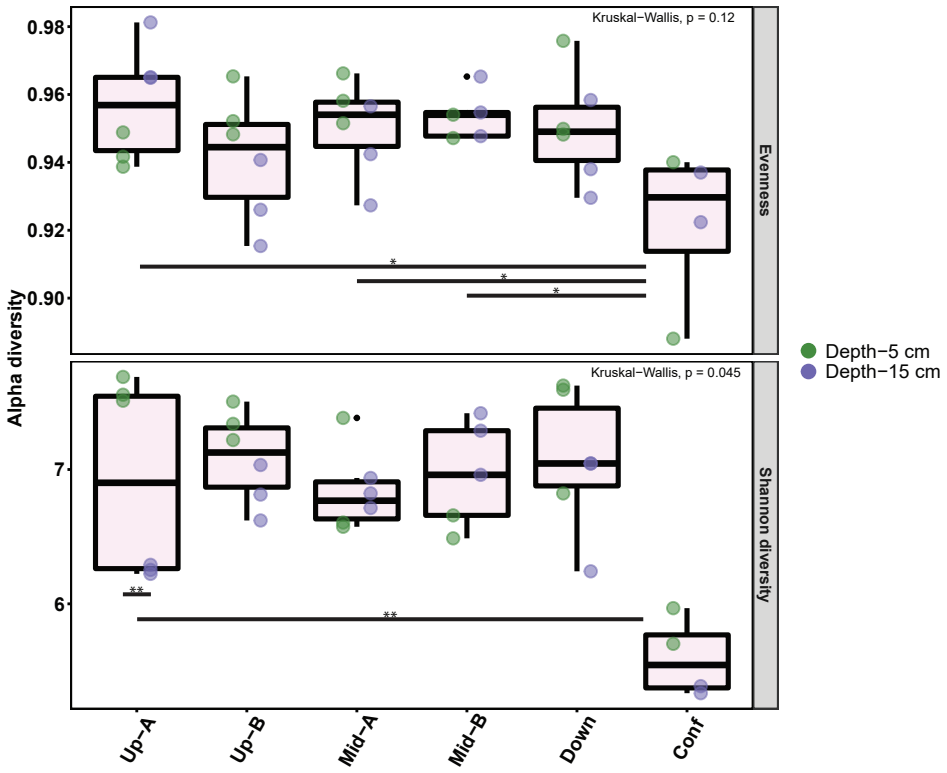

Fig. 3. Alpha diversity of sediment bacterial communities in the Schönbrunnen streambed. Shannon diversity and Shannon diversity based evenness for 16S rRNA gene sequencing data are plotted for each sampling depth and sampling location. Boxplots indicate the mean Shannon diversity and evenness at each sampling location. Asterisks indicate significant differences in Kruskal-Wallis tests with Dunn's Multiple Comparison post-tests (∗: $p < 0.05$; ∗∗: $p < 0.01$).

Fig 4

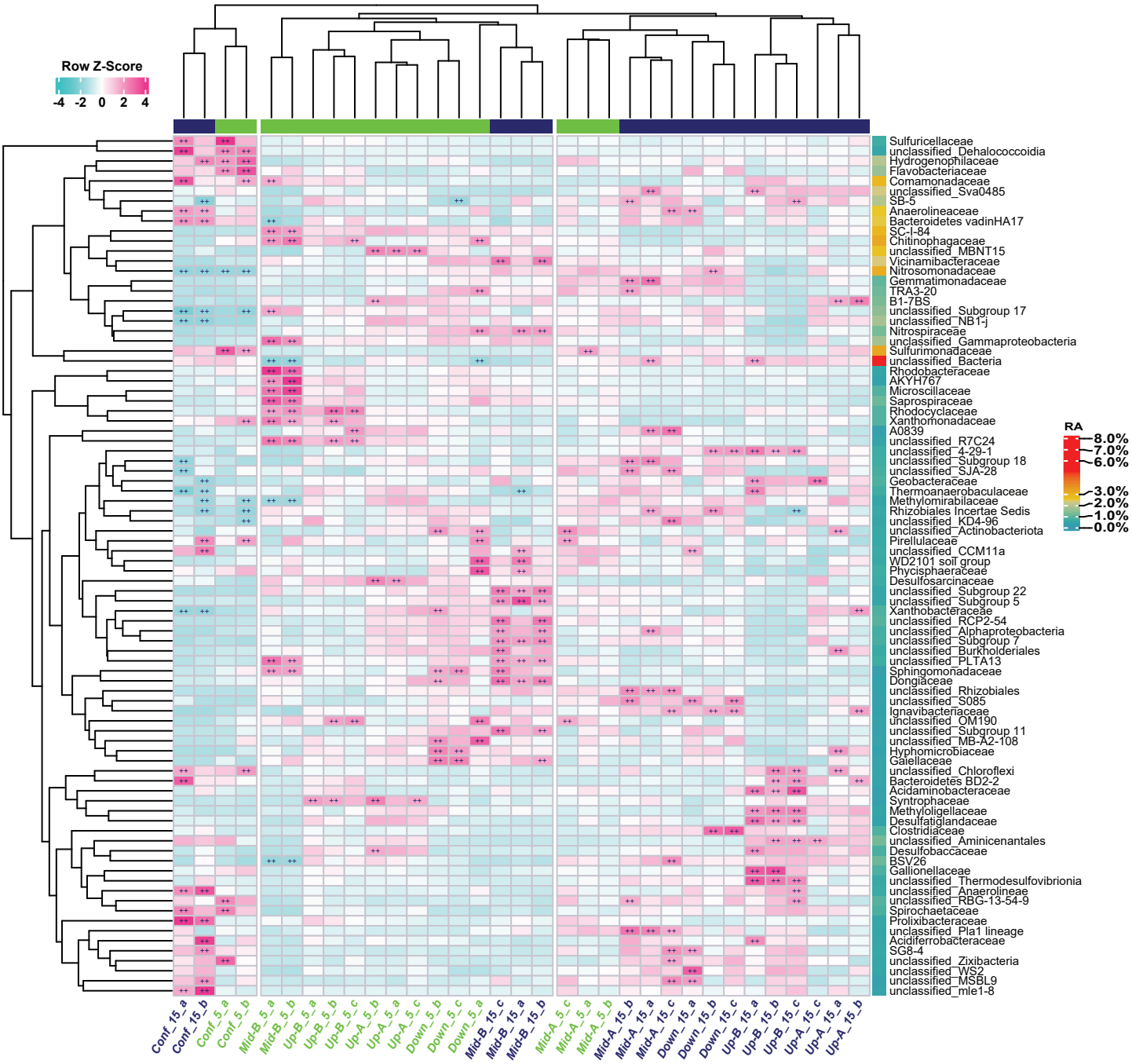

Fig. 4. Heatmap of the most abundant family-level microbial populations in the Schönbrunnen streambed and hierarchical clustering analysis based on Bray-Curtis dissimilarity between samples (ASV level). Z-scores were calculated based on relative abundance (RA) of ASVs agglomerated at the family level. Families with cumulative relative abundances lower than 7% over all samples were excluded from this plot. The last column on the right side additionally shows the mean relative abundance of each family across all samples. Color code for sample names indicates sampling depths (green: 5 cm, purple: 15 cm). Cells were highlighted with '++' symbols if |Z-Score| > 2.

Fig 5

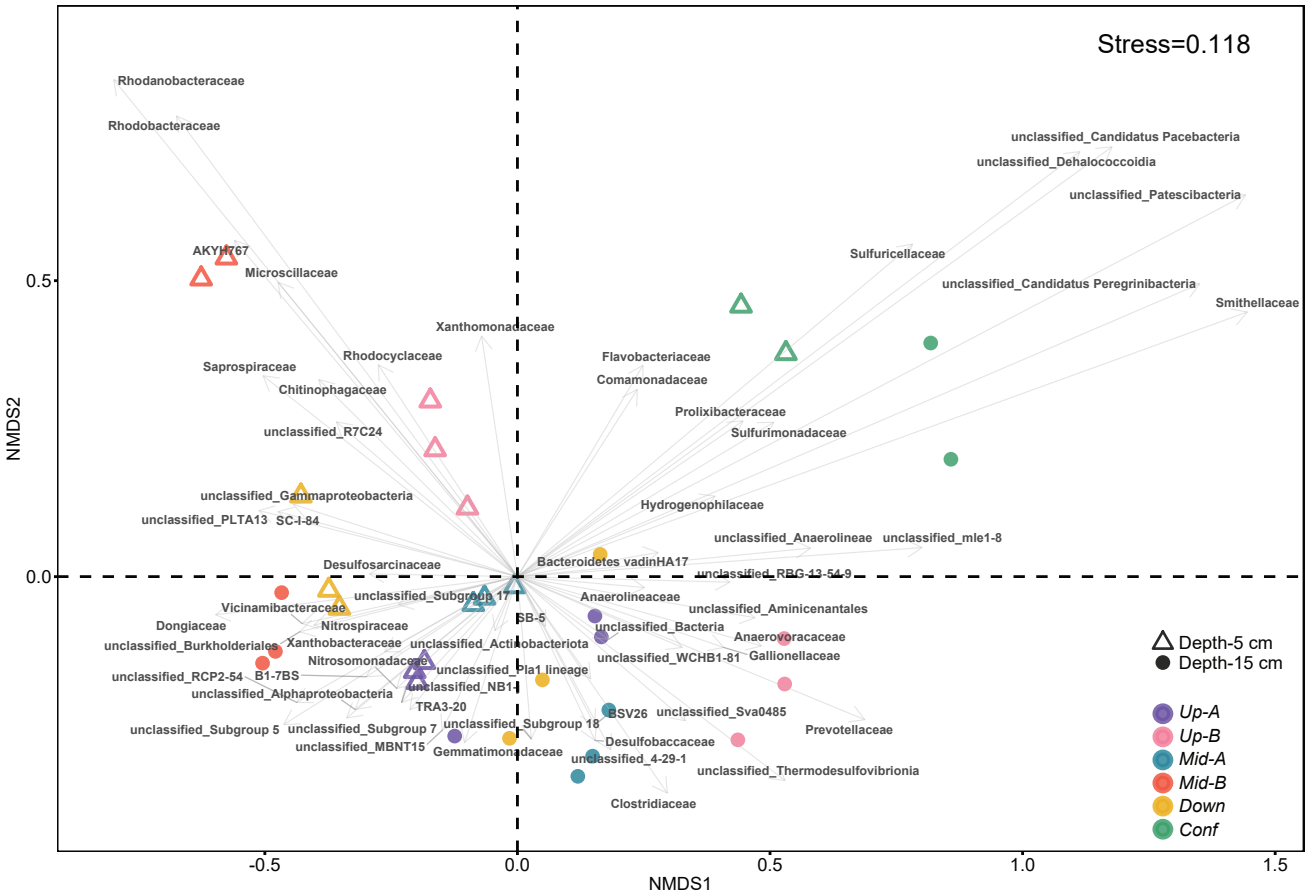

Fig. 5. Bray-Curtis distance-based non-metric multidimensional scaling (NMDS) plot of dissimilarities between streambed microbial communities grouped at the family-level. Selected taxa contributing significantly ($p < 0.05$, together > 50%) to dissimilarities between samples (indicated via SIMPER analyses) were projected onto the NMDS plot. The arrow length and direction of each plotted taxon reflect it's contribution on driving dissimilarities for given sample.

Fig 6

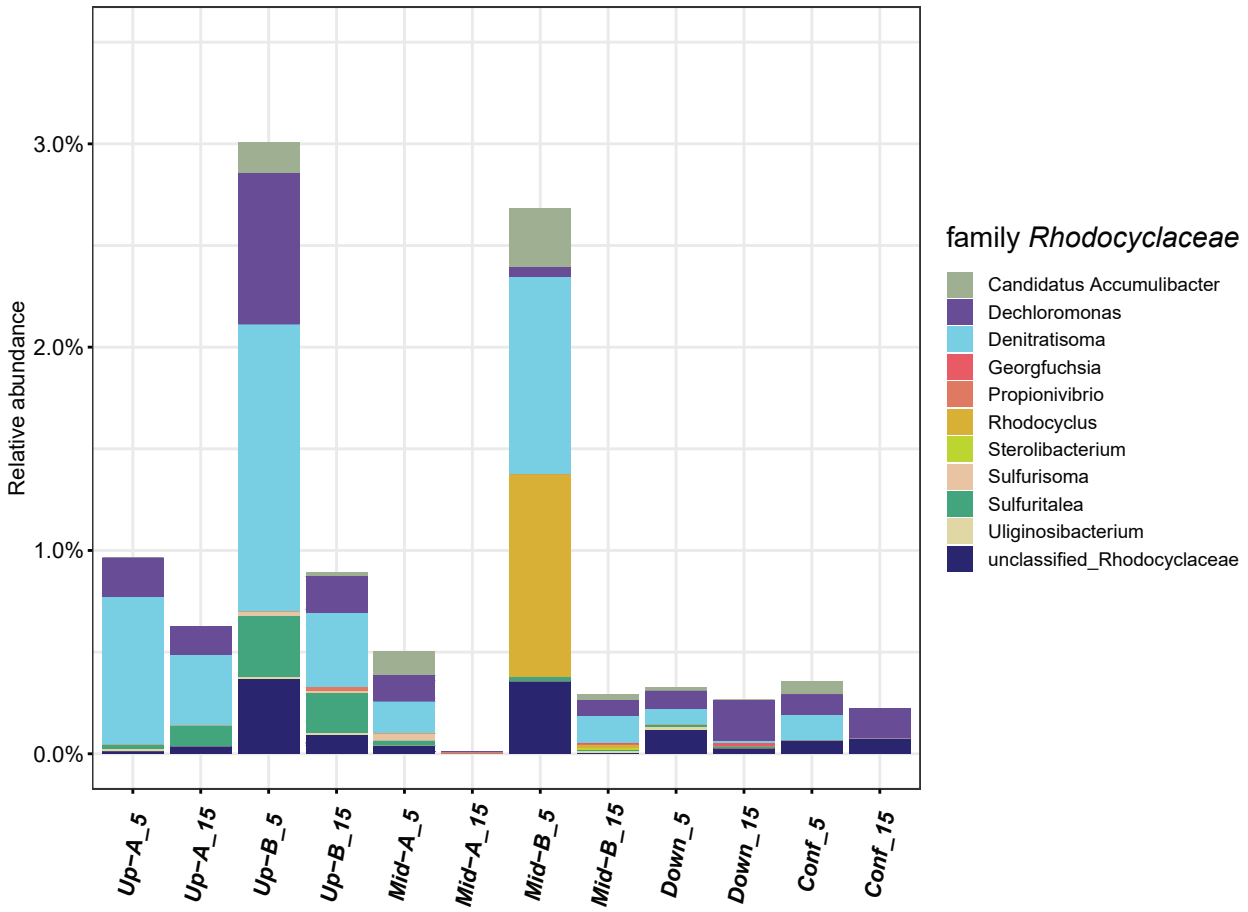

Fig. 6. Relative abundance of members of the *Rhodocyclaceae* across samples from the Schönbrunnen streambed.

Fig 7

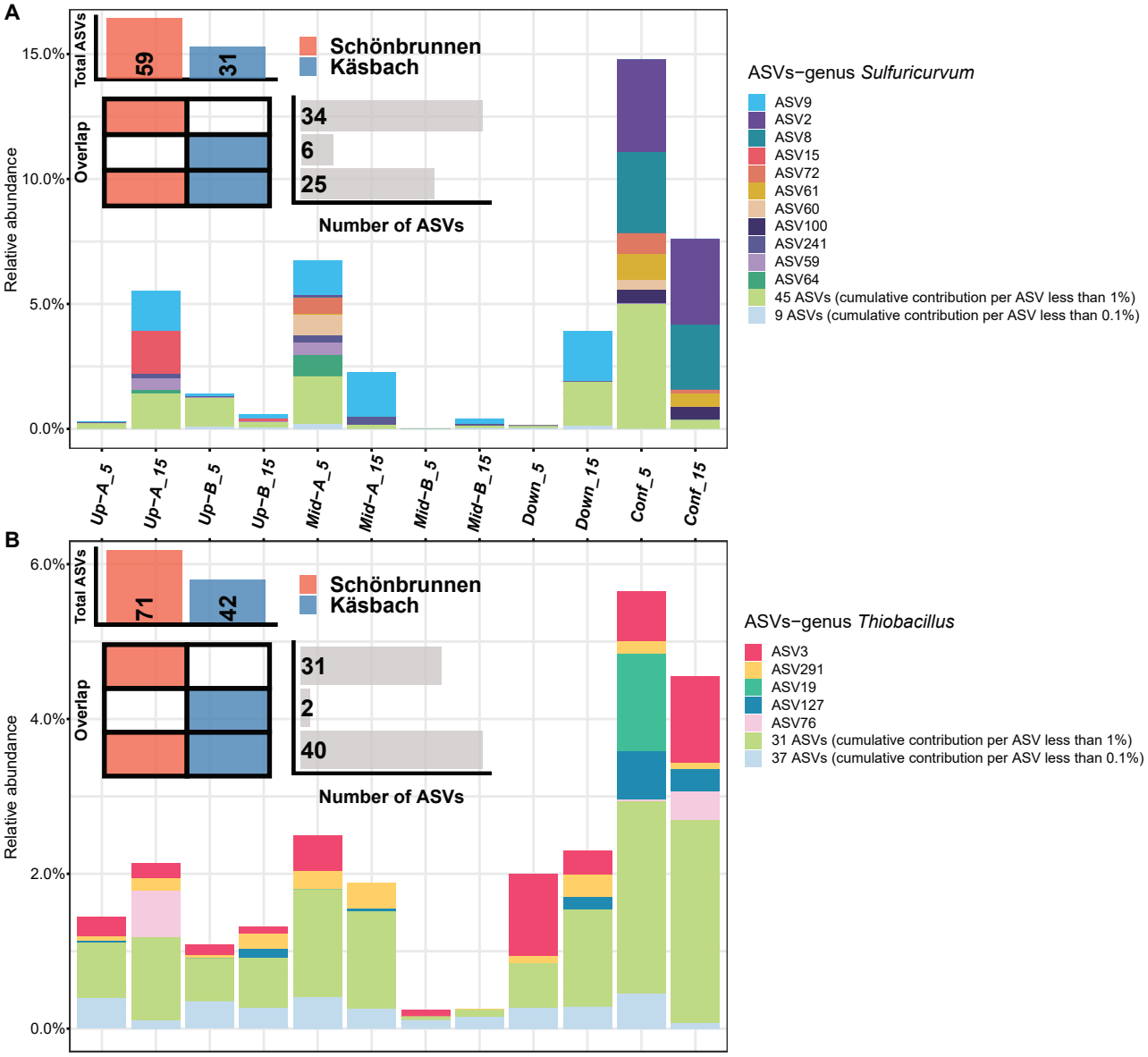

Fig. 7. Relative abundance of potential sulfur-oxidizing bacterial populations across samples of the Schönbrunnen streambed. (A) *Sulfuricurvum* spp., and (B) *Thiobacillus* spp. are resolved at the ASV-level. The upset plots show how many ASVs within both general were unique or shared within Schönbrunnen or Käsbach (i.e. after confluence). Most abundant ASVs were plotted with distinct color codes, whereas lower abundance ASVs were merged into two categories: ASVs with a cumulative abundance <1% across all samples (light green color), and ASVs with a cumulative abundance <0.1% across all samples (light blue color).

Fig 8

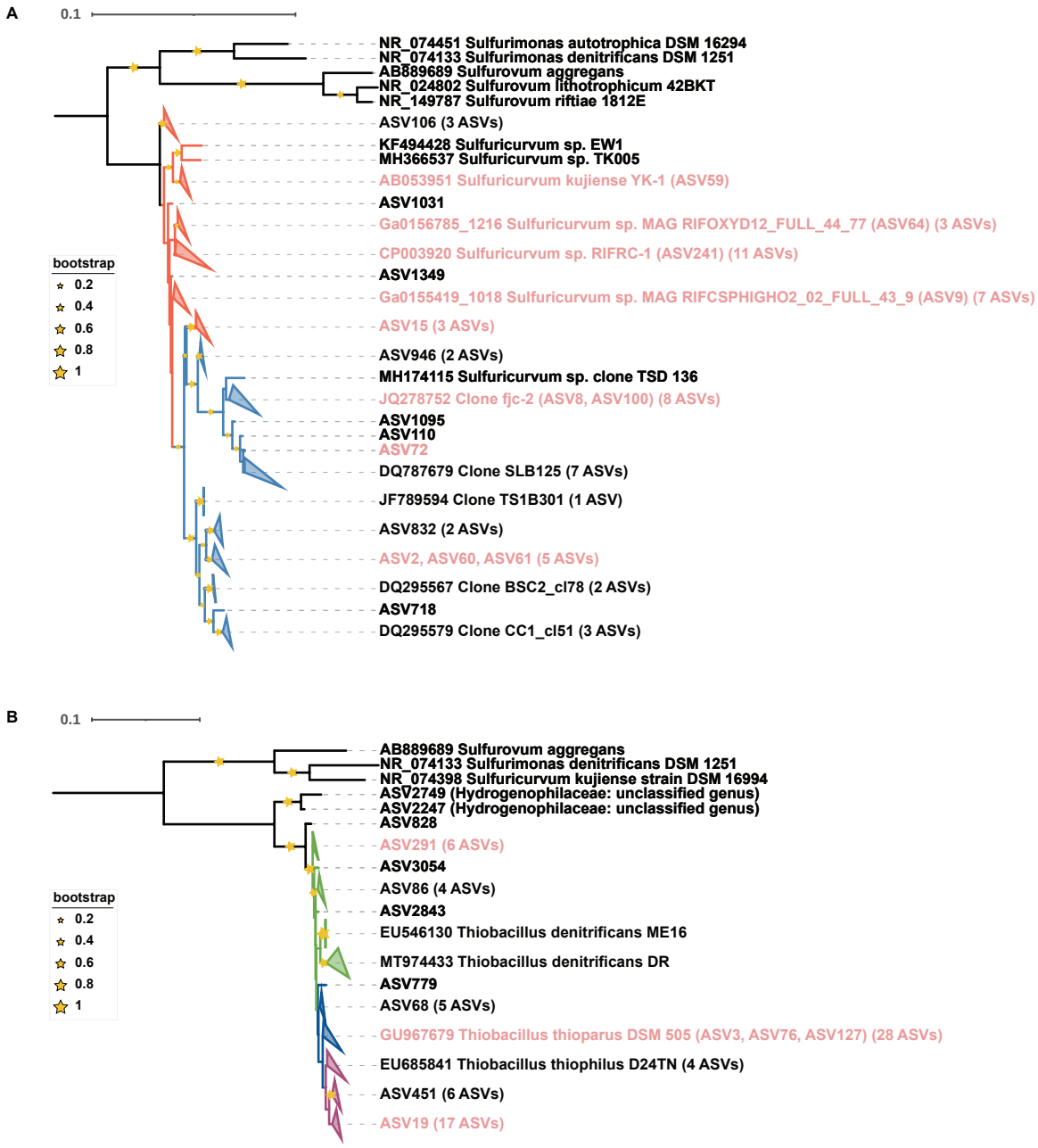

Fig. 8. Maximum likelihood tree of (A) all *Sulfuricurvum* ASVs detected in this study. Tree branches associated with the Schönbrunnen cluster are shown in red, branches of the Käsbach cluster are plotted in blue. In addition, labels of the most abundant ASVs (corresponding to the ASVs with distinct colors in Fig. 7) are highlighted in red. The number of ASVs shown in parentheses (e.g. 6 ASVs) indicate the number of ASVs collapsed in a clade. Similarly, (B) shows the phylogeny of all *Thiobacillus* ASVs detected in this study. The color code for tree branches represents three likely affiliation of ASVs with *T. denitrificans* (green), *T. thioparus* (blue), and *T. thiophilus* (red).

Fig 9

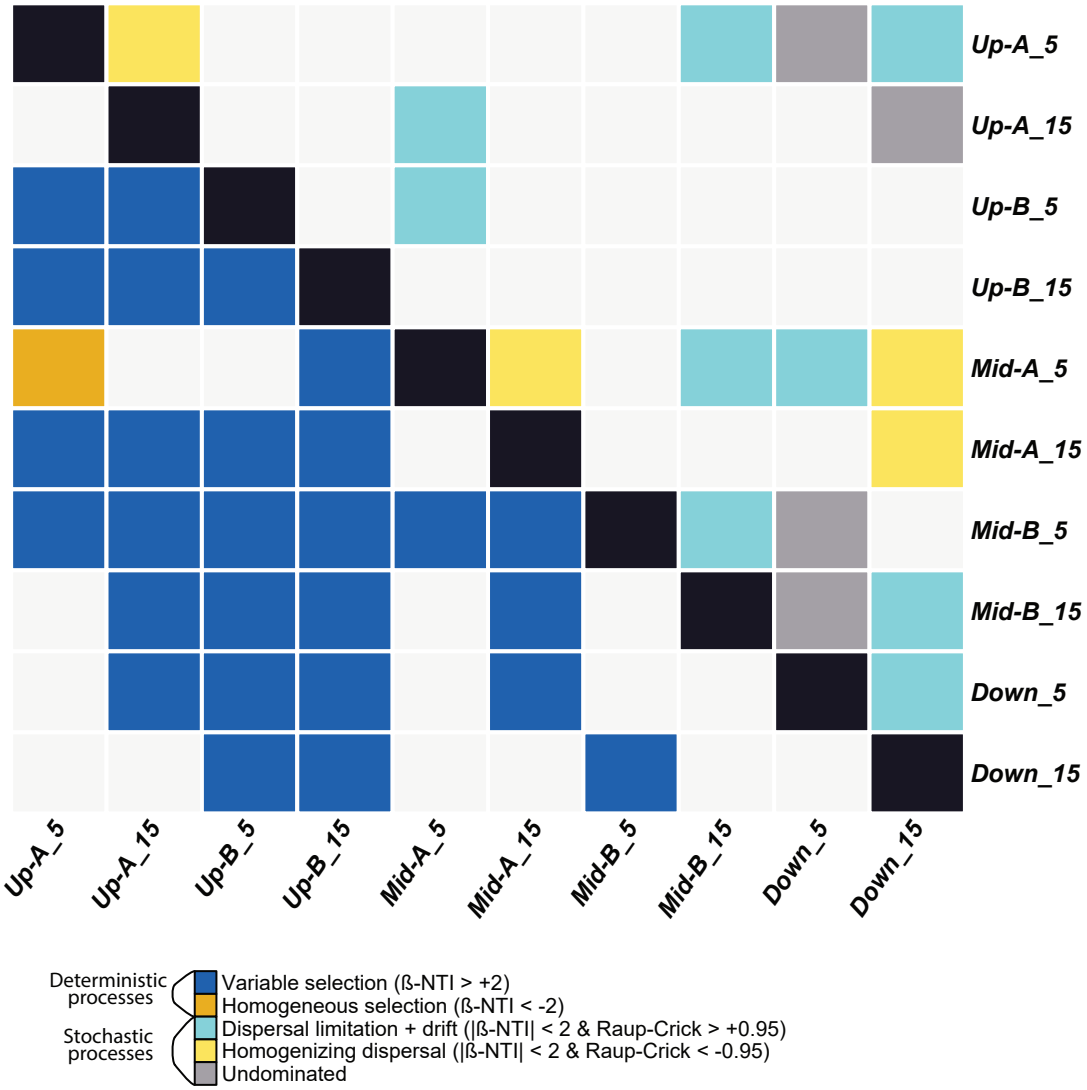

Fig. 9. Heatmap for the βNTI values (lower left triangle) and RC_{bray} values (upper right triangle). Deep blue and yellow colors in the lower triangle indicate deterministic processes like variable selection or homogeneous selection to dominate in pairwise comparison, whereas light blue and yellow colors in the upper triangle indicate stochastic assembly mechanisms, such as dispersal limitation or homogenizing dispersal.

Fig 10

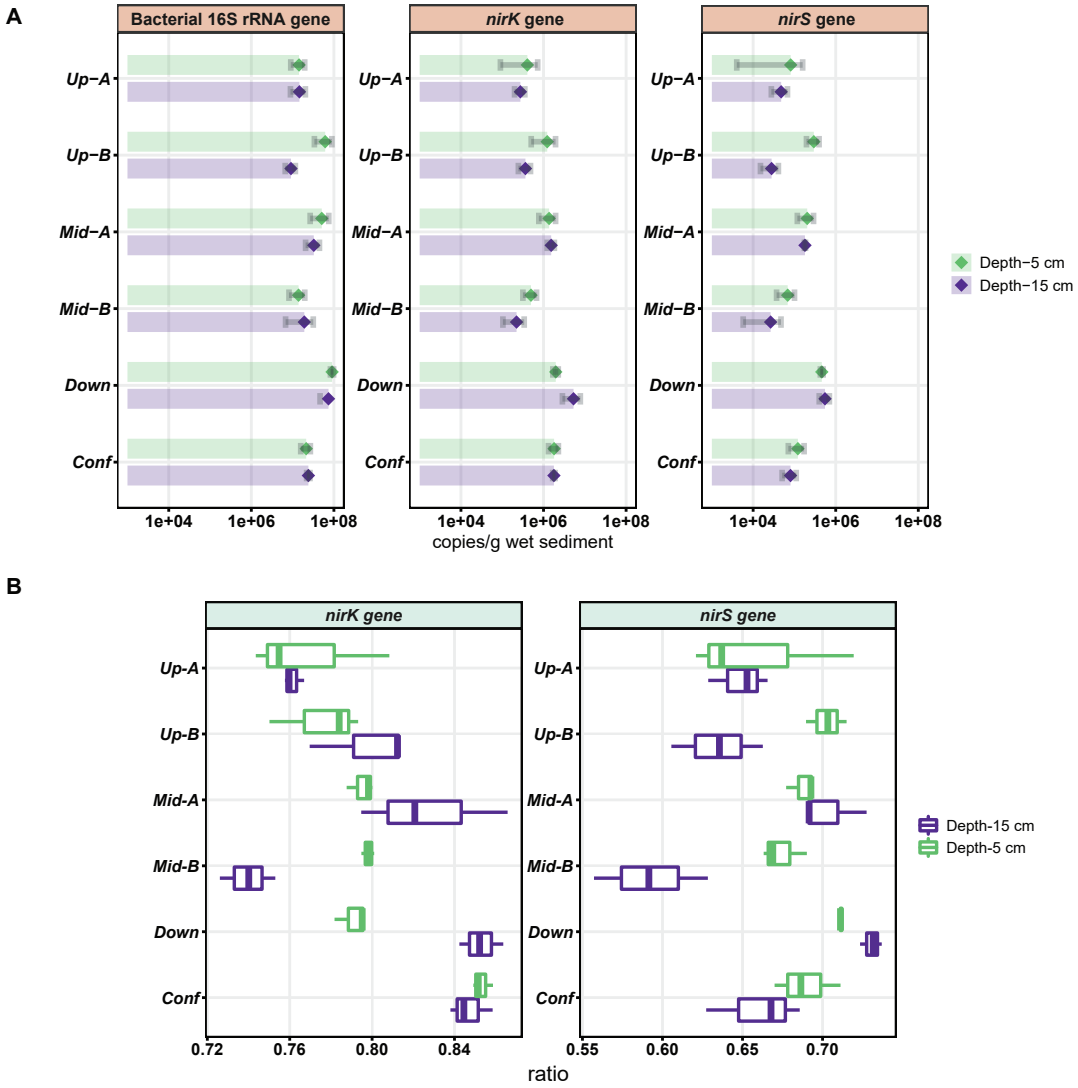

Fig. 10. (A) Abundances of bacterial 16S rRNA, *nirK*, and *nirS* genes in sediments of the Schönbrunnen streambed quantified via qPCR. Gene abundances were calculated as gene copies per g of wet sediment (g_{ww}^{-1} of sediment). Standard deviation of gene abundance in biological (n=3) and technical replication (n=2) are shown as error bar. (B) Relative abundances of *nirK* and *nirS* vs. total bacterial 16S rRNA gene counts. Ratios were calculated as ratios of $\log_{10}$-transformed qPCR counts as shown in (A). Each box indicates variability of biological (n=3) and technical qPCR replicates (n=2).

Click here to access/download
Electronic Supplementary Material (for online publication only)
SI-Wang, Lueders_Manuscript.docx

Hydrological Processes

Groundwater-surface water exchange and hydrologic turnover as key controls for instream and groundwater nitrate concentrations in first-order agricultural stream catchments

Journal:	*Hydrological Processes*
Manuscript ID	Draft
Wiley - Manuscript type:	Research Article
Date Submitted by the Author:	n/a
Complete List of Authors:	Jimenez Fernandez, Oscar; Helmholtz-Centre for Environmental Research - UFZ, Hydrogeology; University of Tübingen, Geosciences Schwientek, Marc; University of Tübingen, Geoscience Osenbrück, Karsten; University of Tübingen, Geoscience Glaser, Clarissa; University of Tübingen, Center for Applied Geoscience Schmidt, Christian; Helmholtz Centre for Environmental Research - UFZ , Department of Hydrogeology Fleckenstein, Jan; Helmholtz Center for Environmental Research (UFZ), Hydrogeology; University of Bayreuth, Bayreuth Center of Ecology and Environmental Research (BayCEER)
Keywords:	riparian groundwater, groundwater-surface water exchange, hydrologic turnover, Radon-222, salt tracer tests, nitrate

SCHOLARONE™
Manuscripts

Groundwater-surface water exchange and hydrologic turnover as key controls for instream and groundwater nitrate concentrations in first-order agricultural stream catchments

Oscar Jimenez-Fernandez [1,2], Marc Schwientek [1,*], Karsten Osenbrück [1], Clarissa Glaser [1], Christian Schmidt [2], Jan H. Fleckenstein [2,3]

[1] Department of Geosciences, University of Tübingen, Schnarrenbergstrasse 94-96, 72076 Tübingen, Germany

[2] Department Hydrogeology, Helmholtz Center for Environmental Research, Permoserstrasse 15, 04318 Leipzig, Germany

[3] Hydrologic Modelling Unit, Bayreuth Center of Ecology and Environmental Research (BayCEER), University of Bayreuth, Bayreuth, Germany

Corresponding authors:

Oscar Jimenez-Fernandez (oscar.jimenez-fernandez@ufz.de)

Prof. Dr. Jan H. Fleckenstein (jan.fleckenstein@ufz.de)

For Peer Review

Keywords: water quality, riparian groundwater, groundwater-surface water exchange, hydrologic turnover, Radon-222, salt tracer tests, nitrate, longitudinal profile.

Running title: Hydrologic turnover shapes water quality

* Landesamt für Geologie, Rohstoffe und Bergbau. Albertstraße 5, 79104 Freiburg im Breisgau, Germany.

Groundwater-surface water exchange and hydrologic turnover as key controls for instream and groundwater nitrate concentrations in first-order agricultural stream catchments

Oscar Jimenez-Fernandez [1,2], Marc Schwientek [1,*], Karsten Osenbrück [1], Clarissa Glaser [1], Christian Schmidt [2], Jan H. Fleckenstein [2,3]

[1] Department of Geosciences, University of Tübingen, Schnarrenbergstrasse 94-96, 72076 Tübingen, Germany

[2] Department Hydrogeology, Helmholtz Center for Environmental Research, Permoserstrasse 15, 04318 Leipzig, Germany

[3] Hydrologic Modelling Unit, Bayreuth Center of Ecology and Environmental Research (BayCEER), University of Bayreuth, Bayreuth, Germany

For Peer Review

Abstract

Lower-order streams define the initial, landscape-related, chemical signature of stream water in catchments. To date, first-order streams have been perceived as predominantly draining systems, which collect water and solutes from the surrounding groundwater and surface runoff and simply mirror the chemical composition of the inputs. In this study, the impact of stream-groundwater exchange fluxes on water chemistry of a first order agricultural stream (Schönbrunnen) and its connected groundwater in south-western Germany was assessed combining ^{222}Rn, dissolved ions (chloride, sulfate, nitrate), and salt tracer tests with investigations of stream discharge and groundwater hydraulic gradients. The findings suggest that stream-water chemistry in lower-order streams is governed by an intricate interplay between dynamic, bidirectional water and solute exchange between groundwater and the stream leading to a pronounced hydrologic turnover along the studied reaches. High nitrate concentrations in stream water were attenuated in downstream direction without an increase in discharge, suggesting that redox processes occurring during sediment passage in sequential infiltration and exfiltration zones affect stream water chemistry. Nitrate in stream water infiltrating into the aquifer at distinct losing spots was subject to denitrification within the first few decimeters of the streambed, while concurrent exfiltration of low-nitrate groundwater into the stream at gaining spots compensated for flow losses and in turn diluted instream nitrate concentrations. In summary the findings imply that (1) instream mixing resulting from the bidirectional exchange of water between groundwater and the stream (hydrologic turnover) affects instream nitrate concentrations, (2) denitrification in the streambed of losing reaches and the near-stream aquifer significantly contributes to reactive nitrate turnover and elimination, and (3) oxidation of ammonium could be a secondary source of nitrate inputs into the stream.

Keywords: water quality, riparian groundwater, groundwater-surface water exchange, hydrologic turnover, Radon-222, salt tracer tests, nitrate, longitudinal profile.

For Peer Review

1. Introduction

Low-order streams are responsible for large fractions of the water and solute fluxes that leave larger catchments at their outlet. Alexander et al. (2007) estimated the contribution of first order streams to the mean annual stream flow and nitrate flux in higher order streams to be up to 70% and 65%, respectively. The large contribution of local groundwater inflow with distinct chemistry to streamflow in lower-order streams creates a significant imprint on their chemical signature (Peterson et al., 2001; Ruiz et al., 2002; Mazurek et al., 2020). Therefore, an improved assessment of the spatio-temporal patterns of exchange between groundwater (GW) and stream water (SW) is important to understand instream water quality patterns and in turn solute exports from agricultural catchments (Ranalli & Macalady, 2010; Covino et al., 2011).

GW-SW interactions have been studied intensively over the last 15 to 20 years with the focus ranging from small-scale hyporheic exchange processes (Cardenas & Wilson, 2006; Briggs et al., 2014; Trauth et al., 2015, Hester et al., 2017) to larger spatial scales of river reaches (Harvey et al., 1996, Ruehl et al., 2006; Zhou et al., 2018) and entire catchments (Covino & McGlynn, 2007, Covino et al., 2011, Maxwell et al., 2016). A large range of methods has been used and further developed to assess patterns of GW-SW interactions and to quantify exchange fluxes, including vertical hydraulic gradients and differential gauging (Kalbus et al., 2006), natural tracers such as specific electrical conductivity (Cirpka et al., 2007; Schmidt et al., 2012), temperature (Schmidt et al., 2006; Hatch et al., 2006; Anibas et al., 2016), stable isotopes of water (Penna et al., 2015), ^{222}Rn (Cook, 2013; Cartwright & Gilfedder, 2015; Oh et al., 2021), artificial tracer injections (Payn et al., 2009; Ward et al., 2013; Kelleher et al. 2019), and numerical modeling (Fleckenstein et al. 2006, Frei et al. 2009; Kaandorp et al. 2018). For an integral, robust, and more holistic assessment of GW-SW exchange processes, several studies have used a combination of different methods (e.g. Osenbrück et al. 2013; Atkinson et al., 2015; Gonzalez-Pinzon et al., 2015; Hoagland et al., 2017; Frederiksen et al., 2018).

Due to the joint exchange of water and solutes, GW-SW interactions also mutually affect solute concentrations in streamflow and in the riparian aquifer (Wriedt et al., 2007; Rahimi et al., 2015; Huizenga et al., 2017; Zhang et al., 2021). While reactive processes such as nitrate reduction

For Peer Review

in riparian buffer zones (Burt et al., 1999; Vidon & Hill, 2004; Henault-Ethier et al., 2017; Lutz et al., 2020) or in the hyporheic zone (Harvey et al., 2013; Zarnetske et al., 2015) are known to attenuate water pollution, GW inflows or SW losses outside reactive hot spots may lead to a persistence of high pollutant concentrations in streamflow or the riparian aquifer respectively (Thompson et al., 2011; Musolff et al., 2017). To evaluate changes in solute concentrations, water balance based artificial tracer methods, which account for simultaneous gains and losses of water over stream reaches (Payn et al., 2009; Covino et al., 2011; Mallard et al. 2014), have great appeal, as they allow to estimate mixing between stream water derived from the upstream reach and the fraction newly gained from the surrounding groundwater. Using such methods, Mallard et al. (2014) demonstrated the potential effects of this so-called “hydrologic turnover” on stream water solute composition using idealized example cases. However, their work mainly addressed network-scale effects under steady-state conditions and did not account for temporal (e.g. seasonal, event-scale) and spatial (nested net gaining and net losing reaches) variations in exchange patterns and flux magnitudes and how they may affect instream concentration and load variability. There are gaps in our understanding of how these dynamic processes ultimately shape concentration signals and the solute loads exported from lower order catchments.

This study aims at narrowing those gaps by systematically evaluating the spatio-temporal patterns of GW-stream exchange and hydrologic turnover along a first order agricultural stream in southwestern Germany. We used a multimethod approach for characterizing GW-stream exchange in order to address the following key questions: (1) How do patterns of gaining and losing reaches and the magnitude of the exchange flux vary in space and time over a year? (2) To what degree can instream concentration variability of nitrate be explained by mixing induced by hydrologic turnover? (3) Are the patterns of nitrate concentrations in riparian groundwater affected by stream water infiltration and hydrologic turnover? To address these questions, we monitored SW and GW over a period from July 2017 to August 2018 using stream gauges, hydrometric measurements at groundwater monitoring wells, and a

For Peer Review

combination of salt tracer experiments and natural tracers (specific electrical conductivity (EC), temperature (T), ^{222}Rn, and major ion composition).

2. Study Site

The Schönbrunnen (SB) is a first order stream 10 km west of the city of Tübingen in Southwest Germany and drains a catchment of approximately one km^2. The land surface is mildly inclined to the west (< 3°) and the elevations within the SB catchment vary between 362 and 390 m asl. In its lower course the stream enters the alluvial Käsbach valley from the west, before it bends to the south and flows parallel to the second-order Käsbach stream, which it joins after a total flow length of 1110 m (Figure 1). Investigations focused on the approximately 550 m long segment of the SB stream between the bend and the confluence with the Käsbach stream. The riparian aquifer connected to the SB is bounded by the Käsbach stream to the east. The mean annual precipitation for the study period ranged from 470 mm (in 2018) to 680 mm (in 2017). The land cover is mainly agricultural fields. In the southern part of the catchment, the majority of these fields are meadows, whereas active cropland and pastures cover most of the northern part and the western hillslopes. The geology of the western hillslopes is dominated by dolomites and claystones of the Lower Keuper, while east of the Käsbach valley, gypsum bearing mudstones and marls of the Middle Keuper prevail. Underlying sediments mainly consist of Quaternary alluvial fills of about 4 to 8 m thickness and comprise silty, clayey, and loamy materials.

3. Materials and Methods

3.1. Hydrological monitoring

Three sharp crested V-notch weirs (W1, W2, and W3) were installed for measuring stream discharge at three locations along the SB stream (Figure 1). Stream stage together with stream

For Peer Review

temperature and specific electrical conductivity (EC) were monitored at 15-min intervals using vented pressure transducers (accuracy: ± 2 mm H_2O) integrated in CTD probes (± 0.1 °C and ± 1 µS/cm; EC compensated to 25°C) with data loggers (UIT GmbH, Dresden, Germany), which were installed immediately upstream of each of the weirs. Discharge Q was calculated from the water level recordings based on the following equation (Henderson, 1966):

$$Q = \frac{8}{15} C \sqrt{2g} \tan\frac{\theta}{2} h^{\frac{5}{2}} \quad (1)$$

where Q is discharge (L/s), C is the non-dimensional runoff coefficient, g is the acceleration due to gravity (m/s^2), θ is the angle included between the sides of the V-notch, given in degrees, and h is the potentiometric head (m) corresponding to the height of the upstream water surface with respect to the vertex of the V-notch. The relative uncertainty of Q is about ± 10 %.

A total of 23 groundwater monitoring wells (1-inch) were installed in the SB catchment between July 2017 and May 2018. The elevation of each well (top of casing) as well as the elevation of selected points along the streambed were levelled with an accuracy of ± 0.002 m. Manual measurements of hydraulic heads were conducted weekly over the study period to characterize the groundwater piezometric surface throughout the study area. In addition, 14 selected wells were equipped with automatic probes (CTD Diver, Schlumberger, Netherlands) to continuously monitor pressure (± 0.5 cm H_2O), EC (± 1% of value in µS/cm; temperature compensation to 25°C) and temperature (± 0.1 K) in 15-min intervals. To calculate atmospheric pressure-corrected hydraulic heads from the pressure recordings, an additional pressure transducer (Baro Diver, Schlumberger, Netherlands) was installed at the stream bank near W2. Precipitation was monitored at the site by a tipping bucket rain gauge (Campbell Scientific, Shepshed, UK).

3.2. Hydrochemical analyses

Water samples for the analysis of major ions were taken from seven stream locations (Figure 1) and from the monitoring wells every four weeks. Groundwater samples were taken using a peristaltic pump (Eijkelkamp, Netherlands) with a pumping rate of about 100 mL/min. Prior to

For Peer Review

sampling, the water volume inside the wells was exchanged at least one to three times, depending on well yield. Glass bottles of 100 mL were filled at each site and filtered through 0.45 µm filters (MillexHA) within 48 hours after sampling. Additional water samples from the streambed sediment were collected in April 2019 using mini piezometers ('mini point samplers'; Duff et al., 1998) sampled with a pumping rate of 2.5 mL/min or less. All filtered samples were kept at 4 °C in the dark before being analyzed by ion chromatography (Dionex DX 500; LOQ = 0.1 mg/L for chloride, nitrate, and 0.3 mg/L for sulfate). Groundwater EC (± 0.5% of value; temperature compensation to 25°C), pH (± 0.5% of value), and temperature (± 0.1 K) were measured in the field using hand-held probes (WTW GmbH, Germany).

3.3. Endmember mixing analysis

Endmember mixing analysis was used to determine the unknown fractions of groundwater inflow, $f_{GW} = Q_{GW}/Q_{Gain}$ and $f_{GE} = Q_{GE}/Q_{Gain}$, where Q_{GW} and Q_{GE} are the groundwater gains from the western and eastern sides of the SB stream, respectively, and Q_{Gain} is the total gross gain from groundwater known from the tracer tests. Due to contrasting sulfate concentrations in the western and eastern parts of the riparian aquifer, sulfate was used as tracer in the mixing analysis. Applying a simple mass balance to the individual stream reaches, the groundwater fractions can be expressed as:

$$f_{GW} = \frac{Q_{down}C_{down} - Q_{up}C_{up} - Q_{Gain}C_{GE} + Q_{Loss}C_{Loss}}{Q_{Gain}\,(C_{GW} - C_{GE})} \quad (2)$$

$$f_{GE} = 1 - f_{GW} \quad (3)$$

where Q_{up}, C_{up}, Q_{down}, and C_{up} are stream discharge and sulfate concentration at the upstream and downstream ends of the considered reach, and C_{GW} and C_{GE} are the mean sulfate concentrations of the western and eastern groundwater endmembers. Stream loss Q_{Loss} was assumed to occur with a concentration C_{Loss} represented by the mean of C_{up} and C_{down}.

3.4. Radon as a tracer for groundwater inflows

For Peer Review

Stream water was sampled for the analysis of dissolved ^{222}Rn on February 9th, 2018 and August 13th, 2018 at the seven stream locations (see Figure 1). Samples were collected from the middle of the stream and assumed to be well-mixed and thus representative for the respective sampling site. Water was filled into 250 mL or 100 mL bottles depending on the prevailing water level in the stream and closed tightly with no headspace in the bottles to avoid degassing. In July 2019, nine monitoring wells that are not affected by infiltrating stream water were sampled for the determination of a representative ^{222}Rn groundwater activity. Groundwater extraction was conducted as described for hydrochemical sampling and water was pumped into a 250mL bottle at low pumping speed to avoid degassing.

The ^{222}Rn activity concentration was measured using a RAD7 Radon Detector (Durridge Company Inc.) and the RAD H_2O accessory (Lee and Kim, 2006). Each sample was degassed for five minutes and then counted up to six times for 30 minutes. These replicated samples led to a relative error between 3 and 7%. Results were corrected for decay between time of sampling and time of measurement and in case of sampling volumes of 100mL multiplied by a correction factor to account for the degassing efficiencies of the measured volume in comparison to the reference volume (250 mL).

Groundwater inflow into the stream was determined based on the ^{222}Rn data from stream and groundwater applying the finite element model FINIFLUX (Frei and Gilfedder, 2015; Glaser et al., 2020). FINIFLUX solves the 1-D mass balance equation for ^{222}Rn where the gain of stream water by groundwater is estimated inversely as part of the optimization process. For the SB stream, degassing was calculated based on the empirical equation of O'Connor & Dobbins (1958) and Cartwright et al. (2011). Hyporheic exchange was assumed to be negligible for the sampling site.

3.5. Salt tracer tests to quantify stream water gains and losses

A series of salt tracer tests were used to quantify stream discharge as well as gross hydrologic exchanges between the stream water and groundwater along six consecutive reaches of the SB following the procedures given by Payn et al. (2009). The selection of the six reaches was

For Peer Review

based on measured longitudinal EC profiles along the stream, assuming changes in EC to reflect groundwater inflows into the stream. Two series of tracer tests at base flow conditions were performed in this study: one in the winter (December 5th-6th, 2017) and one during the summer period (July 18th-19th, 2018). The delineation of the reaches was slightly different for the two experiments due to different hydrological conditions.

Tracer injections of known masses M_{inj} of sodium chloride (NaCl) were performed at the upstream end of each reach, starting at the most downstream reach. For each injection, breakthrough curves of EC were measured with a 5 s resolution at two monitoring points, one after short flow distance allowing for complete transverse mixing of the tracer in the stream cross-section (Kilpatrick & Cobb, 1985) and a second at the downstream end of the reach, which corresponds with the upstream monitoring point of the previous tracer injection. After conversion of measured EC to NaCl concentrations using pre-determined calibration factors, the integrals of the upstream breakthrough curves $C_{up}(t)$ were used to determine stream discharge at the actual upstream end of the reaches:

$$Q_{up} = \frac{M_{inj}}{\int_0^{t_x} C_{up}(t)dt} \tag{4}$$

where t is the time variable of integration and t_x is the time of the experiment. The net change of discharge for the stream reaches is:

$$\Delta Q = Q_{down} - Q_{up} \tag{5}$$

where Q_{down} and Q_{up} are the discharges at the lower end (derived from the previous tracer injection) and upper end of the reach, respectively. The gross loss of stream water (Q_{loss}) along each reach can be calculated from the mass loss M_{Loss} using the breakthrough curve at the downstream monitoring point to derive the mass recovery M_{rec}:

$$Q_{Loss} = \frac{M_{Loss}}{\int_0^{t_{exp}} C_{Loss}(t)dt} = \frac{M_{rec} - M_{inj}}{\int_0^{t_{exp}} C_{Loss}(t)dt} = \frac{Q_{down}\int_0^{t_{exp}} C_{down}(t)dt - M_{inj}}{\int_0^{t_{exp}} C_{Loss}(t)dt} \tag{6}$$

where the concentration C_{Loss} of the water lost from the stream depends on the order in which losses and gains occur. As defined in Eq. (6), Q_{Loss} is a negative number with a minimum vale

For Peer Review

when C_{Loss} is represented by the breakthrough curve at the upstream end C_{up} (losses before gains) and a maximum value for C_{down} at the downstream end of the reach (losses after gains). Gross losses reported here were taken as the mean of the derived minimum and maximum values. Finally, gross gains were calculated by closing the discharge balance over each reach:

$$Q_{Gain} = \Delta Q - Q_{Loss} \tag{7}$$

Relative uncertainties related to the EC measurement and conversion to salt concentrations was usually smaller than 3%. These analytical errors as well as small temporal changes in background EC for the integration of the breakthrough curves were taken into account, which allowed to quantify uncertainties of the calculated discharge and mass recovery. Uncertainties for the resulting gross losses and gains were then obtained from Gaussian error propagation. Systematic errors may be introduced if tracer was lost or diluted within the mixing length. The mixing length was based on stretches were EC remained constant to minimize a contribution of groundwater within these stretches. However, losses to the groundwater cannot be ruled out for stretches with groundwater levels below stream level.

3.6. Assessment of hydrologic turnover

The outcome of the series of tracer tests was used to quantify the fractional hydrologic turnover along the SB stream based on the conceptual model of Covino et al. (2011) and Mallard et al. (2014). This concept allows quantifying the contribution of upstream water to the stream water composition of downstream reaches due to simultaneous loss of stream water and gain of different water from groundwater when moving downstream. Accounting for reaches with both, net losing and net gaining conditions, and assuming complete mixing of inflowing stream discharge and gross gains within reach *i* before losses occur, the stream water contribution from any upstream reach *j* leaving reach *i* at its downstream end is related to the gross loss $Q_{i,Loss}$ [L/s] and gross gain $Q_{i,Gain}$ [L/s] in this reach as follows:

$$Q_{i,j} = Q_{i-1,j}\frac{Q_i}{Q_i + Q_{i,Loss}} = Q_{i-1,j}\frac{Q_i}{Q_{i-1} + Q_{i,Gain}} \tag{8}$$

For Peer Review

where $Q_{i,j}$ [L/s] is the amount of stream water contributed to the discharge leaving reach *i* by any upstream reach *j*, $Q_{i-1,j}$ [L/s] is the stream water contribution to reach *i* -1 from any reach *j*, $Q_{i,Gain}$ [L/s] is the gross gain from groundwater over reach *i*, and Q_i and Q_{i-1} [L/s] are the discharge leaving the downstream end of reach *i*. and *i* -1, respectively. Eq. (8) indicates that the contribution of water from upstream reach decreases in reach *i* when a large portion of stream water in this reach is replenished by gains from or losses to groundwater (i.e., $Q_{i,Gain}$ and/or $Q_{i,Loss}$ becomes large), and vice versa. The contribution to reach *i* by the immediately upstream reach *j* = *i* -1, $Q_{i,i-1}$, can be calculated if the gross gain $Q_{i-1,Gain}$ [L/s] from groundwater in the reach *i* -1 is known (Mallard et al., 2014):

$$Q_{i,i-1} = Q_{i-1,Gain} \frac{Q_i}{Q_{i-1} + Q_{i,\ Gain}} \tag{9}$$

For the uppermost reach (*i* = 1) at the SB stream, $Q_{i-1,Gain}$ was set to the discharge value at weir 1, assuming that stream discharge in this reach mainly originates from groundwater inflow. For all downstream reaches (*i* = 2 to 6), Eq. 8 was applied iteratively to obtain the fractional contributions from all upstream reaches.

4. Results and Discussion

4.1. Spatiotemporal patterns of streamflow

Streamflow (Q) shows a distinct seasonality with low flows in the summer and higher flows in the winter (Figure 2). The substantial increase of cumulative discharge between December 2017 and March 2018 (Figure 2a) indicates that flows during the winter period account for the largest fraction of total annual stream flow. Maximum peak flows typically occur in summer resulting from surface runoff after convective precipitation events. Accordingly, the recession curves are steep and quickly fall back to pre-event conditions (Figure 2b).

In terms of the evolution of discharge along the stream a comparison between the hydrographs from the most upstream weir (W1) and downstream weir (W3) indicates that base flow declined

For Peer Review

between W1 and W3 due to transmission losses along the channel (Figure 2b). This trend of decreasing streamflow in the downstream direction of the SB stream prevailed over most of the monitoring period from June 2017 to August 2018. While relative net losses of base flow were highest during the summer season (up to 90% as compared to 40% during winter), higher total net losses of up to 1.3 L/s occurred during the winter season due to higher base flow at this time.

4.2. Patterns of groundwater heads and groundwater-stream connectivity

Groundwater contour maps based on measured hydraulic heads at the monitoring wells in the shallow alluvial aquifer and at selected stream locations are shown in Figure 3 for representative dates in the winter (January 23rd, 2018) and summer season (August 1st, 2018). According to the contour lines, groundwater flow in both seasons is mainly governed by flow from the hillslopes in the NW and W, and tends to become more parallel to the SB and KB streams in the lower part of the floodplain. In the mid-section, the influence of groundwater inflow from the western hillslopes varies seasonally. While low groundwater heads to the W of the SB stream suggest only minimal groundwater inflow during the summer (Fig. 3b), the more uniform orientation of head contours in winter indicates inflow from the hillslopes over large parts of the western floodplain (Fig. 3a). In the lower part of the study area, contour lines pointing in the upstream direction suggest that groundwater flow converges towards the SB stream from both sides throughout the entire year.

Seasonal variability of heads in single monitoring wells close to the SB stream (e.g., GWS 12 and 19) ranges from 0.7 to 1.3 m. The smallest difference between minimum and maximum groundwater heads of 0.3 m was found in the most northern well (GWS 02) where steady groundwater inflow from the NW dampens seasonal head variations. The highest variation in heads of 1.6 to 2.1 m were observed in wells close to the western fringe of the floodplain (e.g., GWS 11 and 21), probably related to the seasonally variable groundwater inflows from the hillslopes.

For Peer Review

The relative difference between measured elevations of stream stage and nearby groundwater heads (Figure 4) is an indication of the direction and magnitude of the hydraulic gradient between the SB stream and its surrounding groundwater. For that purpose, groundwater heads along hypothetical lines at 10 m distance on each side of the stream were obtained from the interpolated head surfaces in Figure 3. Reaches with groundwater heads below stream stage indicate a potential for stream water losses to the aquifer while the opposite case suggests that the stream is gaining water from groundwater inflows.

During and after recharge by winter precipitation, the hydraulic gradients between the SB and the shallow aquifer are predominantly directed towards the stream. In January 2018, the largest gradients occur at the downstream reaches R4-R6, while in the upstream reaches' gradients are small and groundwater heads are close to the stream stage (Figure 4a). Groundwater heads lower than the stream stage, which indicates local stream water loss to the aquifer, could only be observed along parts of R2 and mainly to the west of the stream. In August 2018 (Figure 4b), groundwater heads are generally lower than stream stages on both sides of the stream from upstream reach R2 until mid of reach R4 indicating substantially larger segments with potentially losing conditions than in the winter season. Gaining conditions continue to prevail at the downstream reaches (second half of R4 to R6), although hydraulic gradients become smaller in August than in January 2018. Generally, the entire studied stream section is characterized by gaining conditions at both upstream (of R1) and downstream ends with a losing section of variable extent in between.

Note that the inference of stream-groundwater exchange from the direction and magnitude of hydraulic gradients between the aquifer and stream is subject to uncertainties, mainly arising from inaccuracies and potential artefacts of the interpolated groundwater head surfaces due to the interpolation method, unknown subsurface heterogeneities, and potentially existing tile drains (e.g., Ohmer et al., 2017). Hence, independent indicators for stream-groundwater exchange patterns were employed to corroborate and refine the results from the head gradient analysis.

For Peer Review

4.3. Radon as indicator of stream water gains from groundwater

The radioactive noble gas radon (^{222}Rn) constitutes a good indicator for groundwater contributions because ^{222}Rn is mainly produced in the aquifer's sediment matrix by the decay of radium-226 contained therein (Glaser et al., 2020). Therefore, profiles of ^{222}Rn activity concentrations were measured along the SB stream (Figure 5a) for an independent characterization of groundwater inflow into the stream at representative dates of the summer and winter seasons. The highest ^{222}Rn activity concentration of 4.8 and 3.8 Bq/L (in the winter and summer season, respectively) was measured at the most upstream sampling location (SB14 in reach R1) close to a focused groundwater input from a spring (Figure 1). The adjacent downstream reaches R2 to R4 are characterized by steadily decreasing concentrations (down to 0.04 Bq/L), while a notable increase in ^{222}Rn (up to 1.7 Bq/L) was observed in the lower part of the studied stream section in reaches R5 and R6. The pattern of ^{222}Rn concentrations along the stream is consistent for both seasons, although during the summer campaign the decrease starting in reach R2 is much steeper, and the subsequent ^{222}Rn increase in R5 and R6 is only weak or absent (Figure 5a). The decrease in ^{222}Rn concentrations along the upstream reaches R1 to R4 is mainly caused by exchange of gaseous ^{222}Rn with the atmosphere and only to a small extend by radioactive decay. The steeper decrease in summer is due to a more pronounced gas exchange resulting from a longer water residence time in the stream segment and a larger surface to volume ratio of the water body (Raymond et al., 2012; Knapp et al., 2019).

Increasing ^{222}Rn concentrations in the stream are attributed to the addition of ^{222}Rn-bearing groundwater from the subsurface. In order to quantify these groundwater inflows, the model FINIFLUX (Frei & Gilfedder, 2015) was applied to the ^{222}Rn data collected along the SB stream and from the alluvial aquifer. The simulated ^{222}Rn concentrations (dashed line in Figure 5a) agree well with measured concentrations and the model yields a cumulative groundwater contribution of 0.25 L/s over reaches R5 and R6 in winter time and of 0.02 L/s in summer time (green bars in Figure 5b). The estimated inflows represent 5 to 25% of total discharge at the downstream weir W3.

For Peer Review

Note that the model simulations assume that ^{222}Rn activity concentrations in groundwater are higher than in stream water and rather homogeneously distributed across the alluvial aquifer. This is the case at the SB site, where measurements of ^{222}Rn in groundwater revealed spatially and temporally uniform concentrations with a mean value of 17.7 ± 2.1 Bq/L (averaged over 11 monitoring wells not influenced by stream water). Only two wells (not included in the average) showed higher ^{222}Rn concentrations of 27 and 38 Bq/L, which most probably are due to local heterogeneities in radium content of the alluvial sediments. The small groundwater inflows indicated by the model between R1 and R4 are within the uncertainty of the ^{222}Rn degassing flux dominating these reaches, and therefore cannot unequivocally interpreted as gross gains over this stream section. The spatially heterogeneous local occurrence of groundwater gains observed at the SB stream corresponds to the findings of previous investigations using ^{222}Rn to quantify groundwater inflow in headwater streams (Schubert et al., 2020).

4.4. Salt tracer injections to assess stream water gains and losses

Stream water losses will not change the concentration of any geochemical tracer present in the remaining water and thus, losing segments can hardly be identified by any concentration profile. Therefore, two series of salt tracer tests were used to quantify gross losses as well as gross gains along six consecutive reaches of the SB stream. The first tracer tests were conducted at the beginning of the recharge period in December 2017, while groundwater levels were already high. Discharge along the stream was between 0.8 and 1.1 L/s. The breakthrough curves from overlapping salt tracer injections in six stream reaches (R1 to R6; Figure 5c) provided total discharge (Eq. 4) as well as gross and net gains (Eq. 7) and losses (Eq. 6) along these reaches. In the upstream reach R1, a net loss of stream water was observed, followed by a small net gain in R2 (Figure 5b). Reaches R3 and R4 showed net losses of water, which amounted for 20% of the upstream inflow from R2. The last two downstream reaches (R5 and R6), again displayed a significant gain of groundwater resulting in an increase in discharge. Overall, discharge along the 535 m long section increased by around 13%.

For Peer Review

The second series of tracer tests was conducted during dry summer conditions in July 2018 when baseflow and groundwater levels were much lower than during the winter season. The loss of water along the tested stream section was pronounced during the second test, when the stream discharge of 0.75 L/s upstream of R1 (at weir W1) decreased by more than 60% by the end of R6 (at W3). The tracer tests indicated net losing conditions for reaches R1 to R4, and R6, with highest gross losses in R2 and R4. Only reach R5 remained as a net gaining reach. As a general pattern, R1 and R4 showed significant net losses of stream water for both seasons, while groundwater gains were observed consistently in R5. These results indicate that net changes in Q are the result of a bidirectional exchange of water between the stream and groundwater over the individual stream reaches.

4.5. General hydrochemistry of stream water and groundwater

Hydrochemical analyses of groundwater and stream water were used to assess the impact of the interlaced gross losses and gross gains leading to hydrologic turnover. Groundwater in most of the monitoring wells at the study site can be classified as calcium-magnesium-bicarbonate-sulfate–type water depicting a neutral to slightly alkaline pH ranging from 6.9 to 7.8. This is in accordance with the predominantly carbonate and gypsum bearing Upper Triassic formations underlying the catchment (D'Affonseca et al. 2020).

Despite the similar hydrochemical characteristics, specific electrical conductivity (EC) revealed a substantial spatial variability between 730 and 2670 µS/cm in the investigated groundwater. The spatial differences are also reflected by ion concentrations, particularly of sulfate (SO_4^{2-}), suggesting that besides agricultural inputs the distribution of the geological formations are the main control of hydrochemical variability in groundwater.

In the upper part of the study area, mean concentrations of SO_4^{2-} in groundwater are in a narrow range of 140-200 mg/L. By contrast, large differences in mean SO_4^{2-} concentrations were observed between the western (50-80 mg/L) and eastern (300-550 mg/L) groundwater in the downstream part (Table 1). Much less variability was observed for chloride (Cl^-) concentrations with an overall range from 9 to 28 mg/L. Only in the downstream part, a small

For Peer Review

difference between the western and eastern groundwater could be observed when using median Cl^- values (Figure 6).

Nitrate concentrations in groundwater and in stream water are generally high (up to 80 mg/L) which is in line with agriculture being the dominant land use (Almasri & Kaluarachchi, 2004). Along the SB stream, nitrate concentrations decrease in the downstream reaches (particularly reaches R5 and R6). In groundwater, nitrate shows a clear spatial pattern with high concentrations (up to 80 mg/L) in the upper (northern) part and close to the hillslopes in the west. In contrast, very low nitrate concentrations (< 2 mg/L) were measured in groundwater wells close to the SB stream along the mid- and downstream reaches and in the eastern part of the alluvial aquifer although agricultural inputs also affect these parts of the study area.

5. Results

5.1. Patterns of stream-groundwater exchange and hydrologic turnover

Overall, the different methods used here to characterize GW-SW exchange fluxes are in good agreement. The combined analyses of water levels, hydraulic gradients, and instream tracer tests reveals a consistent, general pattern of stream-groundwater exchange with net gaining conditions at the up- and downstream ends of the investigated stream segment and a net losing section in between (see Figure 7). This general pattern is corroborated by ^{222}Rn measurements, which consistently showed highest concentrations in the section upstream of R1 and the downstream gaining reaches R4 to R6 due to new inputs from groundwater (Figure 5a). Although the pattern was consistent between winter and summer, the length of the net losing section as well as the intensities of the hydraulic gradients and exchange fluxes showed some seasonal variability. Generally, the length of the losing section expanded during the summer covering parts of the reaches R1 to R3, while the extent of the gaining section at the up- and downstream ends was shrinking (Figure 7).

Despite differences in scale between the different methods and method-specific limitations their combined use provided a relatively consistent picture of exchange patterns at small scales

For Peer Review

and their seasonal dynamics (Figure 7), which might be decisive in shaping stream water composition (Rahimi et al., 2015; Huizenga et al., 2017). The analyzed riparian head-gradients allowed evaluating the general potential for exchange between stream and groundwater (Gu et al., 2008; Voltz et al., 2013) while their combination with ^{222}Rn profiles and instream salt injections allowed us to gain further, valuable insights into the dynamics of bidirectional exchange at sub-reach-scale.

The inferred exchange fluxes indicate that a number of reaches show joint gross losses and gross gains (Figure 5). The observed net changes in stream flow do not have to be caused by gradual losses or gains of water along the entire stream section, but instead are likely to be the result of a series of gross gains and gross losses over individual stream reaches as previously demonstrated by Mallard et al. (2014) and Covino & McGlynn (2007). At SB, the exchange fluxes may be related to small-scale variations of the hydraulic gradient along the reaches (e.g., in R4 during summer; Figure 4b) or may be supported by the simultaneous presence of different hydraulic gradients (e.g., Wroblicky et al., 1998) to the eastern and western sides of the stream (e.g., in reach R3 and R6 during summer; Figure 4b).

Consecutive gains of groundwater and losses of stream water result in an evolution of the stream water source composition. This effect, which has been termed “hydrological turnover” (Mallard et al., 2014), progressively replaces water lost from the stream with groundwater that may have a chemically different signature without a significant change in net stream flow. During the tracer tests in December 2017 only 65% of the SB stream water entering reach R1 (contribution from R_{up}) reached the downstream end of reach R6 close to the confluence with the KB stream (along 535 m reach length) while stream flow increased along the same stream segment by about 10% (Figure 8). The pronounced replacement (or turnover) of water in the stream indicated by the diminished fraction of stream water from upstream reaches at the downstream end of R6 was due to substantial net gains from groundwater in R5 and R6. A comparable decline (more than 60%) in the relative fraction of stream water from upstream R1 occurred at the downstream end of R6 during the tracer test in July 2018 although enhanced stream water losses resulted in a concomitant decline in total stream flow of about 40%. This

For Peer Review

significant hydrologic turnover at the SB stream in both seasons will also affect the chemical composition of the stream water as well as of the adjacent groundwater.

5.2. Impact of hydrological turnover on nitrate in stream water

Stream water quality can be impacted by mixing with groundwater inflows (Wherry et al. 2021), or by reactive processes occurring instream or during hyporheic exchange fluxes (Zarnetske et al., 2015; Trauth et al., 2015). In this study, no distinction was made between conventional groundwater fluxes (recharged by precipitation) and larger scale hyporheic exchange, which might represent part of the observed gains in the downstream section. Nitrate as a potential driver of eutrophication was chosen as a meaningful indicator of stream water quality.

Under the assumption that mixing dominates, the resulting stream water chemistry will depend on which of the distinct groundwater components (western or eastern side) contributes most. The strong contrast in SO_4^{2-} concentrations in groundwater in conjunction with the changes along the SB stream were used in Eq. (3) to quantify the relative contribution f_{GW} and f_{GE} of the two different groundwater endmembers on the western and the eastern side, respectively. For each of the investigated stream reaches, the required average SO_4^{2-} concentration in groundwater at both sides was calculated from data collected from groundwater wells adjacent to these reaches over the summer and winter season (Table 1). The increase in SO_4^{2-} concentration of stream water at lower reaches (Figure 6) implies an enhanced inflow of sulfate-rich groundwater from the East. This is confirmed by the estimated f_{GW} and f_{GE} values shown in Figure 9, revealing that eastern groundwater contributions rise from only 20% in the upstream reaches to more than 80% at the most downstream reach. Using the relative groundwater contributions from Figure 9, hypothetical concentrations of the conservative ion chloride and of the potentially reactive ion nitrate along the SB stream were derived by applying the mass balance underlying Eq. (2) to the experimentally determined water exchange fluxes and measured upstream concentrations (Fig. 8, dashed lines).

For Peer Review

These simulated profiles represent the change in instream ion concentrations given hydrologic turnover is the only process affecting chloride and nitrate during transport. They compare well with the observed concentrations along the stream for both ions (Fig. 8) and lie within the analytical uncertainties for both ions. A good agreement is expected for chloride, which is transported conservatively. Although a clear contrast in chloride concentrations is present between the different groundwater endmembers at the downstream reaches, the low difference between chloride in stream water and the upstream groundwater bodies limits the sensitivity of chloride as an indicator of unaccounted water fluxes.

Similar to Cl^-, there is also a good agreement between simulated and observed NO_3^- concentrations along the SB stream (Figure 6b). An exception are the downstream reaches in the summer period, where measured values are higher than the model prediction. The difference cannot be explained by instream nitrate attenuation (e.g., denitrification or plant uptake) as this would lead to observed values lower than in the model. A possible reactive process that could counteract dilution with nitrate-poor gains is oxidation of ammonium at the groundwater-stream interface (Triska et al., 1993; Butturini et al., 2000). The comparison of measured and modelled data suggests that the observed decrease in nitrate concentrations in downstream direction is dominantly controlled by hydrologic turnover. Without knowledge of groundwater gains and stream water losses, decreasing NO_3^- concentrations along the stream with only marginally changing discharge could have easily been misinterpreted as evidence for reactive processes removing NO_3^- from stream water. Instead, our data and analyses suggest that nitrate removal by instream processes (Ranalli & Macalady, 2010; Miller et al., 2015) or nitrate degradation at the stream-groundwater interface (Puckett et al., 2008) may be of subordinate importance for the evolution of longitudinal nitrate concentration profiles in the stream at the investigated site.

5.3. Impact of hydrologic turnover on nitrate in groundwater

The distribution of NO_3^- concentrations in groundwater, outlined in Figure 10 for the end of the dry summer/fall 2018 and for late winter/early spring 2019, depicts a relatively sharp front

For Peer Review

restricting high NO_3^- concentrations to the North and the West of the floodplain. The subsequent mid- and downstream sections of the aquifer are characterized by low to non-detectable nitrate concentrations in groundwater over the entire period from 2017 to 2019. A comparison of the location of the strong NO_3^- gradient with the spatial patterns of stream-groundwater exchange (Figure 7) suggests that stream water losses may also have an imprint on the near-stream groundwater concentrations of nitrate.

A distinct shift of the nitrate front in groundwater over time is indicated by strong seasonal variations in NO_3^- concentrations in some groundwater monitoring wells close to the SB stream (e.g., GWS12; Figure 10c). Nitrate in most of the other individual wells remained almost constant (although at different levels). The NO_3^- variations in GWS12 coincide with changes in hydraulic conditions and the general hydrochemistry of groundwater at these locations. This suggests an effect of seasonally varying groundwater flow patterns and hydrologic turnover on the NO_3^- distribution in groundwater (Figure 10).

The low nitrate concentrations at GWS12 during late summer until December 2018 may be caused by seasonally varying nitrate reduction within the aquifer (Clément et al., 2003, Lutz et al. 2020) or by seasonally varying inflows of groundwater that have passed through reactive sediments in the riparian or hyporheic zones (Vidon & Hill, 2004; Harvey et al., 2013). This is supported by the low dissolved oxygen concentrations of <2 mg/L and low NO_3^-/Cl^- ratios (Table 1) at GWS12 indicating reducing conditions. We hypothesize that supply of organic carbon via infiltrating stream water facilitates the biogeochemical degradation of nitrate (denitrification) in the transition zone between stream and riparian aquifer. This is supported by the rapid decrease in NO_3^- concentration, with concurrent increase in nitrite (and ammonium) in the first 30 cm of the SB streambed sediment (Figure 11) near the location of the well GWS12. Given the substantial losses of stream water during summer 2018 in this reach (R2; Figure 5b), the significant decline in NO_3^- concentrations at GWS12 (Figure 10c) are attributed to the increased dilution with infiltrating nitrate-reduced stream water resulting from the steeper head gradients from the stream to groundwater over this time period. In

For Peer Review

contrast, rising groundwater tables in late winter and spring lead to a displacement of the low-nitrate groundwater at GWS12 with NO_3^--rich groundwater from the Northwest (Figure 10c). The continuing stream water infiltration further downstream in reaches R3 and R4 (Figure 7) similarly contributes to the extended presence of low NO_3^- concentrations in the aquifer. Denitrification along flow paths of water infiltrating from the stream after sufficient depletion of oxygen has been reported for streambed sediments (Harvey et al., 2013) as well as for zones further into the riparian aquifer (Trauth et al., 2018; Nogueira et al., 2021).

However, the large extent of the region with low NO_3^- concentration in the alluvial aquifer at the study site suggests that in addition to substantial stream water losses, low NO_3^- values in the near-stream groundwater are likely also related to the overall nitrate reduction potential of the floodplain aquifer itself. Efficient denitrification in riparian aquifers is often facilitated be abundant organic matter as an electron donor paired with the evolution of anaerobic zones (Vidon & Hill, 1994, Ranalli & Macalady, 2010; Wherry et al., 2021), but may also be affected by stream water infiltration via delivery of labile organic matter or thermal effects (Trauth et al. 2018). The findings of this study suggest that hydrologic turnover not only changes stream water chemistry, but may also affect the composition of near-stream groundwater at sub-seasonal to seasonal time scales.

6. Conclusions

Using a suite of complementary field methods, we could demonstrate how seasonally varying bi-directional exchange of water and solutes between groundwater and a first order agricultural stream decisively shapes the chemical composition of stream water along a 500m stream segment. The combined use of different methods, with specific merits and limitations, could provide a relatively consistent picture of macroscopic exchange patterns and their seasonal dynamics, while at the same time yielding additional information on water sources and bidirectional exchange volumes. Based on quantified gross losses and gains over all reaches, observed longitudinal instream concentration profiles of nitrate and chloride could be reproduced well using endmember mixing. This suggests that in first-order streams, where

For Peer Review

large fractions of stream flow are made-up of groundwater from the adjoining riparian aquifer, bi-directional exchange of water between the stream and groundwater and the resulting hydrologic turnover are key controls for the seasonal evolution of stream water composition. These findings may also provide a new perspective on instream processing in small agricultural streams, which is often used to explain longitudinal concentration changes (Rahimi et al., 2015; Huizenga et al. 2017). Finally, our results indicate that bidirectional water and solute exchange might also affect near stream groundwater composition, something also reported by Trauth et al. (2018) for a higher order stream. Such changes in groundwater composition may in turn affect the source composition of groundwater inflows to the stream further downstream. Understanding such feedbacks will require further investigations, potentially using transient flow and reactive transport models.

For Peer Review

Acknowledgements

This study was supported by the German Research Foundation (DFG) funded Collaborative Research Centre 1253 CAMPOS (DFG Grant Agreement SFB 1253/1). Additional funding was provided by the 3rd phase of the Helmholtz Research Program (POFIII), Integrated Project “Water and Matter Flux Dynamics in Catchments”. Special thanks go to Sara Cafisso, Bernice Nisch, and Annegret Walz for support in the laboratory, and to Marc Jantz and Toralf Keller for technical support during fieldwork.

Data availability

Data sharing is not applicable to this article.

References

Alexander, R. B., Boyer, E. W., Smith, R. A., Schwarz, G. E., & Moore, R. B. (2007). The role of headwater streams in downstream water quality. *Journal of American Water Resources Association*, **43**(1), 41- 59.

Almasri, M. N., & Kaluarachchi, L. J. (2004). Assessment and management of long-term nitrate pollution of ground water in agriculture-dominated watersheds. *Journal of Hydrology*, **295**, 225- 245.

Anibas, C., Schneidewind, U., Vandersteen, G., Joris, I., Seuntjens, P., & Batelaan, O. (2016). From streambed temperature measurements to spatial-temporal flux quantification: using the LPML method to study groundwater–surface water interaction. *Hydrological Processes*, **30**(2), 203- 216.

Atkinson, A. P., Cartwright, I., Gilfedder, B. S., Hofmann, H., Unland, N. P., Cendón, D. I., & Chisari, R. (2015). A multi-tracer approach to quantifying groundwater inflows to an upland river; assessing the influence of variable groundwater chemistry. *Hydrological Processes*, **29**, 1- 12.

Briggs, M. A., Lautz, L. K., & Hare, D. H. (2014). Residence time control on hot moments of net nitrate production and uptake in the hyporheic zone. *Hydrological Processes*, **28**(11), 3741- 3751.

Burt, T. P., Matchett, L. S., Goulding, K. W. T., Webster, C. P., & Haycock, N. E. (1999). Denitrification in riparian buffer zones: the role of floodplain hydrology. *Hydrological Processes*, **13**(10), 1451- 1463.

Butturini, A., Battin, T. J., & Sabater, F. (2000). Nitrification in stream sediment biofilms: the role of ammonium concentration and DOC quality. *Water Research,* **34**(2), 629- 639.

Cardenas, M. B., & Wilson, J. L. (2006). The influence of ambient groundwater discharge on exchange zones induced by current–bedform interactions. *Journal of Hydrology*, **331**, 103- 109.

Cartwright, I., & Gilfedder, B. (2015). Mapping and quantifying groundwater inflows to Deep Creek (Maribyrnong catchment, SE Australia) using ^{222}Rn, implications for protecting groundwater-dependant ecosystems. *Applied Geochemistry*, **52**, 118- 129.

For Peer Review

Cirpka, O. A., Fienen, M. N., Hofer, M., Hoehn, E., Tessarini, A., Kipfer, R., & Kitanidis, P. K. (2007). Analyzing Bank Filtration by Deconvoluting Time Series of Electric Conductivity. *Groundwater*, **45**(3), 318- 328.

Clément, J.-C., Aquilina, L., Bour, O., Plaine, K., Burt, T. P., & Pinay, G. (2003). Hydrological flowpaths and nitrate removal rates within a riparian floodplain along a fourth-order stream in Brittany (France). *Hydrological Processes*, **17**, 1177- 1195.

Cook, P.G. (2013). Estimating groundwater discharge to rivers from river chemistry surveys. *Hydrological Processes*, **27**(25), 3694- 3707.

Covino, T. P., & McGlynn, B. L. (2007). Stream gains and losses across a mountain-to-valley transition: Impacts on watershed hydrology and stream water chemistry. *Water Resources Research*, **43**(10), 1- 14.

Covino, T. P., McGlynn, B. L., & Mallard, J. (2011). Stream-groundwater exchange and hydrologic turnover at the network scale. *Water Resources Research*, **47**, 1- 11.

D'Affonseca, F.M., Finkel, M. & Cirpka, O.A., 2020. Combining implicit geological modeling, field surveys, and hydrogeological modeling to describe groundwater flow in a karst aquifer. *Hydrogeology Journal*, **28**,2779–2802.https://doi.org/10.1007/s10040-020-02220-z

Deutscher Wetterdienst - DWD. xxx. https://www.dwd.de/.

Deutsches Institut für Normung (1993). Water quality; Determination of electrical conductivity (ISO 7888: 1985); German Version EN 27888.

Duff, J.H., Murphy, F., Fuller, C.C., Triska, F.J., Harvey, J.W., Jackman, A.P. (1998). A mini drivepoint sampler for measuring pore water solute concentrations in the hyporheic zone of sand-bottom streams. *Limnology and Oceanography*, **43**(6), 1378-1383.

Fleckenstein, J. H., Krause, S., Hannah, D. M., & Boano, F. (2009). Groundwater-surface water interactions: New methods and models to improve understanding of processes and dynamics. *Advances in Water Resources*, **33**(11), 1291- 1295.

Frederiksen, R. R., Christensen, S., & Rasmussen, K. R. (2018). Estimating groundwater discharge to a lowland alluvial stream using methods at point-, reach-, and catchment-scale. *Journal of Hydrology*, **564**, 836- 845.

For Peer Review

Frei, S., Fleckenstein, J. H., Kollet, S. J., & Maxwell, R. M. (2009). Patterns and dynamics of river–aquifer exchange with variably-saturated flow using a fully-coupled model. *Journal of Hydrology*, **375**, 383- 393.

Frei, S., & Gilfedder, B. S. (2015). FINIFLUX: An implicit finite element model for quantification of groundwater fluxes and hyporheic exchange in streams and rivers using radon, *Water Resour. Res.*, **51**, 6776–6786, https://doi: 10.1002/2015WR017212.

Fox, A., Laube, G., Schmidt, C., Fleckenstein, J. H., & Arnon, S. (2016). The effect of losing and gaining flow conditions on hyporheic exchange in heterogeneous streambeds. *Water Resources Research*, **52**, 7460- 7477.

Glaser, C., Schwientek, M., Junginger, T., Gilfedder, B.S., Frei, S., Werneburg, M., Zwiener, C., Zarfl, C. (2020). Comparison of environmental tracers including organic micropollutants as groundwater exfiltration indicators into a small river of a karstic catchment. *Hydrological Processes*, **34** (24), 4712-4726.

Gonzalez-Pinzon, R., Ward, A. S., Hatch, C. E., Wlostowski, A. N., Singha, K., Gooseff, M. N., Haggerty, R., Harvey, J. W., Cirpka, O. A., & Brock, J. T. (2015). A field comparison of multiple techniques to quantify groundwater-surface-water interactions. *Freshwater Science*, **34**(1), 139- 160.

Gu, G., Hornberger, G.M., Herman, J.S., Mills, A.L. (2008). Influence of stream-groundwater interactions in the streambed sediments on NO3− flux to a low-relief coastal stream. *Water Resources Research*, **44**(11). W11432, doi:10.1029/2007WR006739

Harvey, J. W., Wagner, B. J., & Bencala, K. E. (1996). Evaluating the Reliability of the Stream Tracer Approach to Characterize Stream-Subsurface Water Exchange. *Water Resources Research*, **32**(8), 2441- 2451.

Harvey, J. W., Bohlke, J. K., Voytek, M. A., Scott, D., & Tobias, C. R. (2013). Hyporheic zone denitrification: Controls on effective reaction depth and contribution to whole-stream mass balance. *Water Resources Research*, **49**(10), 6298- 6316.

For Peer Review

Hatch, C. E., Fisher, A. T., Revenaugh, J. S., Constantz, J., & Ruehl, C. (2006). Quantifying surface water-groundwater in-teractions using time series analysis of streambed thermalrecords: Method development, *Water Resources Research*, **42**, W10410.

Henault-Ethier, L., Larocque, M., Perron, R., Wiseman, N., Labrecque, M. (2017). Hydrological heterogeneity in agricultural riparian buffer strips. *Journal of Hydrology*, **546**, 276- 288.

Henderson, F. M. (1966). Open channel flow. New York: Macmillan.

Hester, E. T., Cardenas, M. B., Haggerty, R., & Apte, S. V. (2017). The importance and challenge of hyporheic mixing. *Water Resources Research*, **53**(5), 3565- 3575.

Hoagland, B., Russo, T. A., Gu, X., Hill, L., Kaye, J., Forsythe, B., & Brantley, S. L. (2017). Hyporheic zone influences on concentration-discharge relationships in a headwater sandstone stream. *Water Resources Research*, **53**(6), 4643- 4667.

Huizenga, A., Bailey, R. T., & Gates, T. K. (2017). Stream-aquifer and in-stream processes affecting nitrogen along a major river and contributing tributary. *Journal of Contaminant Hydrology*, **199**, 24- 35.

Kaandorp, V. P., Molina-Navarro, E., Andersen, H. E., Bloomfield, J. P., Kuijper, M. J. M., & de Louw, P. G. B. (2018). A conceptual model for the analysis of multi-stressors in linked groundwater–surface water systems. *Science of the Total Environment*, **627**, 880- 895. https://doi.org/10.1016/j.scitotenv. 2018.01.259

Kalbus, E., Reinstorf, F., & Schirmer, M. (2006). Measuring methods for groundwater – surface water interactions: a review. *Hydrology and Earth System Sciences*, **10**(6), 873- 887.

Kelleher, C., Ward, A., Knapp, J. L. A., Blaen, P. J., Kurz, M. J., Drummond, J. D., Zarnetske, J. P., Hannah, D. M., Mendoza-Lera, C., Schmadel, N. M., Datry, T., Lewandowski, J., Milner, A. M., & Krause, S. (2019). Exploring Tracer Information and Model Framework Trade-Offs to Improve Estimation of Stream Transient Storage Processes. *Water Resources Research*, **55**(4), 3481- 3501.

Kilpatrick, F. A., & Cobb, E. D. (1985). Measurement of Discharge Using Tracers. U.S. Geological Survey Techniques of Water-Resources Investigations.

For Peer Review

Knapp, J. A., Osenbrück, K., Brennwald, M. S., & Cirpka, O. A. (2019). In-situ mass spectrometry improves the estimation of stream reaeration from gas-tracer tests. *Science of the Total Environment*, **655**, 1062- 1070.

Lee, J. M., & Kimm, G. (2006). A simple and rapid method for analyzing radon in costal and ground waters using a radon-in-air monitor. *Journal of Environmental Radioactivity*, **89**, 219-228.

Lutz, S.R., Trauth, N., Musolff, A., van Breukelen, B.M., Knöller, K., Fleckenstein, J.H., (2020). How important is denitrification in riparian zones? Combining end-member mixing and isotope modeling to quantify nitrate removal from riparian groundwater. *Water Resources Research* **56** (1), e2019WR025528. https://doi.org/10.1029/2019WR025528

Mallard, J., McGlynn, B. L., & Covino, T. P. (2014). Lateral inflows, stream-groundwater exchange, and network geometry influence stream water composition. *Water Resources Research*, **50**, 4603- 4623.

Maxwell, R. M., Condon, L. E., Kollet, S. J., Maher, K., Haggerty, R., & Forrester, M. M. (2016). The imprint of climate and geology on the residence times of groundwater. *Geophysical Research Letters*. **43**(2), 701- 708.

Mazurek, M., Kruszyk, R., & Szpikowska, G. (2020). Source-to-mainstream: Hydrochemical water changes in a channel head in the young glacial area (Pomeranian Lakeland, Poland). *Geomorphology*, **371**, 107445.

Miller, M. P., Tesoriero, A. J., Capel, P. D., Pellerin, B. A., Hyer, K. E., & Burns, D. A. (2015). Quantifying watershed-scale groundwater loading and in-stream fate of nitrate using high-frequency water quality data. *Water Resources Research*, **52**(1), 330- 347.

Musolff, A., Fleckenstein, J. H., Rao, P. S. C., & Jawitz, J. W. (2017). Emergent archetype patterns of coupled hydrologic and biogeochemical responses in catchments. *Geophysical Research Letters*. **44**(9), 4143- 4151.

Nogueira, G. E. H., Schmidt, C., Trauth, N., & Fleckenstein, J. H. (2021). Seasonal and short-term controls of riparian oxygen dynamics and the implications for redox processes. *Hydrological Processes*, **35**(2).

For Peer Review

O'Connor, D.J., & Dobbins, W.E., (1958). Mechanism of Reaeration in Natural Streams. *Transactions of the American Society of Civil Engineers*, **123** (1), 641-666.

Oh, Y. H., Koh, D. C., Kwon, H. I., Jung, Y. Y., Lee, K. Y., Yoon, Y. Y., Kim, D. H., Moon, H. S., & Ha, K. (2021). Identifying and quantifying groundwater inflow to a stream using Rn-220 and Rn-222 as natural tracers. *Journal of Hydrology - Regional Studies*, **33**, 100773.

Ohmer, M., Liesch, T., Goeppert, N., & Goldscheider, N. (2017). On the optimal selection of interpolation methods for groundwater contouring: An example of propagation of uncertainty regarding inter-aquifer exchange. *Advances in Water Resources*, **109**, 121- 132.

Osenbrück, K., Wöhling, T., Lemke, D., Rohrbach, N., Schwientek, M., Leven, C., Castillo Alvarez, C., Taubald, H., & Cirpka, O. A. (2013). Assessing hyporheic exchange and associated travel times by hydraulic, chemical, and isotopic monitoring at the Steinlach Test Site, Germany. *Environmental Earth Sciences*, **69**, 359- 372.

Payn, R. A., Gooseff, M. N., McGlynn, B. L., Bencala, K. E., & Wondzell, S. M. (2009). Channel water balance and exchange with subsurface flow along a mountain headwater stream in Montana, United States. *Water Resources Research*, **45**, 1- 14.

Penna, D., van Meerveld, H. J., Oliviero, O., Zuecco, G., Assendelft, R. S., Dalla Fontana, G., & Borga, M. (2015). Seasonal changes in runoff generation in a small forested mountain catchment. *Hydrological Processes*, **29**(8), 2027- 2042.

Peterson, B. J., Wollheim, W. M., Mulholland, P. J. et al., & Morrall, D. D. (2001). Control of nitrogen export from watersheds by headwater streams. *Science*, **292**(80), 86- 90.

Puckett, L. J., Zamora, C., Essaid, H., Wilson, J. T., Johnson, H. M., Brayton, M. J., & Vogel, J. R. (2008). Transport and fate of nitrate at the ground-water/surface-water interface. *Journal of Environmental Quality*, **37**(3) 1034- 1050.

Rahimi, M., Essaid, H. I., & Wilson, J. T. (2015). The role of dynamic surface water-groundwater exchange on streambed denitrification in a first-order, low-relief agricultural watershed. *Water Resources Research*, **51**(12), 9514- 9538.

Ranalli, A. J., & Macalady, D. L. (2010). The importance of the riparian zone and in-stream processes in nitrate. *Journal of Hydrology*, **389**, 406- 415.

For Peer Review

Raymond, P. A., Zappa, C. J., Butman, D., Bott, T. L., Potter, J., Mulholland, P., Laursen, A. E., McDowell, W. H., & Newbold, D. (2012). Scaling the gas transfer velocity and hydraulic geometry in streams and small rivers. *Limnology and Oceanography: Fluids and Environments*, **2**, 41- 53.

Ruehl, C., Fisher, A. T., Hatch, C., Los Huertos, M., Stemler, G., & Shennan, C. (2006). Differential gauging and tracer tests resolve seepage fluxes in a strongly-losing stream. *Journal of Hydrology*, **330**, 235- 248.

Ruiz, L., Abiven, S., Martin, C., Durand, P., Beaujouan, V., & Molénat, J. (2002). Effect on nitrate concentration in streamwater of agricultural practices in small catchments in Brittany. II: temporal variations and mixing processes. *Hydrology and Earth System Sciences*, **6**, 507-513.

Schmidt, C., Bayer-Raich, M., & Schirmer, M. (2006). Characterization of spatial heterogeneity of groundwater-stream water interactions using multiple depth streambed temperature measurements at the reach scale. *Hydrological and Earth Systems Science*, 10(6), 849-859.

Schmidt, C., Musolff, A., Trauth, N., Vieweg, M., & Fleckenstein, J. H. (2012). Transient analysis of fluctuations of electrical conductivity as tracer in the stream bed. *Hydrological and Earth Systems Science*, **16**(10), 3689- 3697.

Schubert, M., Knoeller, K., Mueller, C., Gilfedder, B. (2020). Investigating river water/ groundwater interaction along a rivulet section by ^{222}Rn mass balancing. *Water*, **12**, 3027.

Thompson, S. E., Basu, N. B., Lascurain, J., Aubeneau, A., & Rao, P. S. C. (2011). Relative dominance of hydrologic versus biogeochemical factors on solute export across impact gradients. *Water Resources Research*, **47**, W00J05.

Trauth, N., Schmidt, C., Vieweg, M., Oswald, S. E., & Fleckenstein, J. H. (2015). Hydraulic controls of in-stream gravel bar hyporheic exchange and reactions. *Water Resources Research*, **51**(4), 2243- 2263.

For Peer Review

Trauth, N., Musolff, A., Knöller, K., Kaden, U. S., Keller, T., Werban, U., & Fleckenstein, J. H. (2018). River water infiltration enhances denitrification efficiency in riparian groundwater. *Water Research*, **130**, 185- 199.

Triska, F. J., Duff, J. H., & Avanzino, R.J. (1993). The role of water exchange between a stream channel and its hyporheic zone in nitrogen cycling at the terrestrial-aquatic interface. *Hydrobiologia*, **251**, 167- 184.

Vidon, P. G. F., & Hill, A. R. (2004). Landscape controls on nitrate removal in stream riparian zones. *Water Resources Research*, **40**(3), W03201.

Voltz, T., Gooseff, M. N., Ward, A. S., Shinga, K., Fitzgerald, M., and Wagener, T. (2013). Riparian hydraulic gradient and stream-groundwater exchange dynamics in steep headwater valleys. *J. Geophys. Res. Earth Surf.,* 118, 953-9369, doi:10.1002/jgrf.20074.

Ward, A. S., Payn, R. A., Gooseff, M. N., McGlynn, B. L., Bencala, K. E., Kelleher, C. A., & Wondzell, S. M. (2013). Variations in surface water-ground water interactions along a headwater mountain stream: Comparisons between transient storage and water balance analyses. *Water Resources Research*, **49**(6), 3359- 3374.

Wherry, S. A., Tesoriero, A. J., & Terziotti, S. (2021). Factors Affecting Nitrate Concentrations in Stream Base Flow. *Environmental Science & Technology*, **55**(2), 902- 911.

Wriedt, G., Spindler, J., Neef, T., Meißner, R., & Rode, M. (2007). Groundwater dynamics and channel activity as major controls of in-stream nitrate concentrations in a lowland catchment system? *Journal of Hydrology*, **343**, 154- 168. https://doi.org/10.1016/j.jhydrol. 2007.06.010

Wroblicky, G. J., Campana, M. E., Valett, H. M., & Dahm, C. N. (1998). Seasonal variation in surface-subsurface water exchange and lateral hyporheic area of two stream-aquifer systems. *Water Resources Research*, **34**(3), 317- 328.

Zarnetske, J. P., Haggerty, R., & Wondzell, S. M. (2015). Coupling multiscale observations to evaluate hyporheic nitrate removal at the reach scale. *Freshwater Science*, **34**(1), 172- 186.

Zhang, Z.Y. Schmidt, C., Nixdorf, E., Kuang, X. and Fleckenstein J.H., (accepted), Effects of Heterogeneous Stream-Groundwater Exchange on the Source Composition of Stream Discharge and Solute Load. *Water Resources Research*.

For Peer Review

Zhou, T., Bao, J., Huang, M. Y., Hou, Z. S., Arntzen, E., Song, X. H., Harding, S. F., Titzler, P. S., Ren, H. Y., Murray, C. J., Perkins, W. A., Chen, X. Y., Stegen, J. C., Hammond, G. E., Thorne, P. D., & Zachara, J. M. (2018). Riverbed Hydrologic Exchange Dynamics in a Large Regulated River Reach. *Water Resources Research*, **54**(4), 2715- 2730.

For Peer Review

Tables

Table 1

Mean concentrations and standard deviations of major anions in stream water and groundwater at the investigated reaches of the SB study site for the winter (W) and summer (S) seasons, respectively.

Stream reach:		R_{up}	R1	R2	R3	R4	R5	R6
Stream water:		Spring	SB14	SB17	SB22	SB26	SB32	SB36	SB40
Cl [mg/L]	W	17 ± 2	16 ± 2	16 ± 2	16 ± 2	17 ± 2	16 ± 3	16 ± 3	16 ± 2
	S	19 ± 3	17 ± 2	16 ± 2	18 ± 4	17 ± 2	17 ± 3	16 ± 2	17 ± 5
SO_4 [mg/L]	W	166 ± 22	152 ± 27	152 ± 28	151 ± 15	151 ± 26	149 ± 28	163 ± 33	199 ± 52
	S	188 ± 35	158 ± 22	158 ± 24	159 ± 22	157 ± 20	156 ± 30	169 ± 34	194 ± 42
NO_3 [mg/L]	W	49 ± 5	48 ± 5	48 ± 5	45 ± 3	48 ± 6	45 ± 7	43 ± 7	36 ± 6
	S	55 ± 11	51 ± 7	49 ± 7	52 ± 10	49 ± 7	49 ± 7	47 ± 11	45 ± 6
Cl/NO_3	W	0.6	0.6	0.6	0.6	0.6	0.6	0.6	0.8
	S	0.6	0.6	0.6	0.6	0.6	0.6	0.7	0.7
GW West:		GWS02	GWS04	GWS12	GWS11	GWS16	GWS19	GWS22	GWS23
Cl [mg/L]	W	18 ± 1	14 ± 1	15 ± 2	8 ± 2	19 ± 1	13 ± 2	14 ± 5	14 ± 2
	S	18 ± 1	14 ± 1	15 ± 1	15 ± 3	21 ± 2	15 ± 1	16 ± 3	14 ± 2
SO_4 [mg/L]	W	164 ± 14	125 ± 8	152 ± 30	46 ± 10	48 ± 5	71 ± 25	65 ± 24	155 ± 30
	S	177 ± 17	135 ± 12	152 ± 18	91 ± 47	53 ± 14	48 ± 10	52 ± 6	151 ± 27
NO_3 [mg/L]	W	52 ± 5	55 ± 3	20 ± 17	25 ± 5	2 ± 1	26 ± 9	14 ± 6	1 ± 1
	S	57 ± 6	55 ± 4	14 ± 12	32 ± 2	3 ± 2	33 ± 8	17 ± 5	2 ± 1
Cl/NO_3	W	0.6	0.5	3.2	0.6	46	1.0	2.2	38
	S	0.5	0.4	4.3	0.8	20	0.8	1.7	16
GW East:			GWS06	GWS07	GWS09	GWS15	GWS17	GWS25	
Cl [mg/L]	W		18 ± 2	16 ± 2	27 ± 3	15 ± 2	12 ± 1	19 ± 2	
	S		18 ± 2	16 ± 1	28 ± 3	16 ± 1	12 ± 1	25 ± 10	
SO_4 [mg/L]	W		164 ± 17	167 ± 23	1170 ± 240	167 ± 19	467 ± 31	526 ± 43	
	S		189 ± 17	164 ± 18	1310 ± 70	194 ± 42	475 ± 64	480 ± 61	
NO_3 [mg/L]	W		41 ± 8	9 ± 6	55 ± 3	1 ± 1	3 ± 4	1 ± 1	
	S		56 ± 2	5 ± 4	55 ± 4	2 ± 1	7 ± 6	2 ± 3	
Cl/NO_3	W		0.8	11.6	611	151	180	186	
	S		0.6	14.4	183	20	5.9	234	

For Peer Review

Figure legends

Figure 1

Location of the Schönbrunnen study site including the field installations (weirs, sampling sites, and monitoring wells) for continuous stream and groundwater monitoring.

Figure 2

(a) Comparison of cumulative discharge Q at weir W2 with weekly precipitation P in the catchment. The dotted section of cumulative Q in June and July 2018 was extrapolated from W3 because of missing data. Dashed lines A and B indicate the times at which hydraulic head contours are depicted in Figure Groundwater head contours based on interpolation (natural neighbor) from monitored hydraulic heads at the groundwater monitoring wells in the alluvial aquifer for representative dates in the (a) winter season (23. January 2018) and (b) summer season (01. August 2018).
4, and T1 and T2 the time at which salt tracer tests were carried out at the SB stream. (b) Hydrographs of typical summer (left panel) and winter (right panel) events measured at the most upstream and downstream weirs W1 and W3, respectively.

Figure 3

Groundwater head contours based on interpolation (natural neighbor) from monitored hydraulic heads at the groundwater monitoring wells in the alluvial aquifer for representative dates in the (a) winter season (23. January 2018) and (b) summer season (01. August 2018).

Figure 4

Comparison of groundwater heads and surface water elevation for representative dates in the (a) winter season (23. January 2018) and (b) summer season (01. August 2018). The blue line indicates the stream stage estimated from average water depth in the stream and streambed elevation measurements. The intervals between measured points were linearly interpolated. The two dashed lines depict groundwater head elevations along two hypothetical lines parallel to the stream, both 10 meters away from the stream in western (green line) and eastern (read line) directions.

Figure 5

(a) Measured (symbols) and simulated (dashed line) Radon-222 activity concentrations in stream water collected in February and July 2018 as representative dates of the two considered seasons. (b) Stream discharge, gross water losses, and gross gains over individual stream reaches R1 to R6 estimated from

For Peer Review

consecutive instream salt tracer tests. The additional green bars show the ^{222}Rn-derived gross gains from groundwater inflows for comparison. (c) Location of the individual reaches (R1 to R6) along the SB stream together with points of tracer injection and monitoring sites (SB14 to SB40) for tracer breakthrough curves, ^{222}Rn, and hydrochemistry.

Figure 6

Mean sulfate, chloride, and nitrate concentrations in stream water (in flow direction) at seven sampling sites bounding the stream reaches R1 to R6 for (a) the summer and (b) winter season. Grey shaded areas represent the inter-quartile ranges of the ions in groundwater at the western (light grey) and eastern (dark grey) sides of the SB stream. For chloride and nitrate, simulated concentrations of these ions are shown for comparison (dashed lines).

Figure 7

Summary of stream-groundwater exchange patterns derived by the different monitoring approaches during the winter (W) and summer (S) seasons. The size of the gain and loss arrows indicates the magnitude of the exchange flux. Not significant fluxes are indicated as 'not sig.'.

Figure 8

Contributions of stream water in the individual reaches (R1 to R6) from upstream reaches based on measured discharge (red line) and estimates of gross gains and losses using Eq. (8) and Eq. (9). R_{up} represents the section upstream of R1. Water losses from the stream can be compensated by gains from groundwater leading to a "hydrologic turnover" of stream water composition.

Figure 9

Relative contributions f_{GW} and f_{GE} to stream discharge from the western and eastern groundwater bodies, respectively. Values are based on sulfate concentrations and gross groundwater gains at the individual reaches. The values of gross gains and gross losses of stream water were taken from the two salt tracer experiments assuming that the results represent averaged seasonal exchange fluxes.

Figure 10

Spatial distribution of nitrate concentrations in groundwater along the SB stream for two dates in different seasons: (a) December 2018, (b) April 2019. Blue arrows indicate different groundwater flow paths leading to distinct nitrate concentrations at the indicated monitoring wells over time. (c) Comparison of the nitrate concentration time series and groundwater levels at well GWS12.

For Peer Review

Figure 11

Concentration profiles of N species (NO_3^- , NO_2^- , and NH_4^+) in streambed sediment in reach R2, where losing conditions prevailed during the summer period. The right panel zooms in on the low concentrated minor N species (different scale).

For Peer Review

Groundwater-surface water exchange and hydrologic turnover as key controls for instream and groundwater nitrate concentrations in first-order agricultural stream catchments

Oscar Jimenez-Fernandez *, Marc Schwientek, Karsten Osenbrück, Clarissa Glaser, Christian Schmidt, Jan H. Fleckenstein *

Graphical abstract:

Bi-directional exchange of water and solutes between groundwater and a first order stream (hydrologic turnover) significantly shapes the chemical composition of the stream water, but also of its surrounding groundwater. The gains from groundwater led to a longitudinal profile of decreasing nitrate concentrations in the stream, even under net losing conditions. Biogeochemical activity in the transition zone between groundwater and stream, result in low nitrate concentrations in near stream groundwater along reaches with substantial gross losses of stream water.

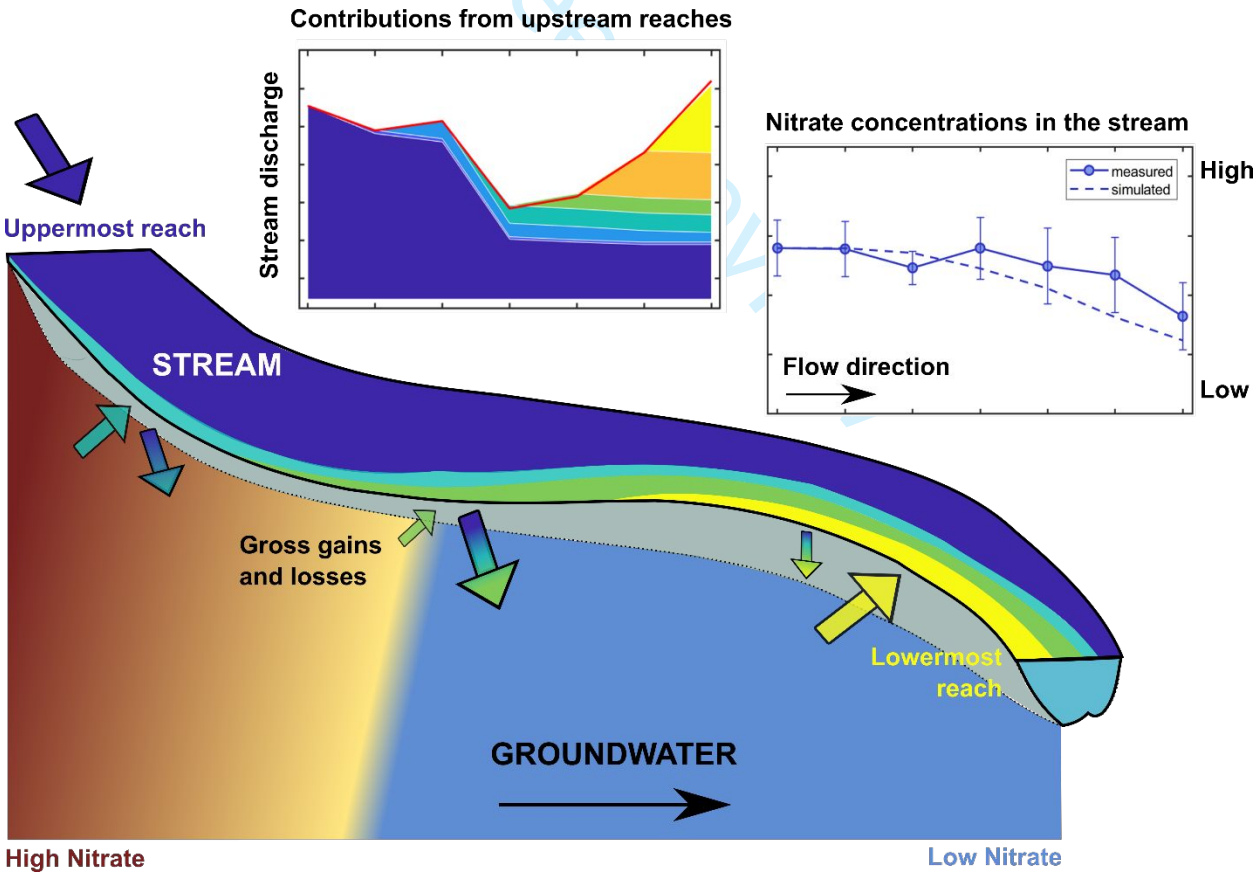

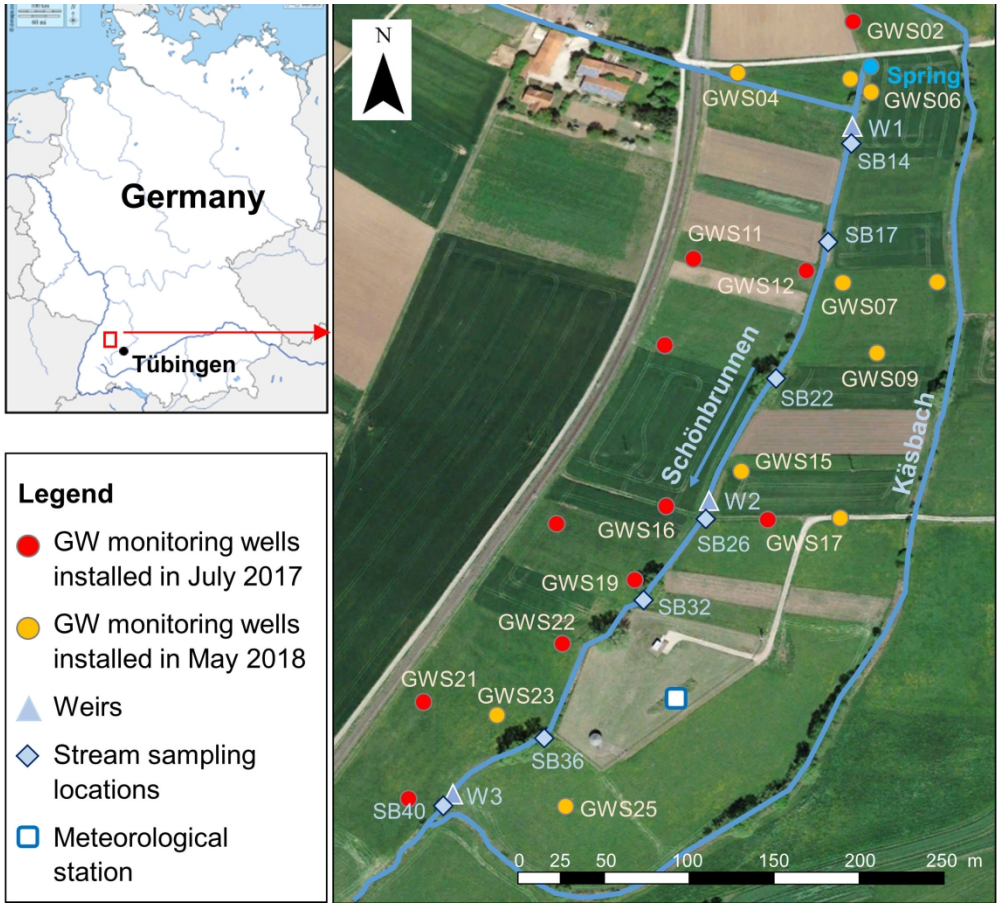

Location of the Schönbrunnen study site including the field installations (weirs, sampling sites, and monitoring wells) for continuous stream and groundwater monitoring.

209x188mm (300 x 300 DPI)

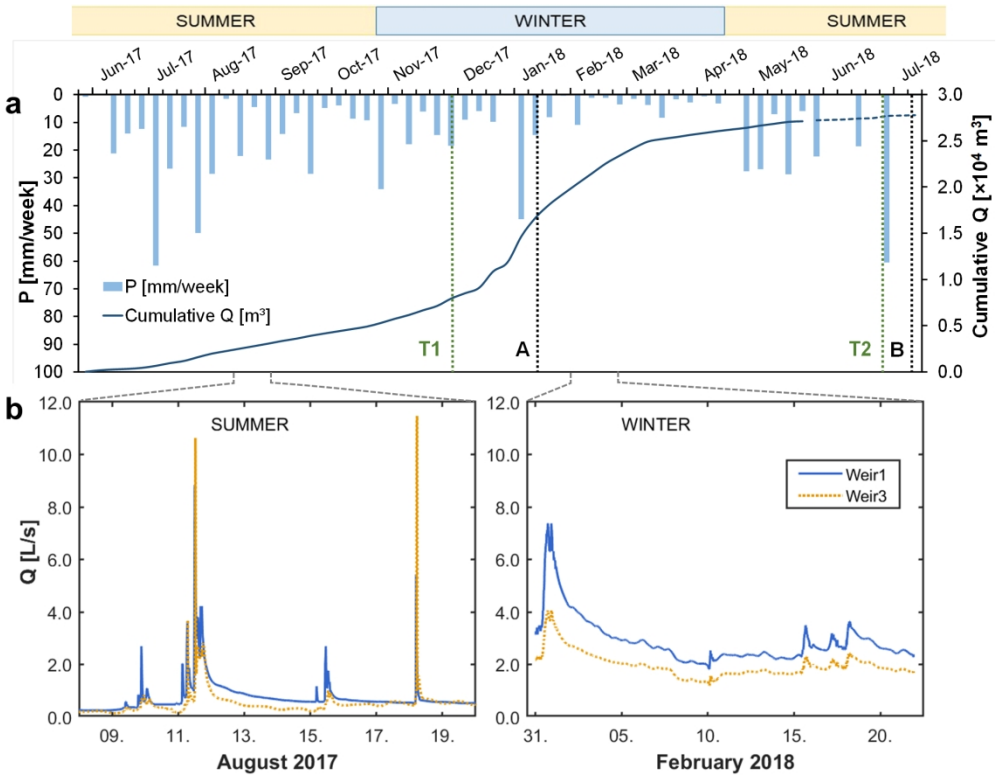

(a) Comparison of cumulative discharge Q at weir W2 with weekly precipitation P in the catchment. The dotted section of cumulative Q in June and July 2018 was extrapolated from W3 because of missing data. Dashed lines A and B indicate the times at which hydraulic head contours are depicted in Figure 4, and T1 and T2 the time at which salt tracer tests were carried out at the SB stream. (b) Hydrographs of typical summer (left panel) and winter (right panel) events measured at the most upstream and downstream weirs W1 and W3, respectively.

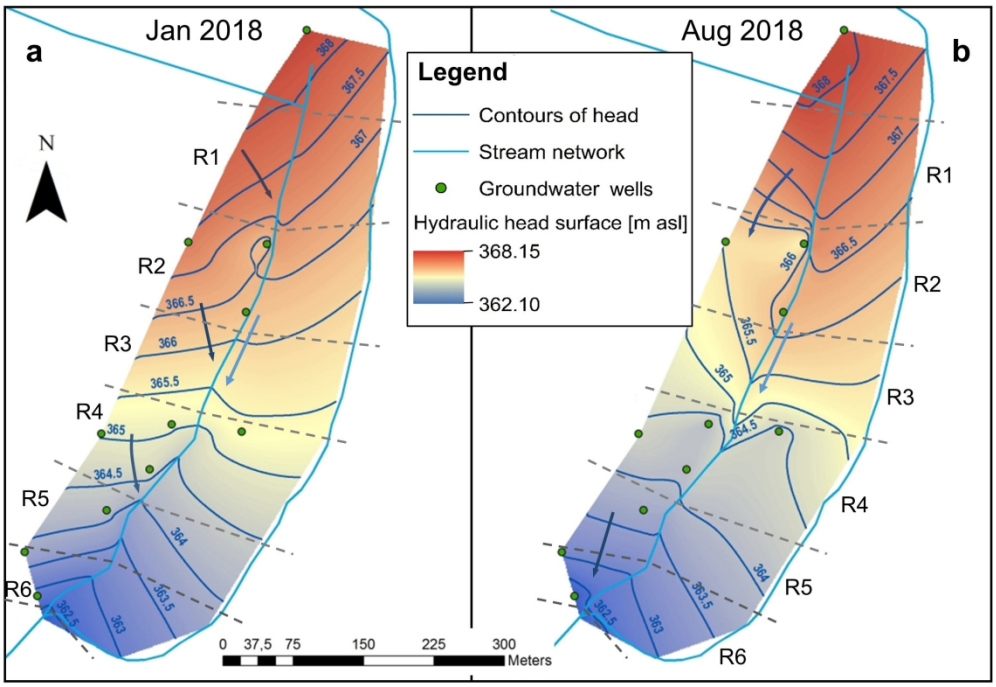

Groundwater head contours based on interpolation (natural neighbor) from monitored hydraulic heads at the groundwater monitoring wells in the alluvial aquifer for representative dates in the (a) winter season (23. January 2018) and (b) summer season (01. August 2018).

223x152mm (300 x 300 DPI)

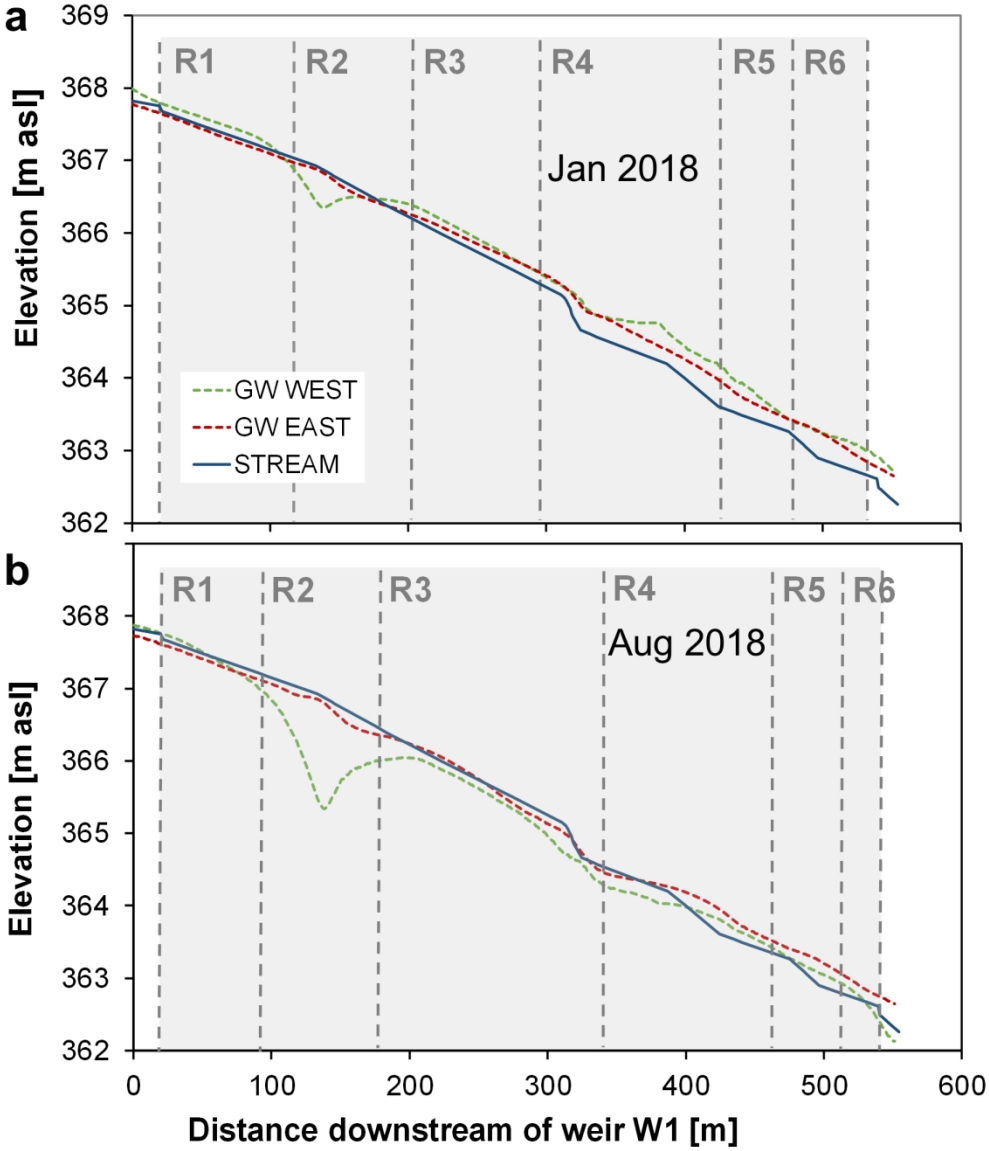

Comparison of groundwater heads and surface water elevation for representative dates in the (a) winter season (23. January 2018) and (b) summer season (01. August 2018). The blue line indicates the stream stage estimated from average water depth in the stream and streambed elevation measurements. The intervals between measured points were linearly interpolated. The two dashed lines depict groundwater head elevations along two hypothetical lines parallel to the stream, both 10 meters away from the stream in western (green line) and eastern (read line) directions.

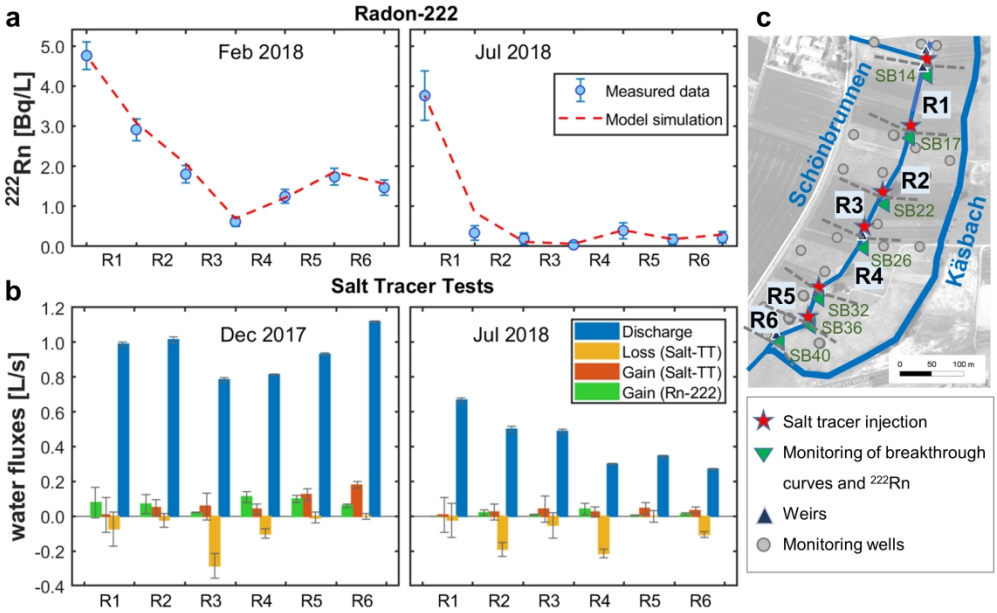

(a) Measured (symbols) and simulated (dashed line) Radon-222 activity concentrations in stream water collected in February and July 2018 as representative dates of the two considered seasons. (b) Stream discharge, gross water losses, and gross gains over individual stream reaches R1 to R6 estimated from consecutive instream salt tracer tests. The additional green bars show the 222Rn-derived gross gains from groundwater inflows for comparison. (c) Location of the individual reaches (R1 to R6) along the SB stream together with points of tracer injection and monitoring sites (SB14 to SB40) for tracer breakthrough curves, 222Rn, and hydrochemistry.

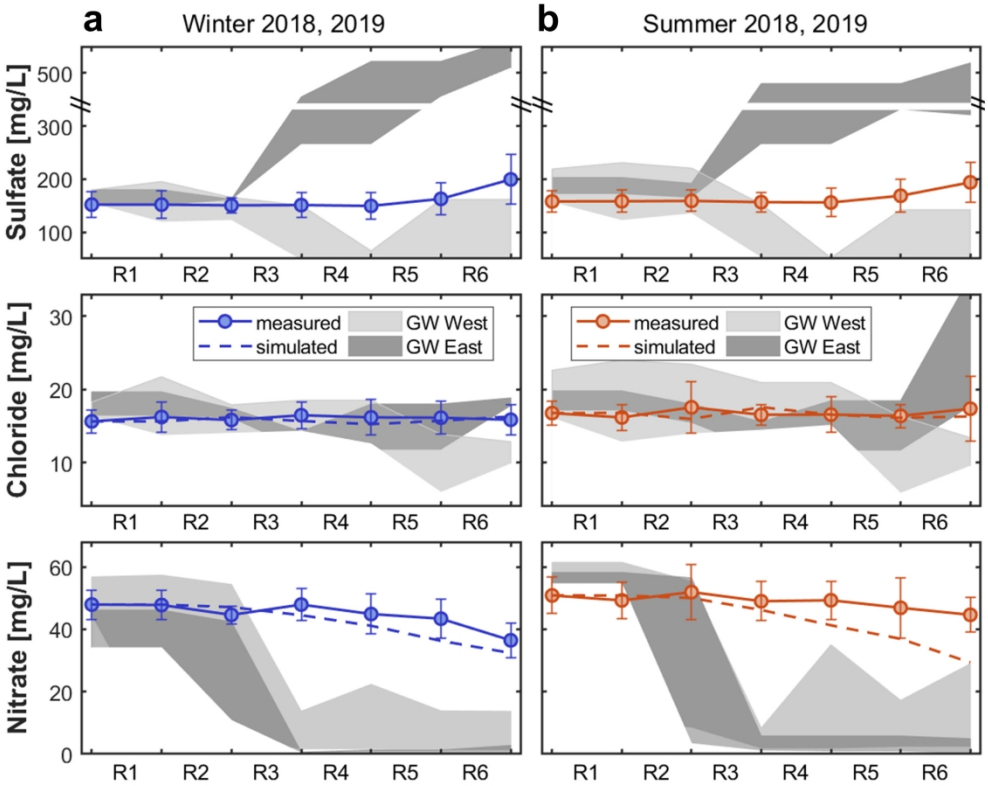

Mean sulfate, chloride, and nitrate concentrations in stream water (in flow direction) at seven sampling sites bounding the stream reaches R1 to R6 for (a) the summer and (b) winter season. Grey shaded areas represent the inter-quartile ranges of the ions in groundwater at the western (light grey) and eastern (dark grey) sides of the SB stream. For chloride and nitrate, simulated concentrations of these ions are shown for comparison (dashed lines).

224x179mm (300 x 300 DPI)

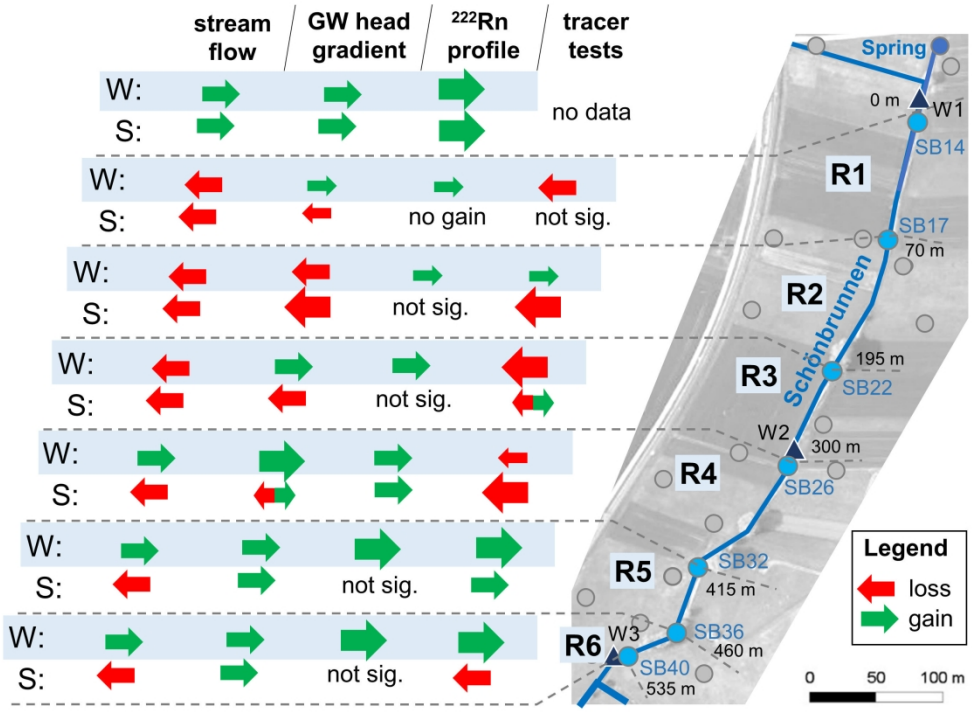

Summary of stream-groundwater exchange patterns derived by the different monitoring approaches during the winter (W) and summer (S) seasons. The size of the gain and loss arrows indicates the magnitude of the exchange flux. Not significant fluxes are indicated as 'not sig.'.

237x170mm (300 x 300 DPI)

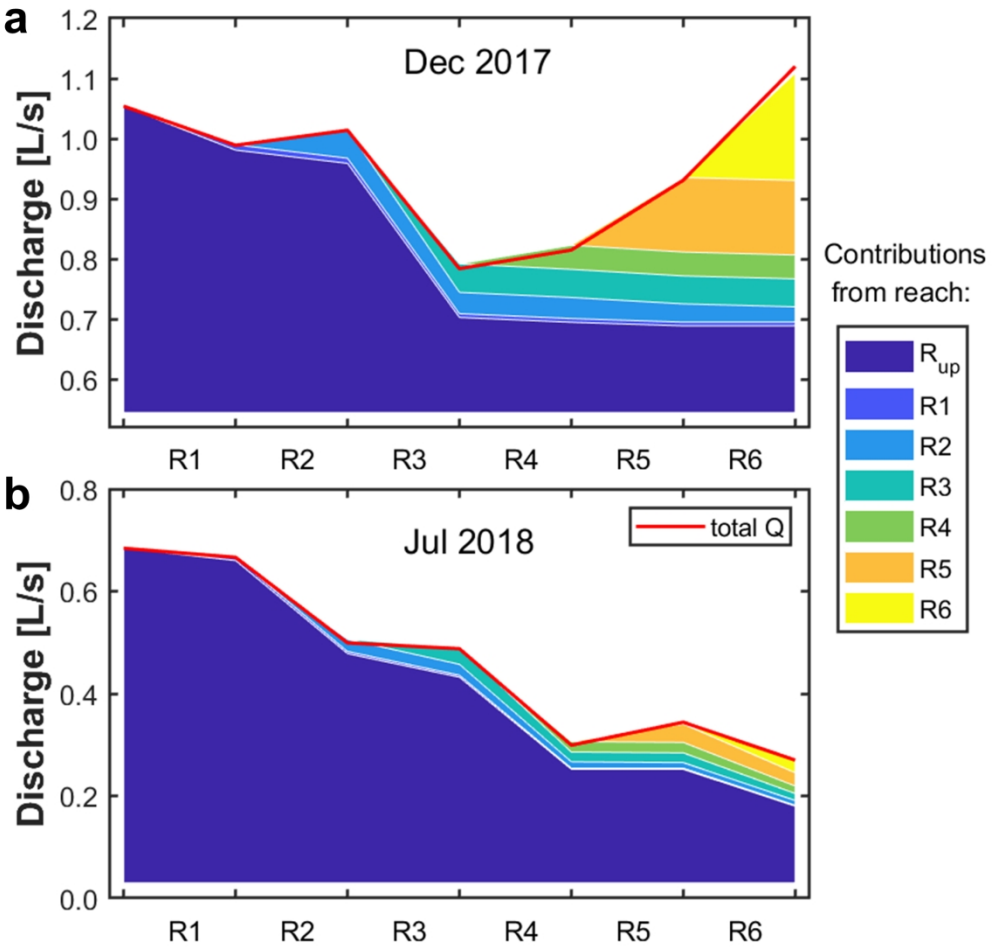

Contributions of stream water in the individual reaches (R1 to R6) from upstream reaches based on measured discharge (red line) and estimates of gross gains and losses using Eq. (8) and Eq. (9). Rup represents the section upstream of R1. Water losses from the stream can be compensated by gains from groundwater leading to a "hydrologic turnover" of stream water composition.

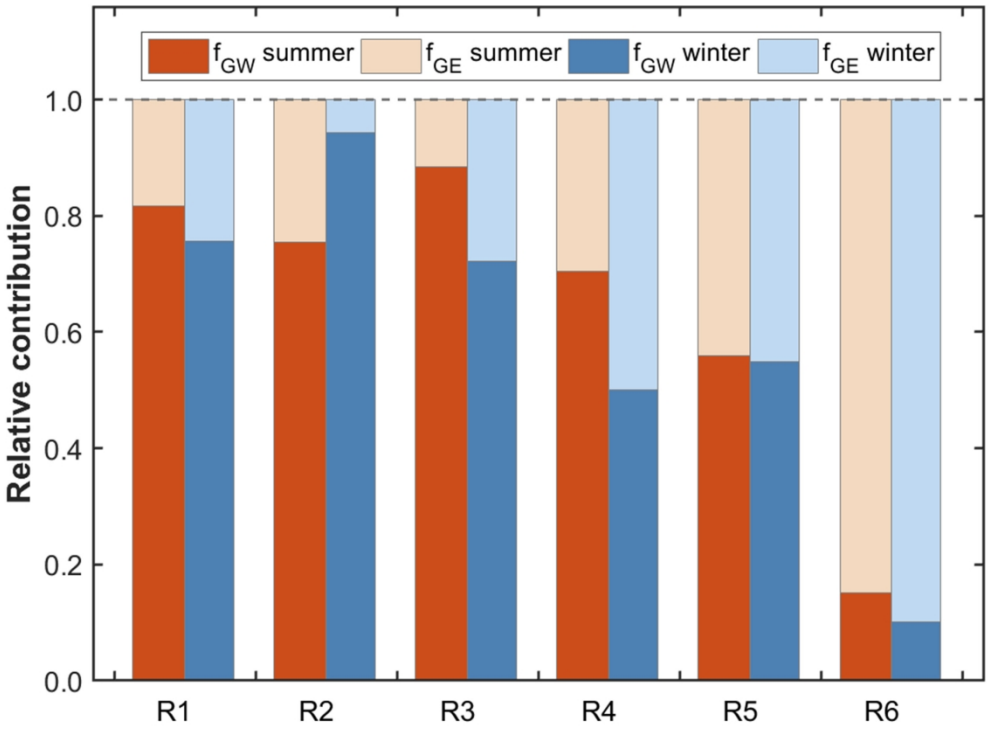

Relative contributions fGW and fGE to stream discharge from the western and eastern groundwater bodies, respectively. Values are based on sulfate concentrations and gross groundwater gains at the individual reaches. The values of gross gains and gross losses of stream water were taken from the two salt tracer experiments assuming that the results represent averaged seasonal exchange fluxes.

230x169mm (300 x 300 DPI)

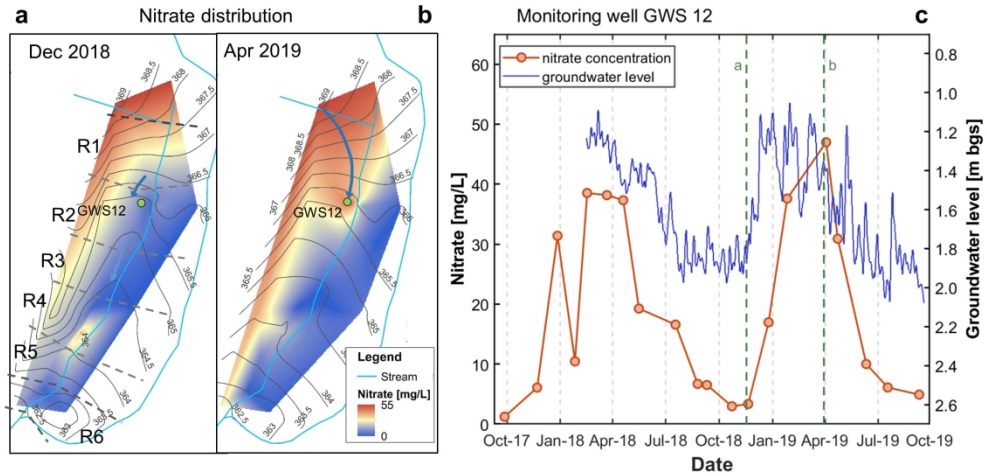

Spatial distribution of nitrate concentrations in groundwater along the SB stream for two dates in different seasons: (a) December 2018, (b) April 2019. Blue arrows indicate different groundwater flow paths leading to distinct nitrate concentrations at the indicated monitoring wells over time. (c) Comparison of the nitrate concentration time series and groundwater levels at well GWS12.

256x123mm (300 x 300 DPI)

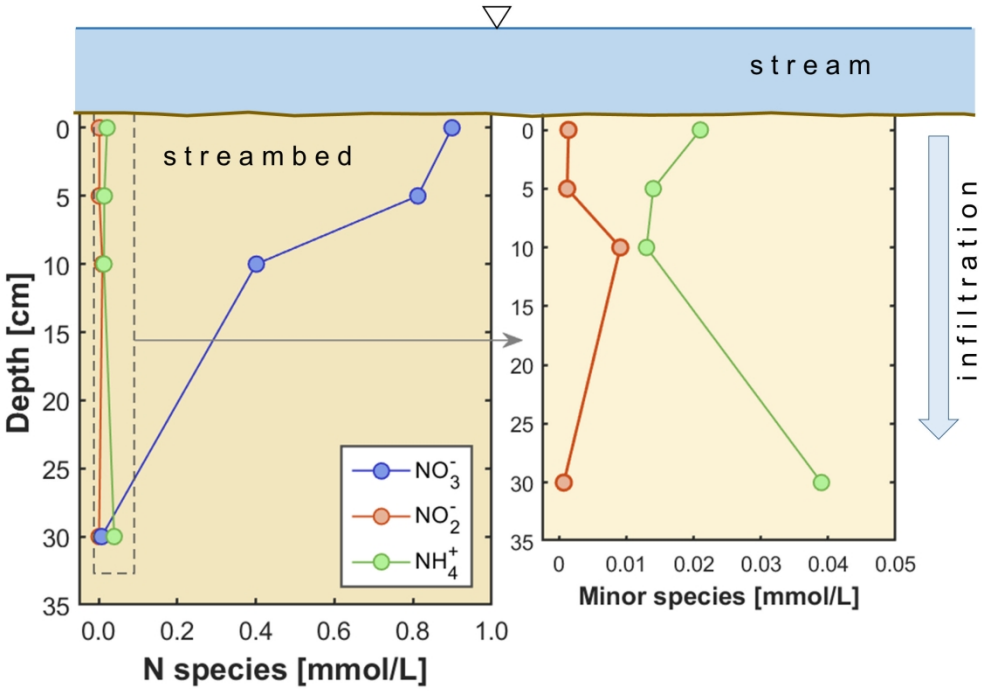

Concentration profiles of N species (NO3- , NO2- , and NH4+) in streambed sediment in reach R2, where losing conditions prevailed during the summer period. The right panel zooms in on the low concentrated minor N species (different scale).

232x161mm (300 x 300 DPI)

Tables

Table 1

Mean concentrations and standard deviations of major anions in stream water and groundwater at the investigated reaches of the SB study site for the winter (W) and summer (S) seasons, respectively.

Stream reach:		R_{up}	R1	R2	R3	R4	R5	R6	
Stream water:		Spring	SB14	SB17	SB22	SB26	SB32	SB36	SB40
Cl [mg/L]	W	17 ± 2	16 ± 2	16 ± 2	16 ± 2	17 ± 2	16 ± 3	16 ± 3	16 ± 2
	S	19 ± 3	17 ± 2	16 ± 2	18 ± 4	17 ± 2	17 ± 3	16 ± 2	17 ± 5
SO_4 [mg/L]	W	166 ± 22	152 ± 27	152 ± 28	151 ± 15	151 ± 26	149 ± 28	163 ± 33	199 ± 52
	S	188 ± 35	158 ± 22	158 ± 24	159 ± 22	157 ± 20	156 ± 30	169 ± 34	194 ± 42
NO_3 [mg/L]	W	49 ± 5	48 ± 5	48 ± 5	45 ± 3	48 ± 6	45 ± 7	43 ± 7	36 ± 6
	S	55 ± 11	51 ± 7	49 ± 7	52 ± 10	49 ± 7	49 ± 7	47 ± 11	45 ± 6
Cl/NO_3	W	0.6	0.6	0.6	0.6	0.6	0.6	0.6	0.8
	S	0.6	0.6	0.6	0.6	0.6	0.6	0.7	0.7
GW West:		GWS02	GWS04	GWS12	GWS11	GWS16	GWS19	GWS22	GWS23
Cl [mg/L]	W	18 ± 1	14 ± 1	15 ± 2	8 ± 2	19 ± 1	13 ± 2	14 ± 5	14 ± 2
	S	18 ± 1	14 ± 1	15 ± 1	15 ± 3	21 ± 2	15 ± 1	16 ± 3	14 ± 2
SO_4 [mg/L]	W	164 ± 14	125 ± 8	152 ± 30	46 ± 10	48 ± 5	71 ± 25	65 ± 24	155 ± 30
	S	177 ± 17	135 ± 12	152 ± 18	91 ± 47	53 ± 14	48 ± 10	52 ± 6	151 ± 27
NO_3 [mg/L]	W	52 ± 5	55 ± 3	20 ± 17	25 ± 5	2 ± 1	26 ± 9	14 ± 6	1 ± 1
	S	57 ± 6	55 ± 4	14 ± 12	32 ± 2	3 ± 2	33 ± 8	17 ± 5	2 ± 1
Cl/NO_3	W	0.6	0.5	3.2	0.6	46	1.0	2.2	38
	S	0.5	0.4	4.3	0.8	20	0.8	1.7	16
GW East:			GWS06	GWS07	GWS09	GWS15	GWS17	GWS25	
Cl [mg/L]	W		18 ± 2	16 ± 2	27 ± 3	15 ± 2	12 ± 1	19 ± 2	
	S		18 ± 2	16 ± 1	28 ± 3	16 ± 1	12 ± 1	25 ± 10	
SO_4 [mg/L]	W		164 ± 17	167 ± 23	1170 ± 240	167 ± 19	467 ± 31	526 ± 43	
	S		189 ± 17	164 ± 18	1310 ± 70	194 ± 42	475 ± 64	480 ± 61	
NO_3 [mg/L]	W		41 ± 8	9 ± 6	55 ± 3	1 ± 1	3 ± 4	1 ± 1	
	S		56 ± 2	5 ± 4	55 ± 4	2 ± 1	7 ± 6	2 ± 3	
Cl/NO_3	W		0.8	11.6	611	151	180	186	
	S		0.6	14.4	183	20	5.9	234	

For Peer Review